AN ABSTRACT OF THE THESIS OF

Youn Kang Chin for the degree of Doctor of Philosophy in Electrical and Computer Engineering presented on May 21, 1982

Title: ANALYSIS AND APPLICATIONS OF MULTIPLE COUPLED LINE STRUCTURES IN AN INHOMOGENEOUS MEDIUM

Abstract approved: Dr. Vijai K. Tripathi

The general expressions for finding the network functions, e.g., the immittance and the scattering parameters, of a general, uniformly coupled n-line structure in an inhomogeneous medium are derived in terms of the normal mode parameters of the system. These are used to compute or to derive the explicit expressions for the elements of the immittance matrix in terms of normal mode parameters.

The scattering parameters of a general non-symmetrical directional coupler with arbitrary terminations are derived in terms of the known scattering parameters with a specified set of terminations such as characteristic non-mode converting terminations. The formulation is quite general and can be applied to various coupled guided wave systems, including coupled microstrip lines, slot lines, comb lines, dielectric waveguides and various other uniformly coupled transmission systems.

The results obtained are used to present the procedure to determine the optimum terminations for directional couplers and sensitivity of various multiports, including couplers, to changes in terminations. It is shown that the coupler performance can be optimized in terms of the terminating impedances.

The analysis and design procedure for both symmetrical and nonsymmetrical four-port coupled structures consisting of the symmetrical three lines in an inhomogeneous medium such as microstrips are presented. Tables and charts for the design of three-line structure are based on the closed form expressions for the immittance parameters.

The analysis and design procedure for open-circuited interdigital multiple coupled microstrip line structures for applications as wideband DC blocks and filters are also presented. As in the case of the other microstrip structures, the initial design is based on the TEM assumption and the final geometry is then determined by the exact computation of the frequency response of the two ports. For larger numbers of lines, the design is based on the equivalent even- and odd-mode parameters of the n-line system. For this case, the TEM design equations, derived in terms of even- and odd-mode impedances of a pair of lines, can be translated into a physical configuration by using published results on coupled lines.

Analysis and Applications of Multiple Coupled Line Structures in an Inhomogeneous Medium

by

Youn Kang Chin

A THESIS

submitted to

Oregon State University

in partial fulfillment of
the requirements for the
degree of
Doctor of Philosophy

Completed May 1982

Commencement June 1983

APPROVED:

Redacted for Privacy

Associate Professor of Electrical and Computer Engineering in charge of major

Redacted for Privacy

Head of the Electrical and Computer Engineering Department

Redacted for Privacy

Dean of Graduate School

Date thesis is presented May 21, 1982

Typed by Mary Ann (Sadie) Airth for Youn K. Chin

ACKNOWLEDGEMENTS

The author wishes to express his deep appreciation to Dr. Vijai K. Tripathi, his major professor, for his encouragement, excellent guidance and suggestions during his course work and the preparation of this research.

The author also expresses thanks to Professors S. John T. Owen, Rudolf Engelbrecht, Thomas K. Plant, and Dale E. Kirk for serving on his graduate committee and reviewing the manuscript.

The author wants to extend his thanks to Mr. H. Lee for his helpful discussions and interest in the development of this research.

The author is deeply grateful to his wife, Bok-Hee and daughter, Soo, for their love, patience, and understanding during the course of this work.

Finally, the author wishes to thank his mother for her encouragement, dedication and inspiration throughout his life, and for his future.

TABLE OF CONTENTS

LIST OF FIGURES

ANALYSIS AND APPLICATIONS OF MULTIPLE COUPLED LINE STRUCTURES IN AN INHOMOGENEOUS MEDIUM

CHAPTER I. Introduction

1.1 BACKGROUND

Wave propagation in coupled distributed parameter systems has been a research topic of continued interest because of its importance in many engineering problems [1-29]. Most of the early work dealt with coupled homogeneous systems and resulted in many applications, including coupled TEM circuits consisting of rectangular and circular bars, strips and other forms of lines for use as filters, directional couplers, phase equalizers, matching networks and others at microwave frequencies [27-29].

Symmetrical two-line (or two-wire and ground) four-port couplers have been investigated by Oliver [4], who suggested that the natural coupling could be used to make directional couplers with the remarkable properties of perfect matching and isolation over the entire frequency band for the dominant TEM mode. Jones and Bolljahn [5] studied the network properties of homogeneous symmetrical coupled line pair by using the four-port impedance matrix. With the advances in integrated circuit technology, the study of the properties and applications of coupled inhomogeneous lines, such as structures consisting of microstrip lines, slot lines [30-34], coplanar lines [35-39] and others, has become quite important in recent years. The network parameters for inhomogeneous symmetrical coupled lines have been derived

by Zysman and Johnson [11]. Allen [40] has utilized these to formulate the design procedure for various two-port circuits for application as filters for the case of large mode velocity ratios. Other problems dealing with coupled inhomogeneous lines include the study and minimization of crosstalk noise in digital circuits since the back plane wiring of a modern high-speed digital computer is best represented by coupled inhomogeneous lines. This has become more significant due to advancements in improved packaging techniques and high-speed semiconductor devices [9, 23-26].

The theory of non-symmetric uniform coupled lines in a homogeneous medium has been formulated by expressing their four-port parameters in terms of the properties of even and odd excitation modes as defined by Cristal [7] and Ekinge [17]. The even voltage-mode, odd current-mode pair, as defined by Ekinge for homogeneous lines, has been considered by Allen [19] and Speciale [20] for the non-symmetrical coupled lines in an inhomogeneous medium. Speciale indicated that these two modes are the normal modes of the coupled lines only if a congruence condition between the parameters is satisfied. Further, Tripathi [21, 22] has developed a convenient procedure to study uniformly coupled non-symmetrical, lossy, inhomogeneous systems in terms of its normal mode parameters and has derived the four-port circuit parameters of two coupled lines in terms of the properties of these mode parameters. These parameters, which are used to study the multiple coupled line structures, are derived in terms of the equivalent self- and mutual-series impedances and shunt-admittances of the lines.

These equivalent self- and mutual-series impedance and shunt-admittance parameters of the coupled inhomogeneous system can be evaluated at low frequencies by assuming a quasi-TEM mode of propagation. This assumption is adequate for designing circuits at low frequencies where the strip width and the substrate thickness are much smaller than the wavelength in the dielectric material. In this case, the equivalent parameters are found by solving the Laplace's or Poisson's equations for the capacitive coefficients of coupling by utilizing various techniques. These include:

(1) Conformal Transformation Method;

An exact conformal transformation for the impedance of zero thickness, homogeneous microstrip line has been given by Schneider [41]. For a single strip conductor or for a system of two-strip conductors, where a high degree of symmetry is present, Schwartz-Christoffel conformal mapping may be used to obtain mathematically exact results in terms of elliptic integrals [42-45]. When the system is not highly symmetrical, the Schwartz-Christoffel method becomes quite cumbersome unless a number of simplifying approximations are made, in which case the results may not be quite accurate.

(2) Finite Difference Method [46-52];

This method is based on the numerical solution of Laplace's equation in finite difference form. This technique is more suitable for an enclosed microstrip conductor, and its finite thickness can be incorporated into the analysis. The most common method of solving finite difference equations is successive over relaxation. Lennartsson [51] has formulated a procedure to evaluate the quasi-TEM param-

eters of shielded asymmetric coupled inhomogeneous lines with good accuracy using a resistive network analog. However, tables or graphical solutions are not available to design such structures. Also, the method is not computationally efficient since a large number of grid points may be required.

(3) Integral Equation Method [26, 53-63];

In this method, one considers the Poisson's equation in terms of line charge distribution and formulates a suitable Green's function which satisfies the boundary conditions at the interface. Using Green's function, an integral equation can be formulated and solved by writing it in the form of a matrix equation and carrying out the matrix inversion numerically. This method has been used for a number of structures, including the non-symmetrical broadside coupled structure in an inhomogeneous medium [63].

(4) Variational Method in Fourier Transform Domain [64-66];

This method is based on Fourier transform and variational technique where the potential function is expanded in the Fourier transform domain and then the variational expression for the capacitances is used in the Fourier transform domain, assuming a trial function for charge or current distribution. This technique can also be used to take into account the effect of finite strip thickness and enclosure and can be extended to microstrips with composite substrates or a dielectric overlay [65].

All the above techniques have been primarily used to obtain the properties of simple and identical coupled lines. In some of the

articles referred to, it has been noted that the same procedure is applicable to the case of non-symmetrical structures.

Recently Lee [67] has formulated an efficient computational procedure to calculate the quasi-TEM parameters (phase constants and line impedances for n modes) for both symmetrical and non-symmetrical multiple lines in an inhomogeneous medium such as coupled microstrip, coplanar lines and waveguides. For the case of multiple microstrip lines, the procedure utilizes a similar approach to that used by Weiss [59] for identical coupled lines.

At higher frequencies, when the wave length in a microstrip line becomes comparable to the transverse dimension of the structure, the quasi-TEM approximation is no longer valid. The line parameters can then be obtained by solving Helmholtz's equation, subject to the given boundary conditions.

The basic techniques include the integral equation method, Galerkin's method in Fourier transform domain and related techniques [68-78].

A great deal of work has been done on the properties and applications of homogeneous coupled lines having commensurate lengths because of their applications in wide variety of microwave circuits [27-29]. The structures are studied by utilizing the line properties, i.e., the characteristic immittances and phase velocities for the two independent even- and odd-modes of excitation. The phase velocity of the two modes is equal for the homogeneous case, and much of the work has been done with the help of lumped equivalent circuits obtained in Richards' frequency plane, $S = j \tan \beta \ell$. This enables

one to utilize various known lumped circuit techniques to study and design these structures.

Inhomogeneous coupled line structures have been designed for the case of identical coupled lines by using simple network techniques and the line properties for even- and odd-modes of excitation [11,40,79-82] primarily for applications as microwave filters. It is seen that the additional degree of freedom obtained through unequal phase velocity of the two modes may result in realization of some unique elements, as shown by Allen[40,79-81] for the case of large velocity-ratios of the two modes. The properties of non-symmetrical coupled lines in an inhomogeneous medium, and their four-port parameters as obtained by Tripathi [21], are used to obtain the equivalent circuits and characteristics of various prototypes for the case of quasi-TEM lossless lines [83]. Such structures have an inherent impedance transforming capability and added flexibility in the design through an additional variable, as compared to identical coupled lines in an inhomogeneous medium.

Wide-band filters with DC-isolated input and output ports [83] have been used as microstrip DC blocks [84-86], which may have improved performance at microwave frequencies as compared to lumped capacitors.

As microwave circuit technology advances, more effective methods for realizing broad-band quadrature hybrids and power dividers/combiners are required for microwave integrated circuits (MIC) applications. In MIC, interdigitated couplers, composed of four coupling strips tied together in pairs, are commonly used to meet tight

coupling conditions. Several quantitative design procedures [87-91] have been proposed since Lange's first investigation [92] of the interdigitated coupler. Later, an unfolded Lange coupler has been presented by Waugh and LaCombe [93] that only needs two bond wires. A 3-dB interdigitated three-line microstrip coupler with two bond wires on alumina substrate (ε_r = 10) has been developed by Tulaja et al. [94]. The immittance parameters for the case of symmetrical coupled three-line microstrip conductors or other inhomogeneous six-port structures were derived in terms of the normal modes of the coupled system by Tripathi [95]. Tripathi [96] has also derived the scattering parameters of coupled symmetrical microstrip three-line structures in an inhomogeneous medium which can be used to study the directional coupler properties, including possible matching and isolation conditions for six-port and interdigitated four-port couplers consisting of symmetrical three-line structures.

1.2 SUMMARY OF THESIS

In chapter II, a general procedure for finding the immittances of a general, uniformly coupled, n-line structure in an inhomogeneous medium is presented. The expressions derived in terms of the normal modes of the system are in a convenient matrix form and can be used to compute or to derive the explicit expressions for the elements of the 2n-port immittance matrix. As an example, the closed form expressions for the elements of the admittance matrix of a symmetrical four-line eight-port structure are given in Appendix A. It is shown that the scattering parameters of a general non-symmetrical

2n-port with arbitrary terminations can be derived in terms of the known scattering parameters with a specified set of terminations such as non-mode converting terminations and the terminating impedances. The formulation is quite general and can be applied to various coupled guided-wave systems, including systems with more than two coupled lines. It is shown that the coupling performance of a general non-symmetrical uniformly-coupled-line four-port coupler with unequal normal mode phase velocities can be optimized in terms of the terminating impedances by using the explicit expressions for the scattering parameters of a non-symmetrical four-port coupler with arbitrary terminations. These expressions can also be used to study the sensitivity of various multiports, including couplers, to changes in terminations.

In chapter III, the sensitivity equations of a four-port coupler to changes in terminations are derived in terms of the known scattering parameters, and the method to determine the optimum terminations by the impedance renormalization procedure are presented with an example for two-line structure.

In chapter IV, the analysis and design procedures for both symmetrical and non-symmetrical interdigitated three-line four-port directional couplers are presented. Table and charts for the design of couplers having typical values of substrate dielectric constants are presented. The procedure to determine the terminations required for optimum coupler performance of the non-symmetrical coupler are also presented in terms of the scattering parameters with characteristic terminations by using impedance renormalization procedure.

In chapter V, the analysis and design procedure for both symmetrical and non-symmetrical open-circuited interdigital multiple coupled microstrip line structures for application as wide-band DC blocks and filters are presented. The design equations for symmetrical and non-symmetrical two-port with a flat frequency response, and symmetrical two-port with a single ripple response having a specified maximum ripple, are formulated. As in the case of the other microstrip structures, the initial design is based on the TEM assumption and the final geometry is then determined by the exact computation of the frequency response of the two ports. For larger numbers of lines, the design is based on the equivalent even- and odd-mode parameters of the n-line system. For this case, the TEM design equation, derived in terms of even- and odd-mode impedances of a pair of lines, can be translated into a physical configuration by using published results on coupled lines.

CHAPTER II. Network Function Characterizing the General 2n-Port

2.1 INTRODUCTION

A coupled transmission line system is a set of transmission lines in which the voltages and currents of each line can influence the voltages and currents of all the others. The systems to be considered are lossless and uniform n-line structures in an inhomogeneous medium. The n-line 2n-port structure can be characterized in terms of an immittance matrix, a chain matrix, or scattering parameters. The immittance matrix is suitable for studying two-port circuits, while the scattering parameters are more suitable for studying multiport circuits, including couplers, since the immittance matrix of a coupler does not conveniently describe the coupler performance. The general forms of the immittance and chain matrices of an n-line structure were derived by Chang [13], Marx [15], and Paul [97, 98]. The explicit closed expressions for non-symmetrical two-line and symmetrical three-line structures were derived by Tripathi [21, 95] in terms of the normal modes of the coupled system.

The expressions derived in terms of the normal mode parameters of an n-line coupled system are in a convenient matrix form and can be used to compute or to derive the explicit expressions for the elements of the 2n-port immittance matrix. These normal mode parameters are the phase constants and the characteristic impedance of the individual lines for all the modes of the system and can be readily computed

for various cases of multiple coupled lines [67]. The closed form expressions for the immittance matrix of the symmetrical four-line structure are given in Appendix A.

The scattering parameters [99] for a 2n-port structure in general can be computed by utilizing the immittance parameters. However, when the number of lines is small, e.g., n = 2 or 3, explicit expressions for these parameters can be derived in a closed form with arbitrary terminations as shown in section 2.3 of this chapter. These expressions for the case of general two-line and symmetrical three-line structures have been derived by Gunton and Paige [100] and Tripathi [96] only for the special case where lines are terminated in non-mode converting impedances. In section 2.3 of this chapter, the scattering parameters of a general coupled line four-port with arbitrary terminations are derived directly from the normal mode parameters of two-line coupled structures by using the definition of the scattering parameters. It is shown that these can also be derived in terms of the scattering parameters of the four-port with non-mode converting terminations and the new arbitrary terminations.

2.2 IMMITTANCE FUNCTIONS

The transmission line equations for the n-line system shown in Fig. 2-1 are given by:

$$\frac{d[V]}{dx} = -[Z]\,[I] \tag{2-1}$$

$$\frac{d[I]}{dx} = -[Y]\,[V] \tag{2-2}$$

where [V] and [I] are the n-dimensional column vectors representing the voltages and currents on the lines, and [Z] and [Y] are n x n impedance and admittance matrices as given by

$$[Z] = \begin{bmatrix} Z_{11} & Z_{12} & \cdots & Z_{1n} \\ Z_{21} & Z_{22} & \cdots & Z_{2n} \\ \vdots & & & \vdots \\ Z_{n1} & Z_{n2} & \cdots & Z_{nn} \end{bmatrix}$$

and

$$[Y] = \begin{bmatrix} Y_{11} & Y_{12} & \cdots & Y_{1n} \\ Y_{21} & Y_{22} & \cdots & Y_{2n} \\ \vdots & \vdots & & \vdots \\ Y_{n1} & Y_{n2} & \cdots & Y_{nn} \end{bmatrix}$$

where Z_{ii} and Y_{ii} $(i = 1, 2, \ldots, n)$ are the equivalent self-impedance and admittance per unit length of the ith line, and Z_{ij} and Y_{ij} $(i \neq j)$ are the mutual impedance and admittance per unit length between the ith line and the jth line.

The voltages and currents for the case of uniformly coupled lines considered here are then the solutions of the following characteristic equations:

$$\frac{d^2[V]}{dx^2} + [Z]\,[Y]\,[V] = 0 \qquad (2\text{-}3)$$

$$\frac{d^2[I]}{dx^2} + [Y]\,[Z]\,[I] = 0 \qquad (2\text{-}4)$$

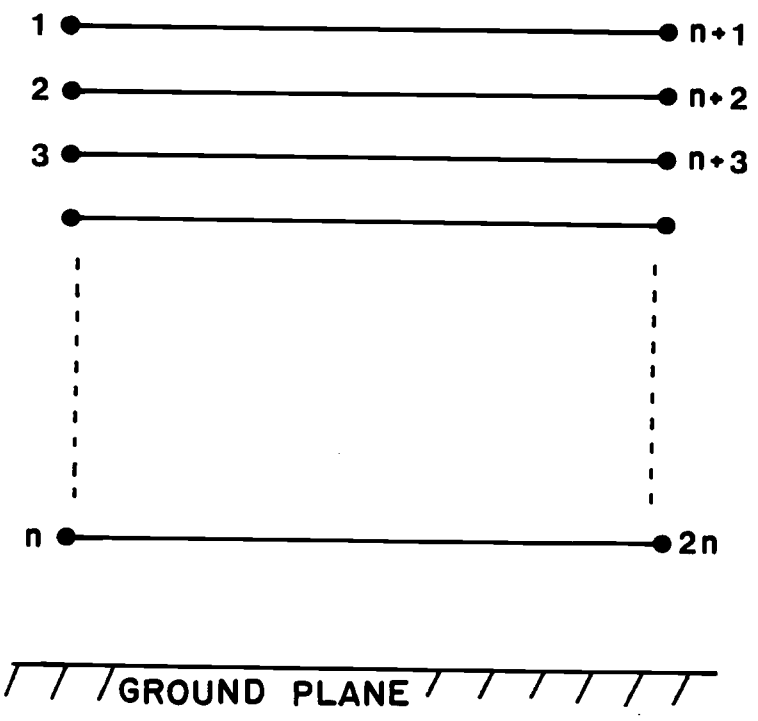

Figure 2-1. Schematic of the coupled line 2n-port.

where, for the n-line 2n-port case

$$[Y]\,[Z] = \{[Z]\,[Y]\}^{T}$$

The general solutions for the port voltages on n-line 2n-port structures are the given by

$$\begin{bmatrix} V_1 \\ V_2 \\ \cdot \\ \cdot \\ \cdot \\ V_n \\ V_{n+1} \\ \cdot \\ \cdot \\ \cdot \\ V_{2n} \end{bmatrix} = \begin{bmatrix} [M_V] & [M_V] \\ [M_V][e^{-j\theta i}]_{diag} & [M_V][e^{j\theta i}]_{diag} \end{bmatrix} \begin{bmatrix} A_1 \\ A_3 \\ \cdot \\ \cdot \\ \cdot \\ A_{2n-1} \\ A_2 \\ \cdot \\ \cdot \\ \cdot \\ A_{2n} \end{bmatrix} \qquad (2\text{-}5)$$

The corresponding currents for n-line 2n-port are determined by substituting the expressions for voltages (2-5) into (2-1). These currents are given by

$$\begin{bmatrix} I_1 \\ I_2 \\ \cdot \\ \cdot \\ \cdot \\ I_n \\ I_{n+1} \\ \cdot \\ \cdot \\ \cdot \\ I_{2n} \end{bmatrix} = \begin{bmatrix} [M_I] & -[M_I] \\ -[M_I][e^{-j\theta_i}]_{diag} & [M_I][e^{j\theta_i}]_{diag} \end{bmatrix} \begin{bmatrix} A_1 \\ A_2 \\ \cdot \\ \cdot \\ \cdot \\ A_{2n-1} \\ A_2 \\ \cdot \\ \cdot \\ \cdot \\ A_{2n} \end{bmatrix} \quad (2\text{-}6)$$

where, $i = 1, 2, \ldots, n$.

In the above equation, the eigenvalues, β_i's, representing the solutions of $\det \{ [Z][Y] + \beta^2 [U] \} = 0$, are the propagation constants for the normal modes of the system.

A_j $(j = 1, 2, \ldots, 2n)$ is an arbitrary amplitude coefficient and $\theta_i = \beta_i \ell$ is the electric length of lines for the n normal modes.

$[M_V]$ is the voltage eigenvector matrix (n by n) corresponding to eigenvalues:

$$[M_V] = \begin{bmatrix} 1 & 1 & \ldots & 1 \\ \alpha_2 & \beta_2 & \ldots & \xi_2 \\ \cdot & & & \cdot \\ \cdot & & & \cdot \\ \cdot & & & \cdot \\ \alpha_n & \beta_n & \ldots & \xi_n \end{bmatrix}$$

$[M_I]$ is the current eigenvector matrix (n by n) defined as $[M_I] \triangleq [Y]_c^T * [M_V]$ with the element $M_{Iij} = Y_{ji} \cdot M_{Vij}$:

$$[M_I] = \begin{bmatrix} Y_{11} & Y_{21} & \cdot & \cdot & \cdot & Y_{n1} \\ \alpha_2 Y_{12} & \beta_2 Y_{22} & \cdot & \cdot & \cdot & \xi_2 Y_{n2} \\ \vdots & & & & & \vdots \\ \alpha_n Y_{1n} & \beta_n Y_{2n} & \cdot & \cdot & \cdot & \xi_n Y_{nn} \end{bmatrix}$$

where, Y_{jk} is the characteristic admittance of line k for mode j.

Eliminating A_1, A_2, . . ., and A_{2n} leads to 2n equations for the 2n-port currents where coefficients represent the immittance parameters. These admittance parameters of the 2n-port are found to be:

$$[Y] = \begin{bmatrix} [M_I] & -[M_I] \\ -[M_I][e^{-j\theta i}]_{diag} & [M_I][e^{j\theta i}]_{diag} \end{bmatrix} \cdot \begin{bmatrix} [M_V] & [M_V] \\ [M_V][e^{-j\theta i}]_{diag} & [M_V][e^{j\theta i}]_{diag} \end{bmatrix}^{-1} \quad (2\text{-}7)$$

where $[\ ]_{diag}$ indicates a diagonal matrix.

The second matrix can be inverted as follows:

$$\begin{bmatrix} [U] + [\frac{e^{-j\theta i}}{2j \sin \theta_i}]_{diag} & -[\frac{1}{2j \sin \theta_i}]_{diag} \\ -[\frac{e^{-j\theta i}}{2j \sin \theta_i}]_{diag} & [\frac{1}{2j \sin \theta_i}]_{diag} \end{bmatrix} \begin{bmatrix} [M_V]^{-1} & [0\ ] \\ [0\ ] & [M_V]^{-1} \end{bmatrix}$$

Hence

$$[Y] = \begin{bmatrix} [M_I][0\,] \\ [0\,][M_I] \end{bmatrix} \begin{bmatrix} -j[\cot\theta_i]_{diag} & j[\csc\theta_i]_{diag} \\ j[\csc\theta_i]_{diag} & -j[\cot\theta_i]_{diag} \end{bmatrix} \begin{bmatrix} [M_V]^{-1}[0\,] \\ [0\,] \quad [M_V]^{-1} \end{bmatrix}$$

Manipulating the above matrices leads to

$$[Y] = \begin{bmatrix} [M_I]\,[\coth\gamma_i\ell]_{diag}\,[M_V]^{-1} & -[M_I]\,[\operatorname{csch}\gamma_i\ell]_{diag}\,[M_V]^{-1} \\ -[M_I]\,[\operatorname{csch}\gamma_i\ell]_{diag}\,[M_V]^{-1} & [M_I]\,[\coth\gamma_i\ell]_{diag}\,[M_V]^{-1} \end{bmatrix} \quad (2\text{-}8)$$

where $\theta_i = j\gamma_i\ell$.

The above matrix elements for the admittance matrix can be readily evaluated for a given 2n-port structure as illustrated for the case of a four-line microstrip structure in the following example.

Example: For a four-line symmetrical microstrip structure, shown in Fig. 2-2, the quasi-TEM normal mode parameters can be computed by the technique given by Lee [67]. The capacitance matrix $[C]_d$ of the structure with the dielectric present is given by:

$$[C]_d = \begin{bmatrix} C_{11} & -C_{12} & -C_{13} & -C_{14} \\ -C_{12} & C_{22} & -C_{23} & -C_{13} \\ -C_{13} & -C_{23} & C_{22} & -C_{12} \\ -C_{14} & -C_{13} & -C_{12} & C_{11} \end{bmatrix}$$

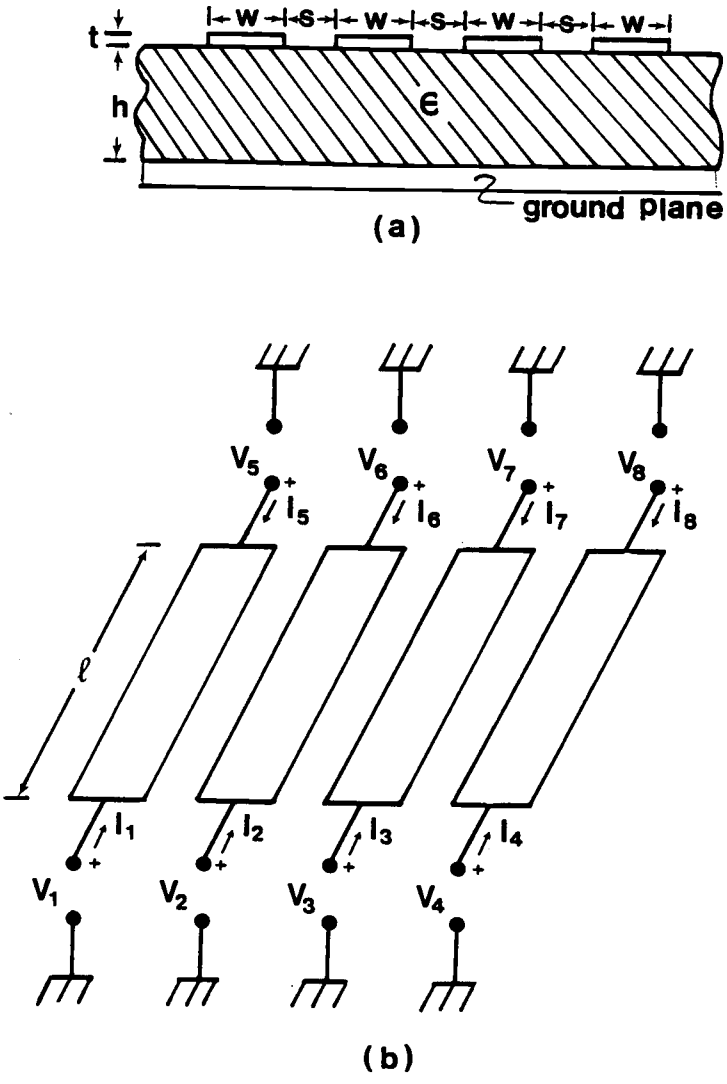

Figure 2-2. (a) Cross sectional view of the symmetrical four-line microstrip structure. (b) Schematic of the coupled line eight-port.

For the relative dielectric constant $\varepsilon_r = 10$ and the geometry given by w/h = 0.11 and s/h= 0.08, these parameters are found to be:

$$C_{11} = 110.38 \text{ pf}, \quad C_{12} = 50.61 \text{ pf}, \quad C_{13} = 9.93 \text{ pf},$$
$$C_{14} = 5.16 \text{ pf}, \quad C_{22} = 134.30 \text{ pf}, \quad C_{23} = 46.52 \text{ pf}.$$

These parameters, together with the same parameters with dielectric removed, lead to the four phase constants, the eigenvector matrix, and the characteristic admittance matrix of the structure, as given by:

$$\beta_1 = 8.502 \times 10^{-9} \text{ sec/m}, \quad \beta_2 = 7.849 \times 10^{-9} \text{ sec/m}$$
$$\beta_3 = 7.824 \times 10^{-9} \text{ sec/m}, \quad \beta_4 = 7.823 \times 10^{-9} \text{ sec/m}$$

where subscript i (=1, 2, 3, 4) indicates mode.

$$[M_V] = \begin{bmatrix} 1. & 1. & 1. & 1. \\ 1.0105 & 0.3436 & -1.5643 & -4.7330 \\ 1.0105 & -0.3436 & -1.5643 & 4.7330 \\ 1. & -1. & 1. & -1. \end{bmatrix}$$

$$[Y]_c = \begin{bmatrix} 1/192.998 & 1/77.272 & 1/39.132 & 1/25.393 \\ 1/305.077 & 1/125.673 & 1/61.856 & 1/41.299 \\ 1/305.077 & 1/125.673 & 1/61.856 & 1/41.299 \\ 1/192.998 & 1/77.272 & 1/39.132 & 1/25.393 \end{bmatrix} \text{ (mho)}$$

The eight-port admittance matrix elements, at the center frequency as defined by $\bar{\theta} = \frac{\Sigma\theta_i}{n} = \frac{\pi}{2}$ are calculated by using equation (2-8) and found to be:

$Y_{11} = -.2144 \times 10^{-3}$mho, $Y_{12} = .3538 \times 10^{-3}$mho

$Y_{13} = .1719 \times 10^{-3}$mho, $Y_{14} = .2053 \times 10^{-3}$mho

$Y_{15} = .1395 \times 10^{-1}$mho, $Y_{16} = -.6552 \times 10^{-2}$mho

$Y_{17} = -.1350 \times 10^{-2}$mho, $Y_{18} = -.7717 \times 10^{-3}$mho

$Y_{22} = -.4697 \times 10^{-3}$mho, $Y_{23} = .2796 \times 10^{-3}$mho

$Y_{26} = .1710 \times 10^{-1}$mho, $Y_{27} = -.5995 \times 10^{-2}$mho

2.3 SCATTERING PARAMETERS

(A) General Expressions [99]

The scattering matrix [S] of a general 2n-port network is defined by

$$b] = [S]\, a] \tag{2-9}$$

where,

$$a] = \begin{bmatrix} a_1 \\ a_2 \\ \cdot \\ \cdot \\ \cdot \\ a_{2n} \end{bmatrix}, \qquad b] = \begin{bmatrix} b_1 \\ b_2 \\ \cdot \\ \cdot \\ \cdot \\ b_{2n} \end{bmatrix}$$

It is assumed that a_i and b_i are normalized so that $1/2\ a_i a_i^*$ is the available power at port i and $1/2\ b_i b_i^*$ is the emergent power at the same port. The a_i's and b_i's are defined by

$$a_i = 1/2 \left(\frac{V_i}{\sqrt{Z_{io}}} + \sqrt{Z_{io}}\, I_i\right) \tag{2-10a}$$

$$b_i = 1/2 \left(\frac{V_i}{\sqrt{Z_{io}}} - \sqrt{Z_{io}}\, I_i\right) \tag{2-10b}$$

where Z_{io}, V_i, and I_i are the terminating impedance, the voltage, and current at port i, respectively.

If one defines

$$[Z_n] = [Z_o]^{-1/2}\, [Z]\, [Z_o]^{-1/2} \tag{2-11a}$$

$$[Y_n] = [Z_o]^{1/2}\, [Y]\, [Z_o]^{1/2} \tag{2-11b}$$

where $[Z_o]^{1/2}$ is a real diagonal matrix, each diagonal entry of which is the square root of Z_{io} and $[Z_o]^{-1/2}$ is the inverse of $[Z_o]^{1/2}$, then

$$[S] = \{[Z_n] - [U]\}\{[Z_n] + [U]\}^{-1} = \{[Z_n] + [U]\}^{-1}\{[Z_n]-[U]\}$$

$$= \{[U] - [Y_n]\}\{[U] + [Y_n]\}^{-1} = \{[U] + [Y_n]\}^{-1}\{[U]-[Y_n]\} \tag{2-12}$$

The above expressions can be used to compute the scattering matrix for multiple coupled line structures in terms of the terminations and the immittance parameters of the 2n-port.

Coupled line four-port:

Substituting the normal mode parameters of two-line coupled structures in the defining expressions for the scattering parameters as given by equation (2-9) [99] leads to the explicit closed expressions for the scattering parameters of a general non-symmetrical

coupled line four-port shown in Fig. 2-3 in an inhomogeneous medium. These parameters can be used to study the properties and applications of non-symmetrical four-port couplers and are found to be:

$$
\begin{aligned}
S_{11} &= S_{44} \\
&= 2 \{ [R_d^2 E F - (R_\pi A - R_c C)(R_\pi B - R_c D)] \cosh (\gamma_\pi + \gamma_c)\ell \\
&\quad + R_d[F(R_\pi A - R_c C) - E(R_\pi B - R_c D)] \sinh (\gamma_\pi + \gamma_c)\ell \\
&\quad - [R_d^2 E F - (R_\pi A + R_c C)(R_\pi B + R_c D) \cosh (\gamma_\pi + \gamma_c)\ell \\
&\quad + R_d[E(R_\pi B + R_c D) - F(R_\pi A + R_c C)] \sinh (\gamma_\pi - \gamma_c)\ell \\
&\quad - 4R_c R_\pi [Z_1/(Z_{c1} Z_{\pi 1} Z_2) - Z_2/(Z_{c2} Z_{\pi 2} Z_1)] \}/\Delta
\end{aligned}
\tag{2-13a}
$$

$$
\begin{aligned}
S_{12} &= S_{21} = S_{34} = S_{43} \\
&= 4R_c R_\pi \{ -(2R_c/Z_{c2} \cdot J + 2R_\pi/Z_{\pi 2} \cdot H) \\
&\quad + (1/Z_{\pi 2} - 1/Z_{c2})[E(R_\pi - R_c) \sinh (\gamma_\pi + \gamma_c)\ell \\
&\qquad + (R_\pi A - R_c C) \cosh (\gamma_\pi + \gamma_c)\ell] \\
&\quad - (1/Z_{\pi 2} + 1/Z_{c2})[F(R_\pi - R_c) \sinh (\gamma_\pi - \gamma_c)\ell \\
&\qquad - (R_\pi B + R_c D) \cosh (\gamma_\pi - \gamma_c)\ell] \}/\Delta
\end{aligned}
\tag{2-13b}
$$

$$
\begin{aligned}
S_{14} &= S_{41} \\
&= 8R_d [R_\pi/Z_{c1} \cdot (1/Z_2 + Z_2/Z_{\pi 2}^2) \sinh \gamma_\pi \ell \\
&\quad + 2R_\pi/(Z_{c1} Z_{\pi 2}) \cosh \gamma_\pi \ell \\
&\quad - R_c/Z_{\pi 1} \cdot (1/Z_2 + Z_2/Z_{c2}^2) \sinh \gamma_c \ell \\
&\quad - 2R_c/(Z_{\pi 1} Z_{c2}) \cosh \gamma \ell]/\Delta
\end{aligned}
\tag{2-13c}
$$

$$
\begin{aligned}
S_{13} &= S_{31} = S_{24} = S_{42} \\
&= 8 [\frac{R_d}{Z_{\pi 1}} (\frac{1}{\sqrt{Z_1 Z_2}} + \frac{\sqrt{Z_1 Z_2}}{Z_{c1} Z_{c2}}) \sinh \gamma_c \ell \\
&\qquad - \frac{R_d}{Z_{c1}} (\frac{1}{\sqrt{Z_1 Z_2}} + \frac{\sqrt{Z_1 Z_2}}{Z_{\pi 1} Z_{\pi 2}}) \sinh \gamma_\pi \ell
\end{aligned}
$$

$$- (R_c/Z_{\pi 1} \cdot G - R_\pi/Z_{c1} \cdot I)(\cosh \gamma_c \ell - \cosh \gamma_\pi \ell) \,]/\Delta \qquad (2\text{-}13d)$$

$$\begin{aligned} S_{22} &= S_{33} \\ &= 2 \{ [R_d^2 \, E \, F + (R_\pi A - R_c C)(R_\pi B - R_c D)] \cosh (\gamma_\pi + \gamma_c)\ell \\ &\quad + R_d [F(R_\pi A - R_c C) + E(R_\pi B - R_c D)] \sinh (\gamma_\pi + \gamma_c)\ell \\ &\quad - [R_d^2 \, E \, F + (R_\pi A + R_c C)(R_\pi B + R_c D)] \cosh (\gamma_\pi - \gamma_c)\ell \\ &\quad + R_d [F(R_\pi A + R_c C) + E(R_\pi B + R_c D)] \sinh (\gamma_\pi - \gamma_c)\ell \\ &\quad + 4R_c R_\pi Z_1/(Z_{c1} Z_{\pi 1} Z_2) - Z_2/(Z_{c2} Z_{\pi 2} Z_1))] \} /\Delta \end{aligned} \qquad (2\text{-}13e)$$

$$\begin{aligned} S_{23} &= S_{32} \\ &= 8R_d \, [-R_c/Z_{c2} (1/Z_1 + Z_1/Z_{\pi 1}^2) \sinh \gamma_\pi \ell \\ &\quad - 2R_c/(Z_{\pi 1} Z_{c2}) \cosh \gamma_\pi \ell \\ &\quad + R_\pi/Z_{\pi 2} (1/Z_1 + Z_1/Z_{c1}^2) \sinh \gamma_c \ell \\ &\quad + 2R_\pi/(Z_{c1} Z_{\pi 2}) \cosh \gamma_c \ell \,]/\Delta \end{aligned} \qquad (2\text{-}13f)$$

where Z_1 and Z_2 are terminations on line 1 and line 2, respectively. The notation here follows Tripathi [21].

$$\begin{aligned} R_d &= R_\pi - R_c \\ \Delta &= 8R_c R_\pi \, H \, J + 2[R_d^2 \, E^2 + (R_\pi A - R_c C)^2 \cosh (\gamma_\pi + \gamma_c)\ell \\ &\quad + 4R_d \, E \, (R_\pi A - R_c C) \sinh (\gamma_\pi + \gamma_c)\ell \\ &\quad - 2[R_d^2 \, F^2 + (R_\pi B + R_c D)^2 \cosh (\gamma_\pi - \gamma_c)\ell \\ &\quad + 4R_d \, F \, (R_\pi B + R_c D) \sinh (\gamma_\pi - \gamma_c)\ell \end{aligned} \qquad (2\text{-}13g)$$

where,

$$A = \frac{1}{Z_{c1}} \sqrt{\frac{Z_1}{Z_2}} + \frac{1}{Z_{\pi 2}} \sqrt{\frac{Z_2}{Z_1}} \quad , \quad B = \frac{1}{Z_{c1}} \sqrt{\frac{Z_1}{Z_2}} - \frac{1}{Z_{\pi 2}} \sqrt{\frac{Z_2}{Z_1}}$$

$$C = \frac{1}{Z_{\pi 1}} \sqrt{\frac{Z_1}{Z_2}} + \frac{1}{Z_{c2}} \sqrt{\frac{Z_2}{Z_1}} \quad , \quad D = \frac{1}{Z_{\pi 1}} \sqrt{\frac{Z_1}{Z_2}} - \frac{1}{Z_{c2}} \sqrt{\frac{Z_2}{Z_1}}$$

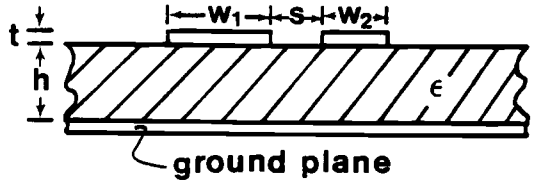

(a)

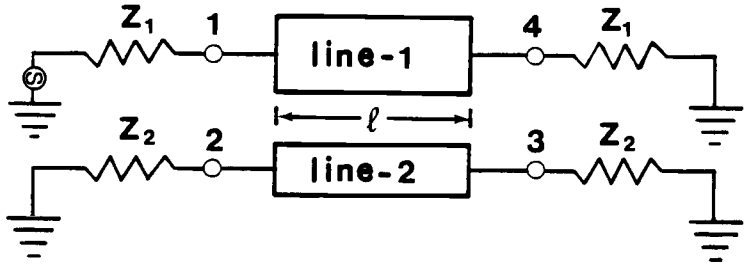

(b)

Figure 2-3. (a) Cross sectional view of the non-symmetrical two-line microstrip structure. (b) Schematic of the coupled line four-port.

$$E = \frac{1}{\sqrt{Z_1 Z_2}} + \frac{\sqrt{Z_1 Z_2}}{Z_{c1} Z_{\pi 2}} \quad , \quad F = \frac{1}{\sqrt{Z_1 Z_2}} - \frac{\sqrt{Z_1 Z_2}}{Z_{c1} Z_{\pi 2}}$$

$$G = \frac{1}{Z_{c1}} \sqrt{\frac{Z_1}{Z_2}} + \frac{1}{Z_{c2}} \sqrt{\frac{Z_2}{Z_1}} \quad , \quad H = \frac{1}{Z_{c1}} \sqrt{\frac{Z_1}{Z_2}} - \frac{1}{Z_{c2}} \sqrt{\frac{Z_2}{Z_1}}$$

$$I = \frac{1}{Z_{\pi 1}} \sqrt{\frac{Z_1}{Z_2}} + \frac{1}{Z_{\pi 2}} \sqrt{\frac{Z_2}{Z_1}} \quad , \quad J = \frac{1}{Z_{\pi 1}} \sqrt{\frac{Z_1}{Z_2}} - \frac{1}{Z_{\pi 2}} \sqrt{\frac{Z_2}{Z_1}}$$

The above expressions have been verified numerically by evaluating them for some typical cases from equations (2-13) and comparing them with the same parameters computed by the general expressions, equation (2-12). In addition, the above expressions reduce to the known expressions for symmetrical coupled line four-port in a homogeneous medium with $R_c = -R_\pi = 1$, $\beta_c = \beta_\pi = \beta$, $Z_{c1} = Z_{c2} = Z_{eo}$, and $Z_{\pi 1} = Z_{\pi 2} = Z_{oo}$.

(B) Scattering Parameters by Using Impedance Renormalization

Let [S] be the scattering matrix for a 2n-port terminated in Z_{io}, i = 1, 2, . . ., 2n, and [S'] be the scattering matrix of the same network terminated in Z_i, i = 1, 2, . . ., 2n. Then these scattering matrices are defined as

$$b] = [S]\ a] \tag{2-14a}$$

$$b'] = [S']\ a'] \tag{2-14b}$$

According to equation (2-10), for the termination Z_i

$$a'_i = \frac{1}{2} \left(\frac{V_i}{\sqrt{Z_i}} + \sqrt{Z_i}\ I_i \right) \tag{2-15a}$$

$$b'_i = \frac{1}{2} \left(\frac{V_i}{\sqrt{Z_i}} - \sqrt{Z_i}\ I_i \right) \tag{2-15b}$$

From equations (2-10)

$$V_i = \frac{1}{2}(a_i + b_i)\sqrt{Z_{io}} \qquad (2\text{-}16a)$$

$$I_i = \frac{1}{2}(a_i - b_i)\sqrt{Z_{io}} \qquad (2\text{-}16b)$$

Substituting the above equations (2-16) into equation (2-15) gives

$$2a_i' = Z_{si}a_i + Z_{di}b_i$$

$$2b_i' = Z_{di}a_i + Z_{si}b_i$$

where

$$Z_{si} \triangleq \sqrt{\frac{Z_{io}}{Z_i}} + \sqrt{\frac{Z_i}{Z_{io}}}$$

$$Z_{di} \triangleq \sqrt{\frac{Z_{io}}{Z_i}} - \sqrt{\frac{Z_i}{Z_{io}}}$$

a'] and b'] can then be expressed in terms of a] and b] as:

$$2a'] = [Z_s]\,a] + [Z_d][S]\,a]$$

$$2b'] = 2[S']\,a'] = [Z_d]\,a] + [Z_s][S]\,a]$$

The above relation together with the definition of scattering parameters leads to the following equation relating the desired scattering parameters [S'] in terms of the known parameters [S] and the arbitrary new terminations Z_i's.

$$[S'] = \{[Z_d] + [Z_s][S]\}\{[Z_s] + [Z_d][S]\}^{-1} \qquad (2\text{-}17)$$

where $[Z_s]$ and $[Z_d]$ are diagonal matrices with diagonal terms given by Z_{si} and Z_{di}.

Equation (2-17), expressing the scattering parameters of a 2n-port with arbitrary terminations, in terms of the same known parameters, can be used to study sensitivity of multi-port circuits to changes in various terminations and also to optimize the circuit performance in terms of the terminating impedances. The matrix $\{[Z_s] + [Z_d][S]\}^{-1}$ is readily determined if only two of the terminations are to be changed, as in the case for a uniformly coupled line four-port. For the general non-symmetrical coupled line four-port with non-mode converting terminations, only the ratio (Z_{2o}/Z_{1o}) is specified., which enables us to choose either $Z_1 = Z_{1o}$ or $Z_2 = Z_{2o}$. The new scattering parameters with arbitrary terminations $Z_1 = Z_4$ and $Z_2 = Z_3$ are found by normalizing with respect to changes in two terminations only. That is, for a four-port terminated in arbitrary impedances Z_1 and Z_4,

$$\{[Z_s]+[Z_d][S]\}^{-1} = \begin{bmatrix} Z_{s1}+Z_{d1}S_{11} & Z_{d1}S_{12} & Z_{d1}S_{13} & Z_{d1}S_{14} \\ 0 & 2 & 0 & 0 \\ 0 & 0 & 2 & 0 \\ Z_{d1}S_{14} & Z_{d1}S_{13} & Z_{d1}S_{12} & Z_{s1}+Z_{d1}S_{11} \end{bmatrix}^{-1} \qquad (2\text{-}18)$$

which is easily inverted. In the above equation, the characteristic terminations have been chosen to be $Z_{2o} = Z_2$ and then $Z_{1o} = Z_2/(-R_c R_\pi)$ [21]. Substituting in equation (2-17) leads to the scattering parameters for the four-port as given by:

$$S'_{11} = S'_{44} = [(Z_{d1} + Z_{s1}S_{11})(Z_{s1} + Z_{d1}S_{11}) - Z_{s1}Z_{d1}S_{14}^2]/\Delta \qquad (2\text{-}19a)$$

$$S'_{14} = S'_{41} = [Z_{s1}S_{14}(Z_{s1} + Z_{d1}S_{11}) - Z_{d1}S_{14}(Z_{d1} + Z_{s1}S_{11})]/\Delta \qquad (2\text{-}19b)$$

$$S'_{12} = S'_{21} = S'_{34} = S'_{43} = [2S_{12}(Z_{s1} + Z_{d1}S_{11}) - 2Z_{d1}S_{14}S_{13}]/\Delta \quad (2\text{-}19c)$$

$$S'_{13} = S'_{31} = S'_{24} = S'_{42} = [2S_{13}(Z_{s1} + Z_{d1}S_{11}) - 2Z_{d1}S_{1s}S_{14}]/\Delta \quad (2\text{-}19d)$$

$$S'_{22} = S'_{33} = S_{22} - [Z_{d1}(Z_{s1} + Z_{d1}S_{11})(S_{12}^2 + S_{13}^2) - 2Z_{d1}^2 S_{12}S_{13}S_{14}]/\Delta \quad (2\text{-}19e)$$

$$S'_{23} = S'_{32} = S_{23} - [2Z_{d1}(Z_{s1} + Z_{d1}S_{11})S_{12}S_{13} - Z_{d1}^2 S_{14}(S_{12}^2 + S_{13}^2)]/\Delta \quad (2\text{-}19f)$$

where, $\Delta = (Z_{s1} + Z_{d1}S_{11})^2 - Z_{d1}^2 S_{14}^2$.

Similarly, if the terminations on line 1 are fixed and those on line 2 are changed, a complimentary set of equations are given by

$$S'_{11} = S'_{44} = S_{11} - Z_{d2}[(Z_{s2} + Z_{d2}S_{22})(S_{12}^2 + S_{13}^2) - 2Z_{d2}S_{12}S_{13}S_{23}]/\Delta \quad (2\text{-}20a)$$

$$S'_{12} = S'_{21} = S'_{34} = S'_{43} = Z_{s2}S_{12}/2 - Z_{d2}[Z_{s2}^2(S_{12}S_{22} + S_{13}S_{23}) + Z_{d2}^2(S_{12}S_{22} - S_{13}S_{23}) + Z_{s2}Z_{d2}S_{12}(S_{22}^2 - S_{23}^2 + 1)]/(2\Delta) \quad (2\text{-}20b)$$

$$S'_{13} = S'_{31} = S'_{24} = S'_{42} = Z_{s2}S_{13}/2 - Z_{d2}[Z_{s2}^2(S_{12}S_{23} + S_{13}S_{22}) - Z_{d2}^2(S_{12}S_{23} - S_{13}S_{22}) + Z_{s2}Z_{d2}S_{13}(S_{22}^2 - S_{23}^2 + 1)]/(2\Delta) \quad (2\text{-}20c)$$

$$S'_{14} = S'_{41} = S_{14} - Z_{d2}[2S_{13}S_{12}(Z_{s2} + Z_{d2}S_{22}) - Z_{d2}S_{23}(S_{12}^2 + S_{13}^2)]/\Delta \quad (2\text{-}20d)$$

$$S'_{22} = S'_{33} = [(Z_{d2} + Z_{s2}S_{22})(Z_{s2} + Z_{d2}S_{22}) - Z_{s2}Z_{d2}S_{23}^2]/\Delta \quad (2\text{-}20e)$$

$$S'_{23} = S'_{32} = [Z_{s2}S_{23}(Z_{s2} + Z_{d2}S_{22}) - Z_{d2}S_{23}(Z_{d2} + Z_{s2}S_{22})]/\Delta \quad (2\text{-}20f)$$

where, $\Delta = (Z_{s2} + Z_{d2}S_{22})^2 - (Z_{d2}S_{23})^2$

The above equations for the elements of the matrix [S'] represent the scattering parameters of the four-port with arbitrary terminations and are expressed in terms of the known scattering parameters with characteristic non-mode converting terminations and

the new impedances. The elements of the known scattering parameters for two-line and symmetrical three-line four-port with non-mode converting terminations were derived by Tripathi [96] and are given in Appendix C.

2.4 CONCLUDING REMARKS

The procedure for finding the immittance of a general n-line coupled structure in an inhomogeneous medium has been presented in terms of the normal mode parameters of the n-line coupled system. The expressions are in a convenient form for both computational purposes and for deriving the explicit closed form expressions for the elements of the 2n-port immittance matrix. As an example, the closed form expressions for the elements of the admittance matrix of a symmetrical eight-port structure are given in Appendix A.

The scattering parameters of a general coupled line four-port with arbitrary terminations are derived directly from the normal mode parameters of two-line structure by using the definition of the scattering parameters. It is shown that these can also be derived in terms of the scattering parameters of the four-port with non-mode converting terminations and the new arbitrary terminations.

CHAPTER III. Sensitivity Analysis and Optimization of Four-Port (Directional Couplers)

3.1 INTRODUCTION

The effect of any changes in various parameters (strip width, spacing between strips, substrate dielectric constant, etc.) on the characteristics of single and coupled microstrip line structure has been analyzed by using the sensitivity approach [101, 102]. The equations for perturbation of scattering parameters, which are useful for 10% variation in the even- and odd-mode characteristic impedances as well as the phase velocities for symmetrical two-line couplers, were presented by Brenner [103].

In this chapter, the sensitivities of scattering parameters for two-line, interdigitated three-line and four-line couplers, with respect to changes in terminations, have been derived by using the impedance renormalization procedure prescribed in the previous chapter.

The study of directional couplers consisting of general, uniformly coupled non-symmetrical lines in an inhomogeneous medium has been confined to the case where the structure is terminated in a set of impedances that allows for the excitation of the individual normal modes of the system [96, 100]. Examples of such structures

include coupled microstrip lines, slot lines, comb lines, dielectric waveguides and various other uniformly coupled transmission systems. The scattering parameters of two-line four-port [100], three line interdigitated four-port [96] with such characteristic non-mode converting terminations are known. Sun [104] has also derived the solution for port voltages when the lines are terminated in impedances satisfying Cristal's [7] homogeneous (non-symmetrical TEM lines) conditions which is a special case of non-mode converting terminations. In this chapter it is shown that the performance of directional couplers consisting of such non-symmetrical lines with unequal normal mode phase velocities can be optimized in terms of the terminating impedances. A method to determine the optimum terminations with examples of non-symmetrical edge coupled microstrip coupler is presented.

3.2 SENSITIVITY ANALYSIS

The sensitivity of scattering parameters S_{ij} with respect to changes in a termination is defined as:

$$S_{ij}^{(i)} = \frac{1}{S_{ij}} \frac{\Delta S_{ij}}{\Delta Z_i} \Bigg|_{Z_{io} = \text{constant}} \qquad (3\text{-}1)$$

where Z_{io} is the termination for the known scattering parameter S_{ij} and Z_i is the changed, new termination for S'_{ij}, a scattering parameter with arbitrary termination as given by equations (2-19) and (2-20). $\Delta Z_i = Z_{io} - Z_i$ and $\Delta S_{ij} = S'_{ij} - S_{ij}$. Hence, the sensitivity for symmetrical and non-symmetrical coupled four-port

structures is represented in terms of the known scattering parameters with respect to changes in line terminations. The sensitivity equations can be derived from equations (2-19) and (2-20) and they are defined as follows.

If the terminating impedance of line 2, Z_{20}, is fixed, the sensitivity parameters of the four-port with respect to changes in Z_1 are found to be:

$$S_{11}^{(1)} = S_{44}^{(1)} = \frac{1}{S_{11}} \frac{\Delta S_{11}}{\Delta Z_1} = \frac{(k_1 + S_{11})(1/S_{11} - S_{11}) - \frac{S_{14}^2}{S_{11}} (k_1 - S_{11})}{D_1 \Delta Z_1} \tag{3-2a}$$

$$S_{12}^{(1)} = S_{21}^{(1)} = S_{34}^{(1)} = S_{43}^{(1)} = \frac{1}{S_{12}} \frac{\Delta S_{12}}{\Delta Z_1}$$

$$= \frac{(k_1 + S_{11})[(1 + \frac{2}{Z_{d1}} - S_{11})/(k_1 + 1) - 1] - S_{14}(\frac{2 S_{13}}{S_{12} Z_{d1}} - S_{14})}{D_1 \Delta Z_1} \tag{3-2b}$$

$$S_{13}^{(1)} = S_{31}^{(1)} = S_{24}^{(1)} = S_{42}^{(1)} = \frac{1}{S_{13}} \frac{\Delta S_{13}}{\Delta Z_1}$$

$$= \frac{(k_1 + S_{11})[(1 + \frac{2}{Z_{d1}} - S_{11})/(k_1 + 1) - 1] - S_{14}(\frac{2 S_{12}}{S_{13} Z_{d1}} - S_{14})}{D_1 \Delta Z_1} \tag{3-2c}$$

$$S_{14}^{(1)} = S_{41}^{(1)} = \frac{1}{S_{14}} \frac{\Delta S_{14}}{\Delta Z_1}$$

$$= -\frac{(1 - S_{11} - S_{14})(1 - S_{11} + S_{14}) + 2 S_{11} (k_1 + 1)}{D_1 \Delta Z_1} \tag{3-2d}$$

$$S_{22}^{(1)} = S_{33}^{(1)} = \frac{1}{S_{22}} \frac{\Delta S_{22}}{\Delta Z_1}$$

$$= - \frac{(k_1 + S_{11})\,(S_{12}^2 + S_{13}^2)/S_{22} - 2\,S_{12}\,S_{13}\,S_{14}/S_{22}}{D_1\,\Delta Z_1} \quad (3\text{-}2e)$$

$$S_{23}^{(1)} = S_{32}^{(1)} = \frac{1}{S_{23}} \frac{\Delta S_{23}}{\Delta Z_1}$$

$$= - \frac{2\,(k_1 + S_{11})\,S_{12}\,S_{13}/S_{23} - S_{14}\,(S_{12}^2 + S_{13}^2)/S_{23}}{D_1\,\Delta Z_1} \quad (3\text{-}2f)$$

Similarly, if the terminating impedance of line 1, Z_{1o}, is fixed, the sensitivity parameters of the four-port with respect to changes in Z_2 are found to be:

$$S_{11}^{(2)} = S_{44}^{(2)} = \frac{1}{S_{11}} \frac{\Delta S_{11}}{\Delta Z_2}$$

$$= - \frac{(k_2 + S_{22})(S_{12}^2 + S_{13}^2)/S_{11} - 2S_{12}\,S_{13}\,S_{23}/S_{11}}{D_2\,\Delta Z_2} \quad (3\text{-}2g)$$

$$S_{12}^{(2)} = S_{21}^{(2)} = S_{34}^{(2)} = S_{43}^{(2)} = \frac{1}{S_{12}} \frac{\Delta S_{12}}{\Delta Z_2}$$

$$= \frac{Z_{d2}}{2\,\Delta Z_2} \left[\left(k_2 - \frac{2}{Z_{d2}}\right) - \frac{(S_{22}+S_{13}S_{23}/S_{12})\,k_2^2 + (S_{22}-S_{23}+1)k_2 + (S_{22}-S_{13}S_{23}/S_{12})}{D_2} \right] \quad (3\text{-}2h)$$

$$S_{13}^{(2)} = S_{31}^{(2)} = S_{24}^{(2)} = S_{42}^{(2)} = \frac{1}{S_{13}} \frac{\Delta S_{13}}{\Delta Z_2}$$

$$= \frac{Z_{d2}}{2\,\Delta Z_2}\left[\left(k_2 - \frac{2}{Z_{d2}}\right) - \frac{(S_{22}+S_{12}S_{23}/S_{13})k_2^2+(S_{22}^2-S_{23}^2+1)k_2+(S_{22}-S_{12}S_{23}/S_{13})}{D_2}\right] \tag{3-2i}$$

$$S_{14}^{(2)} = S_{41}^{(2)} = \frac{1}{S_{14}}\frac{\Delta S_{14}}{\Delta Z_2}$$

$$= \frac{S_{23}\,(S_{12}^2 + S_{13}^2)/S_{14} - 2S_{12}\,S_{13}\,(k_2 + S_{22})/S_{14}}{D_2\,\Delta Z_2} \tag{3-2j}$$

$$S_{22}^{(2)} = S_{33}^{(2)} = \frac{1}{S_{22}}\frac{\Delta S_{22}}{\Delta Z_2}$$

$$= \frac{(1 + S_{23}^2) - S_{22}(k_2 + S_{22}) + k_2(1 - S_{23}^2)/S_{22}}{D_2\,\Delta Z_2} \tag{3-2k}$$

$$S_{23}^{(2)} = S_{32}^{(2)} = \frac{1}{S_{23}}\frac{\Delta S_{23}}{\Delta Z_2}$$

$$= -\frac{1 + (2k_2 + S_{22})S_{22} - S_{23}^2}{D_2\,\Delta Z_2} \tag{3-2l}$$

where

$$Z_1 = Z_{1o} - \Delta Z_1$$

$$Z_2 = Z_{2o} - \Delta Z_2$$

$k_1 = Z_{s1}/Z_{d1}$ and $k_2 = Z_{s2}/Z_{d2}$, k_i $(i = 1,2)$ has a negative sign for $Z_i > Z_{io}$ and a positive sign for $Z_i < Z_{io}$.

$$D_1 = (k_2 + S_{11})^2 - S_{14}^2$$

$$D_2 = (k_2 + S_{22})^2 - S_{23}^2$$

3.3 OPTIMIZATION OF COUPLER

The scattering parameters for the general case of a non-symmetrical coupler terminated in non-mode converting impedances were derived by Gunton and Paige [100]. Examination of these parameters reveals that, for such structures with unequal normal mode phase velocities, such as non-symmetrical coupled microstrip lines, ideal couplers with $S_{ii} = 0$ for all i's and $S_{ij} = 0$ where parts i and j are to be isolated, can not be realized. However, examination of the scattering parameters with arbitrary terminations, as given by equations (2-19) and (2-20), reveals that both matching and isolation can in general be improved in terms of terminating impedances. For a given coupled system, the above formulation can be used to solve for the terminations Z_1 and Z_2 such that both matching and isolation conditions are optimized. The solution, Z_1 and Z_2, is generally complex if we demand perfect matching ($S_{ii} = 0$, all i's) at a given frequency which can be implemented with open- or short-circuited stubs at all the ports of the coupler. Choice of real terminations can only lead to the maximation of isolation or directivity of the coupler. It should be noted here that from the unitary property of the scattering matrix we have a choice of either minimizing the reflection coefficients at all the ports or minimizing the reflection coefficients at the input port and the transmission coefficient between the input and isolated port. This condition can be derived by the unitary property of the scattering matrix for a lossless four-port coupler in a homogeneous medium as follows:

In the case of a lossless, reciprocal, non-symmetrical, and contra-directional four-port (Fig. 2-3) with $S_{11} = S_{33} = S_{13} = 0$, the definition of a unitary condition, $[U] - [S^*]^T[S] = [0]$, leads to

$$|S_{12}|^2 + |S_{14}|^2 = 1$$

$$|S_{23}|^2 + |S_{34}|^2 = 1$$

$$|S_{12}|^2 + |S_{22}|^2 + |S_{23}|^2 + |S_{24}|^2 = 1$$

$$|S_{14}|^2 + |S_{24}|^2 + |S_{34}|^2 + |S_{44}|^2 = 1$$

Add the last two equations and substitute the other two equations to obtain

$$|S_{22}|^2 + 2\,|S_{24}|^2 + |S_{44}|^2 = 0$$

Since these quantities are all non-negative, the following results must be given by

$$|S_{22}|^2 = |S_{24}|^2 = |S_{44}|^2 = 0 \qquad (3\text{-}3)$$

and the resultant scattering matrix must have the following form:

$$[S] = \begin{bmatrix} 0 & S_{12} & 0 & S_{14} \\ S_{12} & 0 & S_{23} & 0 \\ 0 & S_{23} & 0 & S_{24} \\ S_{14} & 0 & S_{34} & 0 \end{bmatrix}$$

Hence, any lossless coupler, two of whose ports are matched and isolated, must be matched and isolated at the other two ports. For a general four-port coupler, $S_{11} = S_{44}$ and $S_{22} = S_{33}$.

Evaluation of Z_1 and Z_2:

One method to determine the terminations Z_1 and Z_2 required for optimum performance is to use the impedance renormalization procedure as given by equations (2-19) and (2-20) in an iterative manner. To illustrate this, let us consider a general, non-symmetrical, contra-directional coupler such as coupled microstrip lines (Fig. 2-3(b)). The coupled system can be characterized in terms of its characteristic parameters for the two normal modes c and π of the system [21], which are derived from the self- and mutual-equivalent series inductances and shunt-capacitances per unit length of the lines. These parameters are the two phase constants β_c and β_π, the characteristic impedance of the two lines for the two modes (Z_{1c}, Z_{2c}, $Z_{1\pi}$, $Z_{2\pi}$), and the elements of the voltage eigenvector matrix R_c and R_π representing the ratio of voltages on the two lines for the two normal modes of the system. The scattering parameters of the four-port, when terminated in non-mode converting impedances as given by Cristal's homogeneous medium values [7], i.e., $Z_{1o} = \sqrt{Z_{1c}Z_{1\pi}}$ and $Z_{2o} = \sqrt{Z_{2c}Z_{2\pi}}$ $= - Z_{1o}R_cR_\pi$, can be evaluated from the results obtained by Gunton and Pagie [100]. This non-mode converting set of terminations is a suitable starting point since it results in an ideal coupler if the two normal mode phase velocities are equal [7,100].

However, for the general case of the coupled system with $\beta_c \neq \beta_\pi$, this set of terminations gives good isolation but a mismatch of all the ports, depending upon the difference between the normal mode velocities. In order to match the structure and keep the isolation

maximum, new terminations, Z_1 and Z_2, can be found by utilizing equations (2-19) and (2-20) in an iterative manner at a given frequency, e.g., the center frequency of the coupler represented by $\theta = (\beta_c + \beta_\pi)\,\ell/2 = \frac{\pi}{2}$. That is, S'_{11} is minimized by keeping Z_2 fixed and evaluating Z_1 for minimum S'_{11}. Then Z_1 is fixed to this new value and a new Z_2 is found such that the new, renormalized S'_{22} ($S'_{33} = S'_{22}$) is a minimum, which results in minimizing S'_{13}. Then the process is repeated until either the solutions for Z_1 and Z_2 converges to a final value or the reflection coefficient and isolation or directivity meet a required specification. Again, it should be noted that perfect matching and isolation at the center frequency can be obtained only by choosing complex solutions for Z_1 and Z_2.

Example: The quasi-TEM parameters of a two-line non-symmetrical coupled microstrip structure can be computed by using a number of techniques, including the Green's function integral equation method [105]. A nominal 6 dB non-symmetrical coupler was designed with $\varepsilon_r = 10$ by computing the normal mode parameters as a function of the microstrip widths and the spacing between the strips. The normal mode parameters for the physical dimensions, $w_1/h = 0.4$, $w_2/h = 0.11$, and $s/h = 0.08$, are found to be;

Mode c: $\varepsilon_{eff} = 6.4468$, $R_c = .993$, $Z_{c1} = 92.45\ \Omega$, $Z_{c2} = 190.86\ \Omega$

Mode ¶: $\varepsilon_{eff} = 5.5152$, $R_\pi = -2.0778$, $Z_{¶1} = 26.94\ \Omega$, $Z_{¶2} = 55.61\ \Omega$

The scattering parameters, representing matching and isolation of the coupler when terminated in characteristic non-mode converting values satisfying Cristal's homogeneous conditions [7] $Z_{1o} = \sqrt{Z_{c1} Z_{¶1}} = 49.9\ \Omega$

and $Z_{2o} = \sqrt{Z_{c2} Z_{\pi 2}}$ = 103.2 Ω at the center frequency represented by $\theta = (\beta_c + \beta_\pi)\ell/2 = \pi/2$, are found to be:

$\|S_{11}\|$	$\|S_{12}\|$	$\|S_{13}\|$	$\|S_{14}\|$	$\|S_{21}\|$	$\|S_{22}\|$	$\|S_{23}\|$	$\|S_{24}\|$
0.1955	0.5119	0.0402	0.8355	0.5119	0.1967	0.8352	0.0402

To determine the optimum terminations, the following formulations for $S'_{11} = 0$ and $S'_{22} = 0$ can be derived by equations (2-19) and (2-20).

(1) For $S'_{11} = 0$

$$Z_1 = Z_{1o}\sqrt{\frac{k/2 - 1}{k/2 + 1}} \qquad (3\text{-}4a)$$

where

$$k = \frac{S_{14}^2 - S_{11}^2 - 1}{S_{11}}$$

(2) For $S'_{22} = 0$

$$Z_2 = Z_{2o}\sqrt{\frac{k/2 - 1}{k/2 + 1}} \qquad (3\text{-}4b)$$

where

$$k = \frac{S_{23}^2 - S_{22}^2 - 1}{S_{22}}$$

Equation (3-4a) when terminated in Z_{1o} = 49.9 Ω and Z_{2o} = 103.2 Ω, then, gives

$$Z_1 = 62.9\ \Omega$$

The new scattering parameters with $Z_1 = 69.9\ \Omega$ and $Z_{2_o} = 103.2\ \Omega$ are given by

$\|S_{11}\|$	$\|S_{12}\|$	$\|S_{13}\|$	$\|S_{14}\|$	$\|S_{21}\|$	$\|S_{22}\|$	$\|S_{23}\|$	$\|S_{24}\|$
0.0256	0.5152	0.0659	0.8541	0.5152	0.1663	0.8382	0.0659

Next, equation (3-4(b)), when terminated in $Z_1 = 62.9\ \Omega$ and $Z_{20} = 103.2\ \Omega$, gives

$$Z_2 = 85.17\ \Omega.$$

The new scattering parameters, with $Z_1 = 62.9\ \Omega$ and $Z_2 = 85.17\ \Omega$, are found to be;

$\|S_{11}\|$	$\|S_{12}\|$	$\|S_{13}\|$	$\|S_{14}\|$	$\|S_{21}\|$	$\|S_{22}\|$	$\|S_{23}\|$	$\|S_{24}\|$
0.0278	0.5220	0.0429	0.8514	0.5220	0.0263	0.8515	0.0427

The coupling, reflection coefficient and directivity are also plotted as a function of normalized frequency in Fig. 3-1 for both cases and, as seen, the coupler matching is considerably improved with minimum change in directivity.

The procedure described here can be used to evaluate the optimum terminations for a non-symmetrical interdigitated three-line four-port coupler. A method to determine the optimum terminations is presented in Chapter IV.

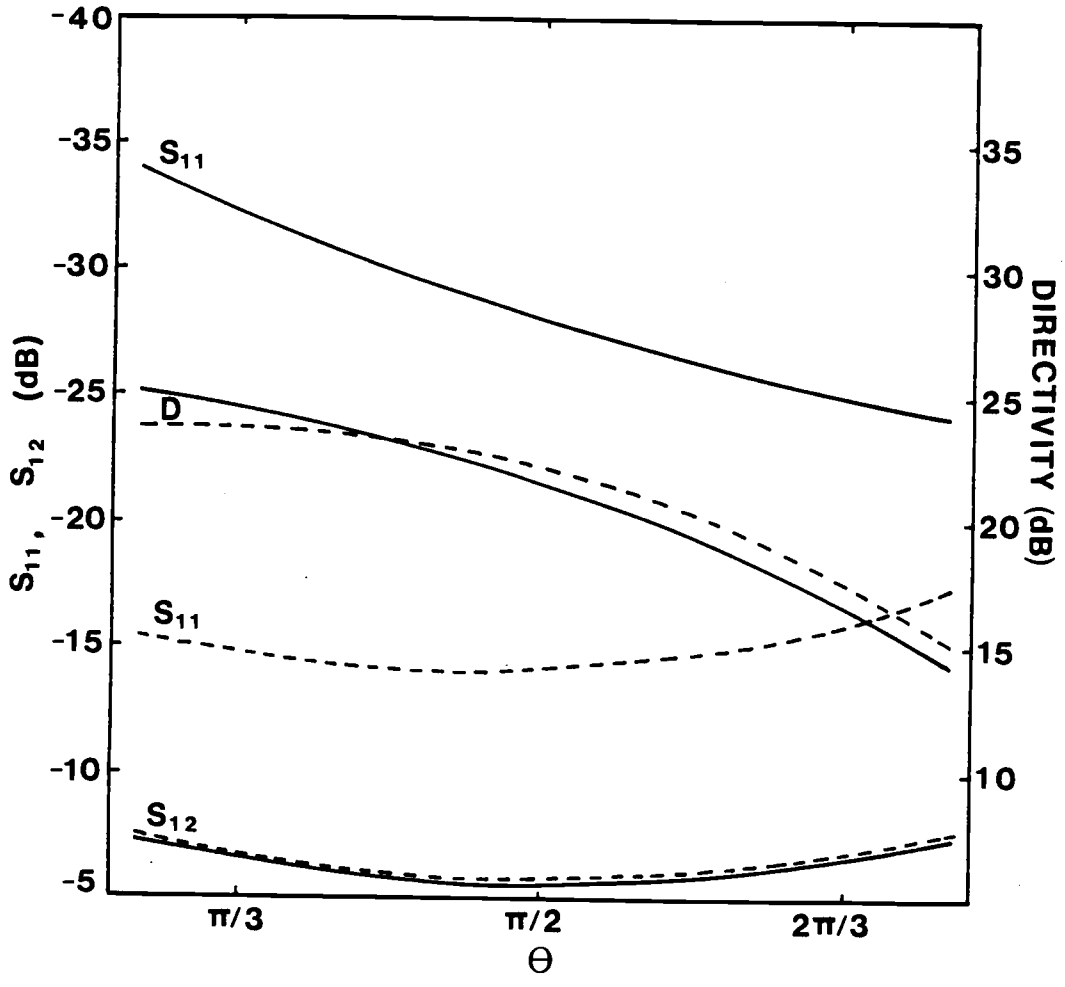

Figure 3-1. Coupling $|S_{12}|$, reflection coefficient $|S_{11}|$ and directivity D vs normalized frequency Θ with $\varepsilon_r = 10$.
------ Characteristic terminations, $Z_{10} = 49.9$ ohms and $Z_{20} = 103.2$ ohms
——— Optimized terminations, $Z_1 = 62.9$ ohms and $Z_2 = 85.17$ ohms

3.4 CONCLUDING REMARKS

The sensitivities of scattering parameters for a general uniformly coupled four-port structure to changes in terminations are presented in terms of the known scattering parameters with the given terminations. These are derived from the expressions for the scattering parameters with arbitrary terminations described in Section 2.3 of Chapter II.

The procedure to determine the terminations required for optimum coupler performance by using the expressions for the scattering parameters of the general, uniformly coupled non-symmetrical lines with arbitrary terminations has been presented. The formulation is quite general and can be applied to various coupled guided wave systems, including systems with more than two coupled lines.

CHAPTER IV. Design of Three-Line Couplers

4.1 INTRODUCTION

Multiple coupled line structures, including the three-line structures, have been studied for various applications as directional couplers and other circuit elements [83-96, 106-110]. The interdigitated directional coupler has been the most effective means for achieving tight coupling in microstrip circuits. The main advantages are its small size and the relatively large gaps between conductors as compared to a conventional two-line coupler case. The interdigitated 3 dB four-line microstrip coupler was introduced by Lange [92], who did not provide any design information in terms of the coupled line parameters of a line pair or the parameters derived from a rigorous electromagnetic field analysis of the four-line structure. Later, the unfolded form of a 3 dB Lange coupler was reported by Wangh and LaCombe [93]. The general design equations for such couplers with an arbitrary even number of coupled lines have been derived by Ou [87]. The equations are written in terms of even- and odd-mode admittances of only two adjacent coupled lines, which are assumed to be identical to any other pair of lines in the structure.

Various design procedures for the Lange coupler have been described by Paolino [91] Rizzoli et al. [108], and others

[89,90,107,111,112]. Paolino's procdure is based on the even- and odd-mode excitations, and requires a numerical solution for the self-and mutual-capacitance per unit length of a system of n equal conductors. Rizzoli's procedure is based on the assumption that capacitances between nonadjacent lines can be neglected for the coupler analysis. He has developed design charts to find the geometry of the structure for a prescribed coupling and bounds on directivity and VSWR. The directional coupler with a spiral-shaped construction has also been presented by Shibata et al.[106]. This coupler is formed by coiling two edge-coupled lines, which leads to the multiple lines structure with the assumption that capacitances between nonadjacent lines can be neglected.

In this chapter, analysis and design procedures for the symmetrical and non-symmetrical interdigitated four-port structures consisting of symmetrical three lines shown in Fig. 4-1 is presented. The configuration is simple and a lesser number of bond wires are required as compared to the four-line couplers. The 3 dB interdigitated three-line coupler on alumina substrate (ε_r = 10) was fabricated by Tulaja et al [94]. This work was mostly experimental and did not provide the design procedure for the three-line case. The properties of the three-line structures have been studied by Yamamoto et al.[113] for TEM case and by Pavlidis et al.[114], and Tripathi [95] for the general inhomogeneous structure. The general solutions for normal mode propagation constants, eigenvectors, and impedances, etc., are expressed in matrix form for the general case

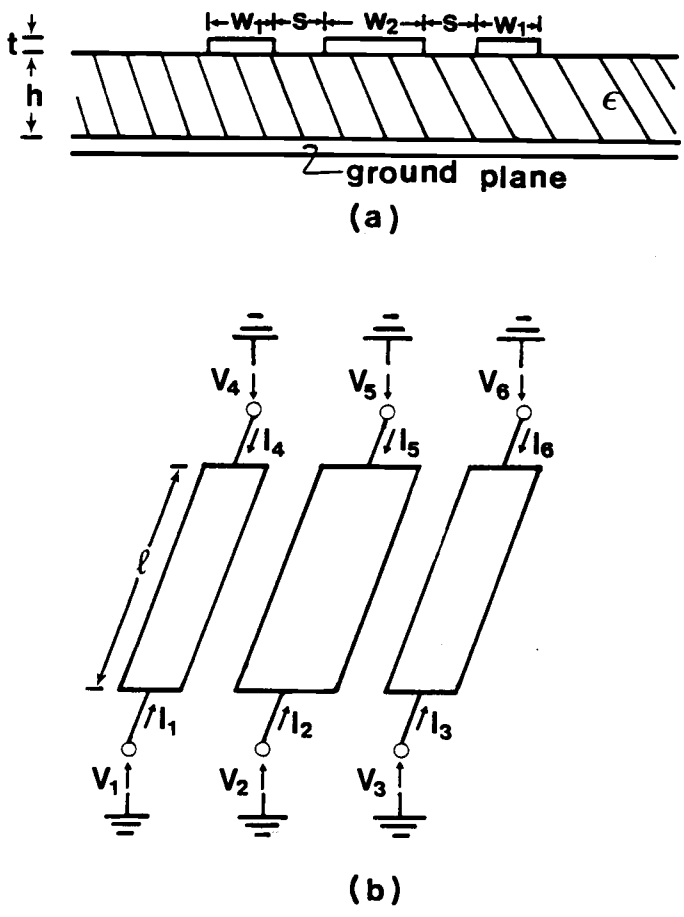

Figure 4-1. (a) Cross sectional view of the symmetrical three-line microstrip structure. (b) Schematic of the coupled line six-port.

of the multiconductor system by Marx [15]. However, the explicit expressions [95] for six-port circuit parameters for the symmetrical three-line case, in terms of the self- and mutual-line impedances and admittances per unit length, are desirable and convenient to study and formulate design procedures for couplers and other circuit elements.

In this chapter, the exact analysis procedures for both the symmetrical and non-symmetrical interdigitated four-port coupled structures consisting of symmetrical three-lines in an inhomogeneous medium shown in Fig. 4-2(b) are presented. The table and charts for designing both cases have been provided.

The procedure to determine the terminations required for optimum coupler performance of the non-symmetrical coupler are also presented in terms of the scattering parameters with characteristic terminations by using impedance renormalization procedures.

4.2 ANALYSIS AND DESIGN

(A) Analysis: The expressions for scattering parameters prescribed in Chapter II are used to analyze the performance of symmetrical and non-symmetrical interdigitated three-line four-port couplers in this section. Since the closed form expressions for the scattering parameters of the non-symmetrical interdigitated three-line four-port coupler with arbitrary terminations are very complicated, it is convenient to derive these parameters in terms of the elements of the equivalent admittance matrix. For this

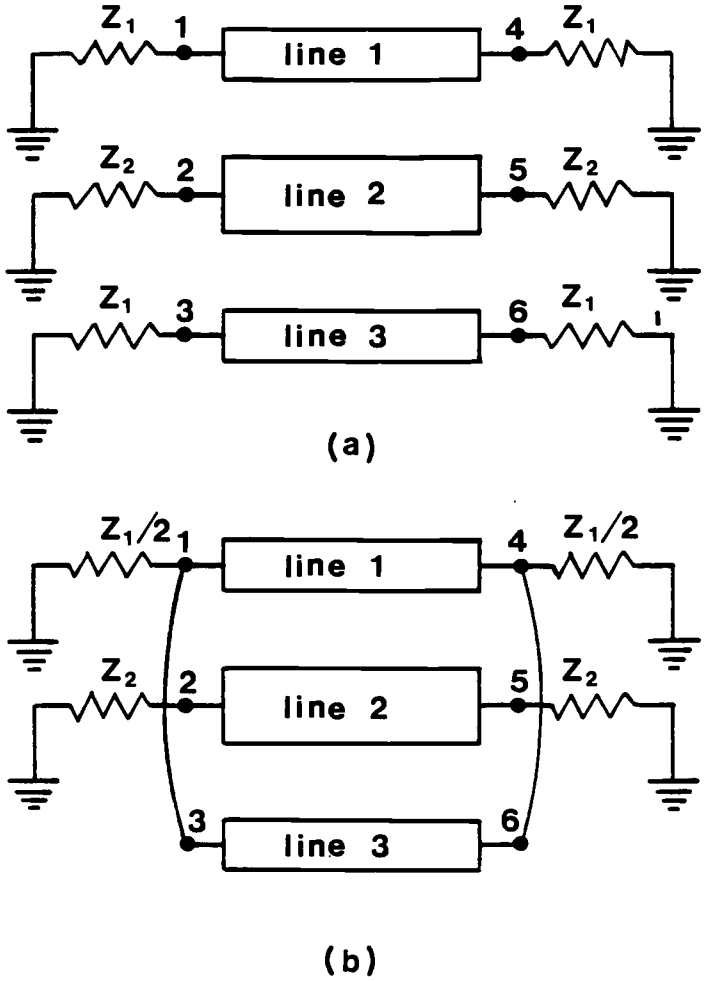

Figure 4-2. Schematic of characteristically terminated coupled three-line structure. (a) Six-port. (b) Interdigitated four-port.

non-symmetrical case, these are numerically computed by utilizing the general expressions given in section 2.3, and are given by

$$[S] = \{[U] - [Y_n]\}\ \{[U] + [Y_n]\}^{-1} \qquad (2\text{-}12)$$

where

$$[Y_n] =$$

$$\begin{bmatrix} \sqrt{Z_1} & 0 & 0 & 0 \\ 0 & \sqrt{Z_2} & 0 & 0 \\ 0 & 0 & \sqrt{Z_2} & 0 \\ 0 & 0 & 0 & \sqrt{Z_1} \end{bmatrix} \begin{bmatrix} Y_{11} & Y_{12} & Y_{13} & Y_{14} \\ Y_{12} & Y_{22} & Y_{23} & Y_{13} \\ Y_{13} & Y_{23} & Y_{22} & Y_{12} \\ Y_{14} & Y_{13} & Y_{12} & Y_{11} \end{bmatrix} \begin{bmatrix} \sqrt{Z_1} & 0 & 0 & 0 \\ 0 & \sqrt{Z_2} & 0 & 0 \\ 0 & 0 & \sqrt{Z_2} & 0 \\ 0 & 0 & 0 & \sqrt{Z_1} \end{bmatrix}$$

The admittance matrix of an interdigitated three-line four-port, shown in Fig. 4-2(b), can be found from the following boundary conditions:

$$I_a = I_1 + I_3,\quad I_c = I_4 + I_6,\quad V_a = V_1 = V_3,\quad I_1 = I_3,$$

$$\text{and } I_4 = I_6$$

The equivalent admittance matrix for four-port is, then, given by

$$[Y] = \begin{bmatrix} Y_{11} & Y_{12} & Y_{13} & Y_{14} \\ Y_{12} & Y_{22} & Y_{22} & Y_{13} \\ Y_{13} & Y_{23} & Y_{22} & Y_{12} \\ Y_{14} & Y_{13} & Y_{12} & Y_{11} \end{bmatrix}$$

$$= \begin{bmatrix} 2(y_{11} + y_{13}) & 2y_{12} & 2y_{15} & 2(y_{14} + y_{16}) \\ 2y_{12} & y_{22} & y_{25} & 2y_{15} \\ 2y_{15} & y_{25} & y_{22} & 2y_{12} \\ 2(y_{14} + y_{16}) & 2y_{15} & 2y_{12} & 2(y_{11} + y_{13}) \end{bmatrix}$$

where y_{ij} is a component of the coupled line six-port admittance matrix[95].

The explicit expressions for scattering parameters given by equation (C-3) in Appendix C are very convenient in the analysis of the coupler performance of a general symmetrical and non-symmetrical two-line or interdigitated three-line four-port couplers.

For both cases of three-line four-port, the scattering parameters can be expressed by equation(C-3),in which Z_{1o}/Z_{2o} has been taken as $-2/R_{vb}R_{vc}$ where $R_c = R_{vb}$ and $R_\pi = R_{vc}$. The examination of scattering parameters reveals that, while for the symmetrical interdigitated three-line four-port when terminated in $Z_1 = Z_{1o}/2 = \sqrt{Z_{b1}Z_{c1}}/2$ and $Z_{2o} = \sqrt{Z_{b2}Z_{c2}} = Z_1$ [96] the coupler is matched and the isolation is maximum at the center frequency given by $(\beta_a + \beta_b + \beta_c)\ell/3 = \frac{\pi}{2}$, for the non-symmetrical case with terminations given by Cristal's homogeneous medium values [7], i.e., $Z_1 = Z_{1o}/2 = \sqrt{Z_{b1}\ Z_{c1}}/2$ and $Z_{2o} = \sqrt{Z_{b2}Z_{c2}}$, the isolation is maximum at the center frequency but the coupler is not matched. In order to match the structure and keep the isolation maximum, the terminations Z_1 and Z_2 required for optimum performance of the coupler can be found by utilizing the impedance normalization procedure described in Section 3.3.

(B) Design: The normalized physical dimensions, w_1/h, w_2/h and s/h of a symmetrical three-line microstrip structure in an inhomogeneous medium are shown in Fig. 4-1(a). These dimensions, such that both symmetrical and non-symmetrical interdigitated four-port couplers shown in Fig. 4-2(b) have the desired coupling, i.e., 3 dB, 6 dB and

10 dB, were found by trial and error methods as follows: The quasi-TEM mode parameters for given relative dielectric constants, $\varepsilon_r = 10$ and $\varepsilon_r = 2.55$ representing alumina and polystyrene, and arbitrarily chosen physical dimensions of the structure was first determined using the technique given by Lee[67]. These parameters were then substituted into the equivalent admittance parameters for both the structures. The general expressions for scattering parameters, given by equations (2-12) in which terminations of $Z_1 = Z_2 = 50\ \Omega$ have been used, are derived in terms of the previous admittance parameters. These expressions were then used to find the coupling. The above procedure has been repeated until one can find the desired coupling. The results obtained are given in Table 4-1.

The length of the coupler is determined by the center frequency. The correct values of the coupling, reflection coefficient, directivity, isolation and bandwidth for a symmetrical interdigitated four-port when terminated in non-mode converting impedances as given by Cristal's homogeneous medium values [7], i.e., $\sqrt{Z_{b1}Z_{c1}}/2 = \sqrt{Z_{b2}Z_{c2}} = 50\ \Omega$, can be evaluated by utilizing the explicit expressions for scattering parameters given by equation(C-3). This is also plotted as a function of normalized frequency given by $\theta = \omega\sqrt{\mu_o\varepsilon_o}\,(\sqrt{\varepsilon_{ra}} + \sqrt{\varepsilon_{rb}} + \sqrt{\varepsilon_{rc}})\cdot \ell/3$ in Figure 4-3, 4, 5, 6 and 7.

The non-mode converting terminations given by $Z_{1o} = \sqrt{Z_{b1}Z_{c1}}/2$ and $Z_{2o} = \sqrt{Z_{b2}Z_{c2}}$ are plotted as a function of the relative width of the middle strip (w_2/h) for 3 dB, 6 dB and 10 dB coupling, with the relative width of the outer strips (w_1/h) and the relative spacing

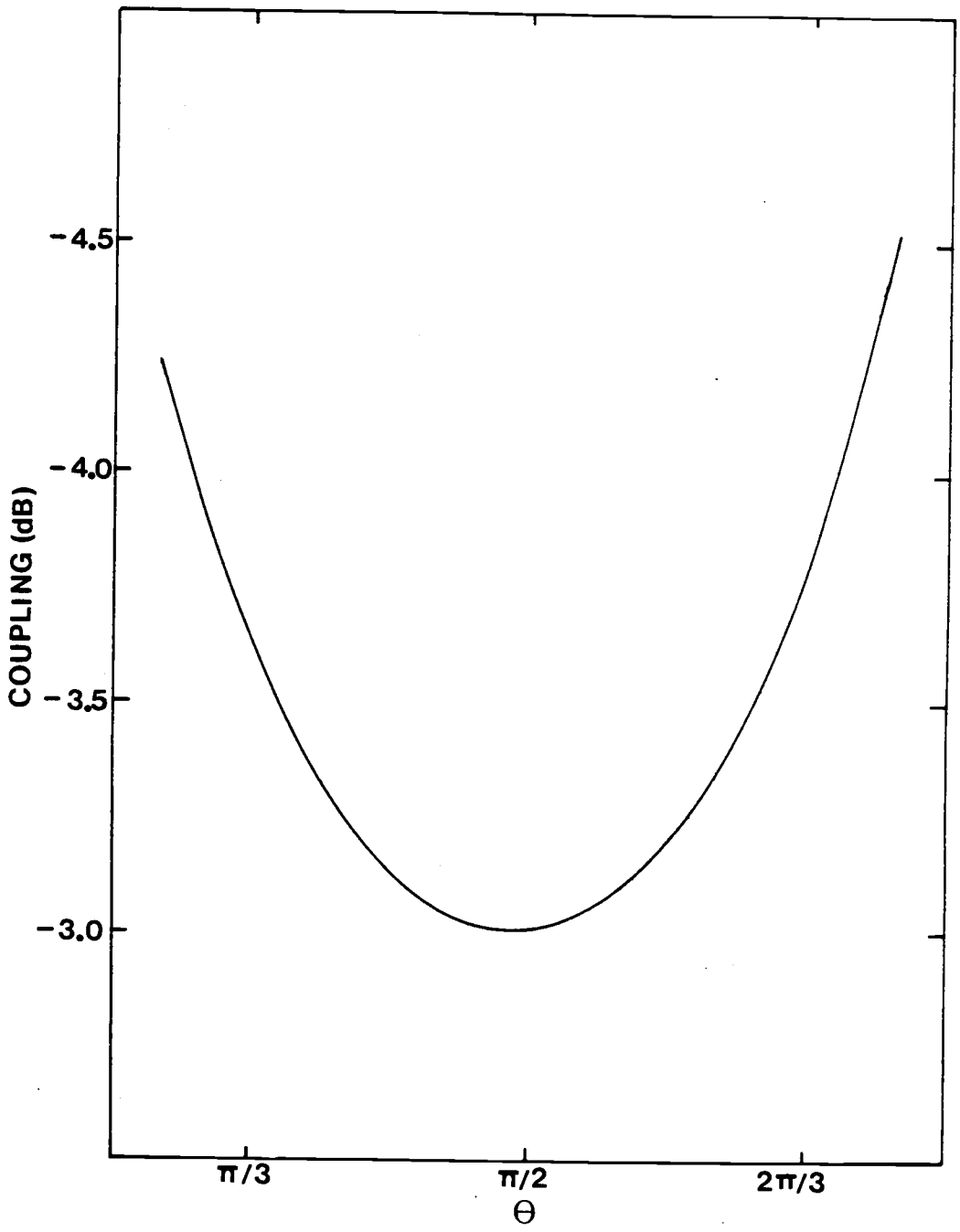

Figure 4-3(a). Coupling $|S_{12}|$ vs normalized frequency Θ for nominal 3-dB coupling with $\varepsilon_r = 10$ (where $w_1/h = w_2/4h = 2s/h = 0.078$), when terminated in $Z_1 = Z_2 = 50$ ohms.

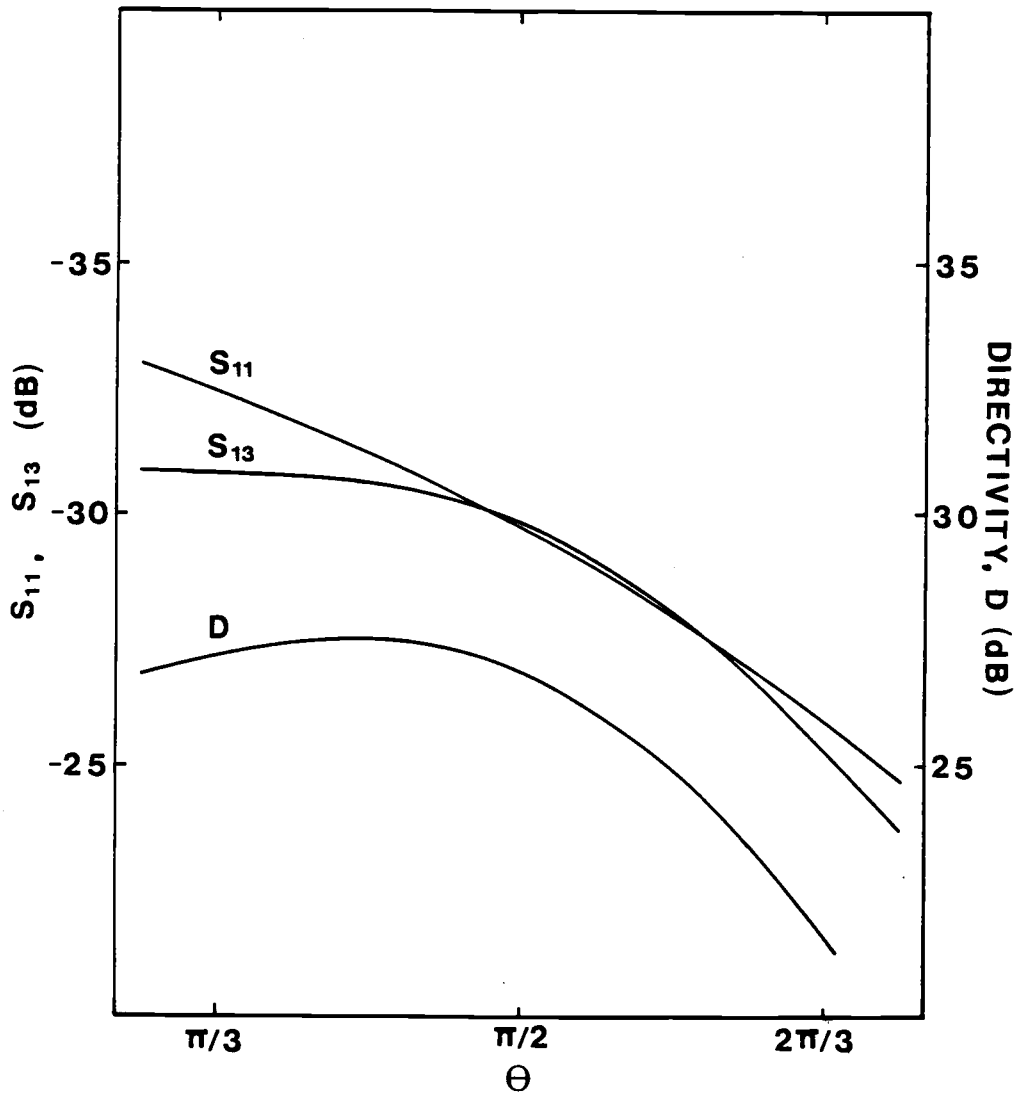

Figure 4-3(b). Reflection coefficient $|S_{11}|$, isolation $|S_{13}|$ and directivity D vs normalized frequency Θ for nominal 3-dB coupling with $\varepsilon_r = 10$ (where $w_1/h = w_2/4h = 2s/h = 0.078$), when terminated in $Z_1 = Z_2 = 50$ ohms.

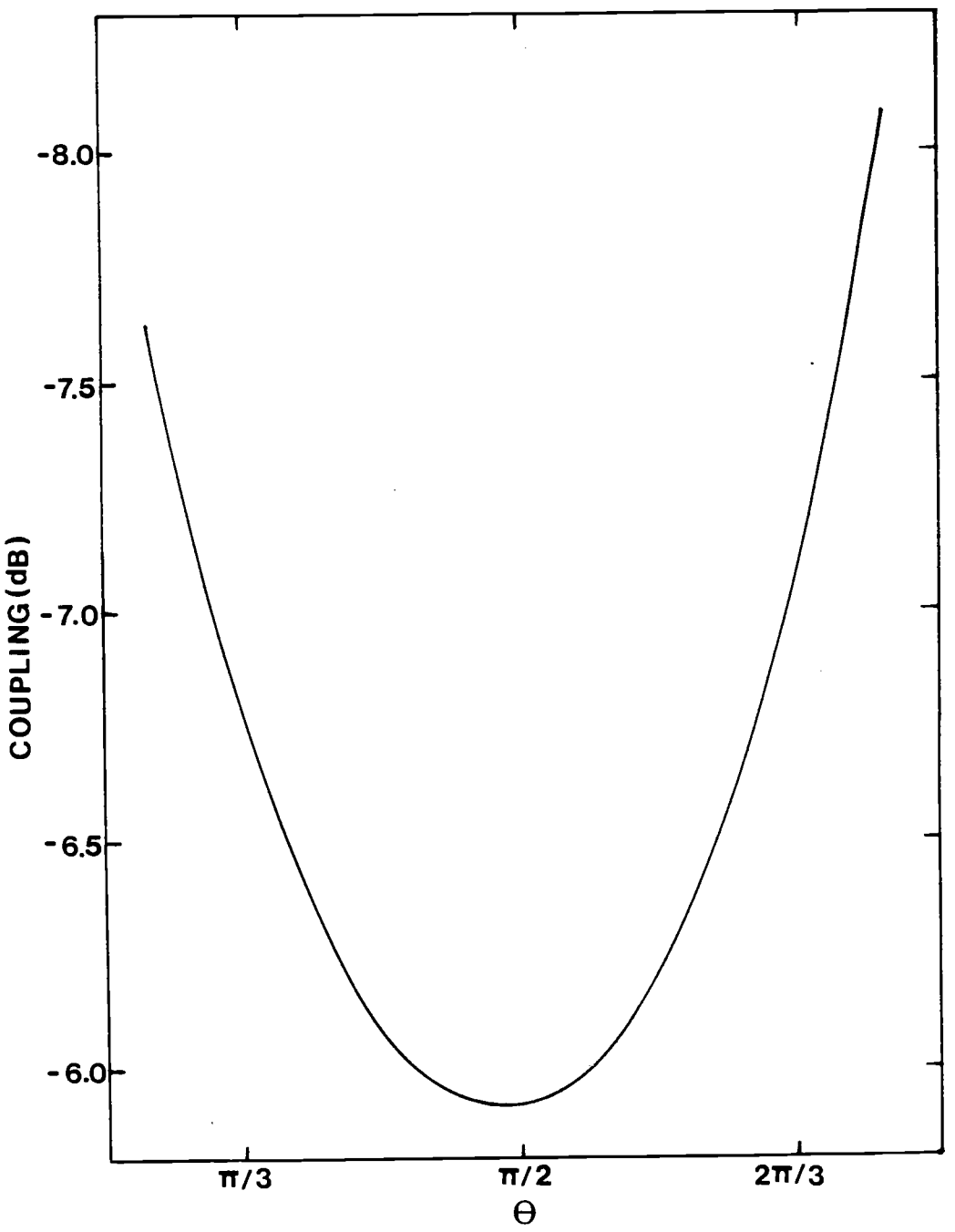

Figure 4-4(a). Coupling $|S_{12}|$ vs normalized frequency Θ for nominal 6-dB coupling with $\varepsilon_r = 10$ (where $w_1/h = 0.125$, $w_2/h = 2s/h = 0.374$), when terminated in $Z_1 = Z_2 = 50$ ohms.

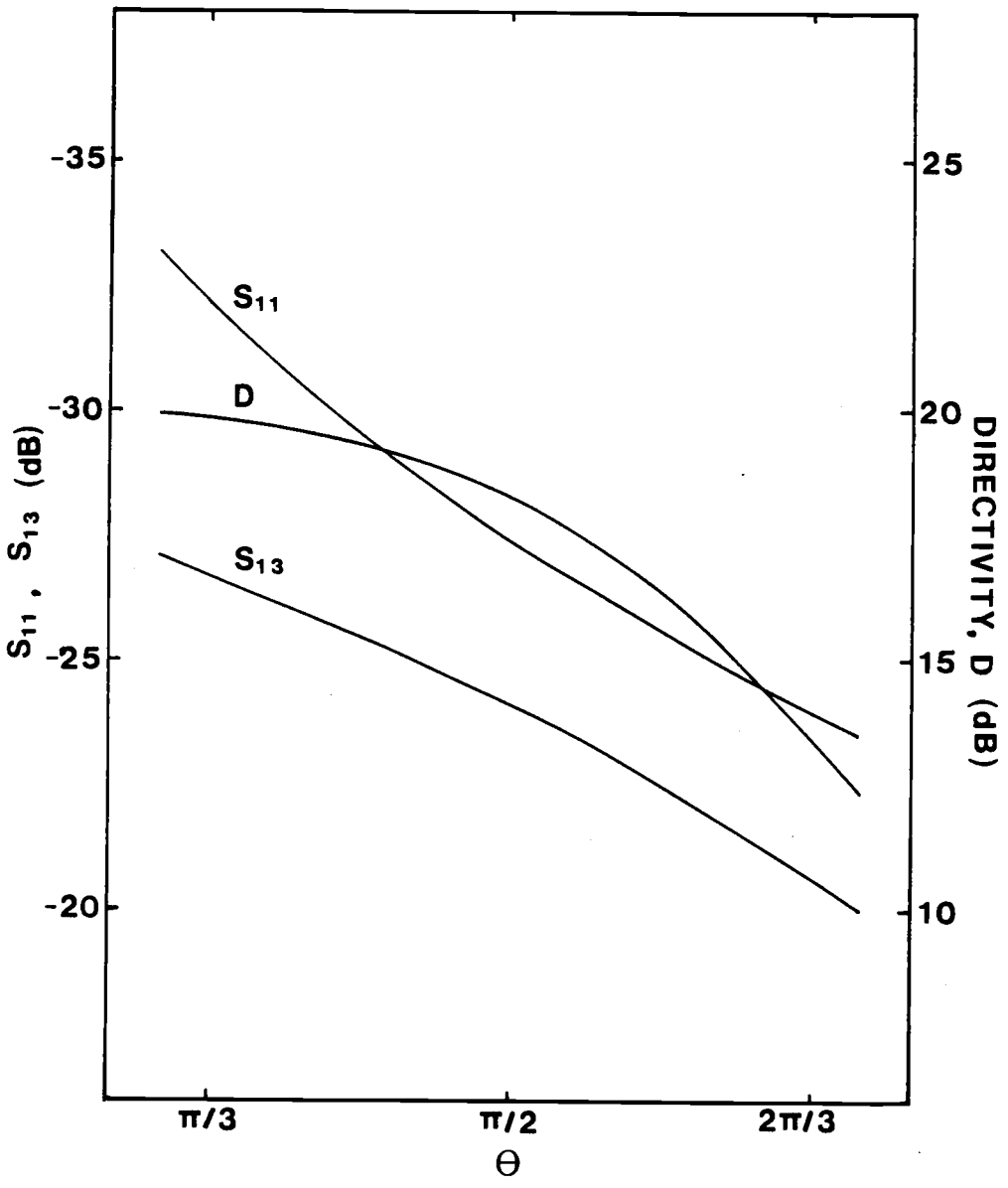

Figure 4-4(b). Reflection coefficient $|S_{11}|$, isolation $|S_{13}|$ and directivity D vs normalized frequency Θ for nominal 6-dB coupling with $\varepsilon_r = 10$ (where $w_1/h = 0.125$, $w_2/h = 2s/h = 0.374$), when terminated in $Z_1 = Z_2 = 50$ ohms.

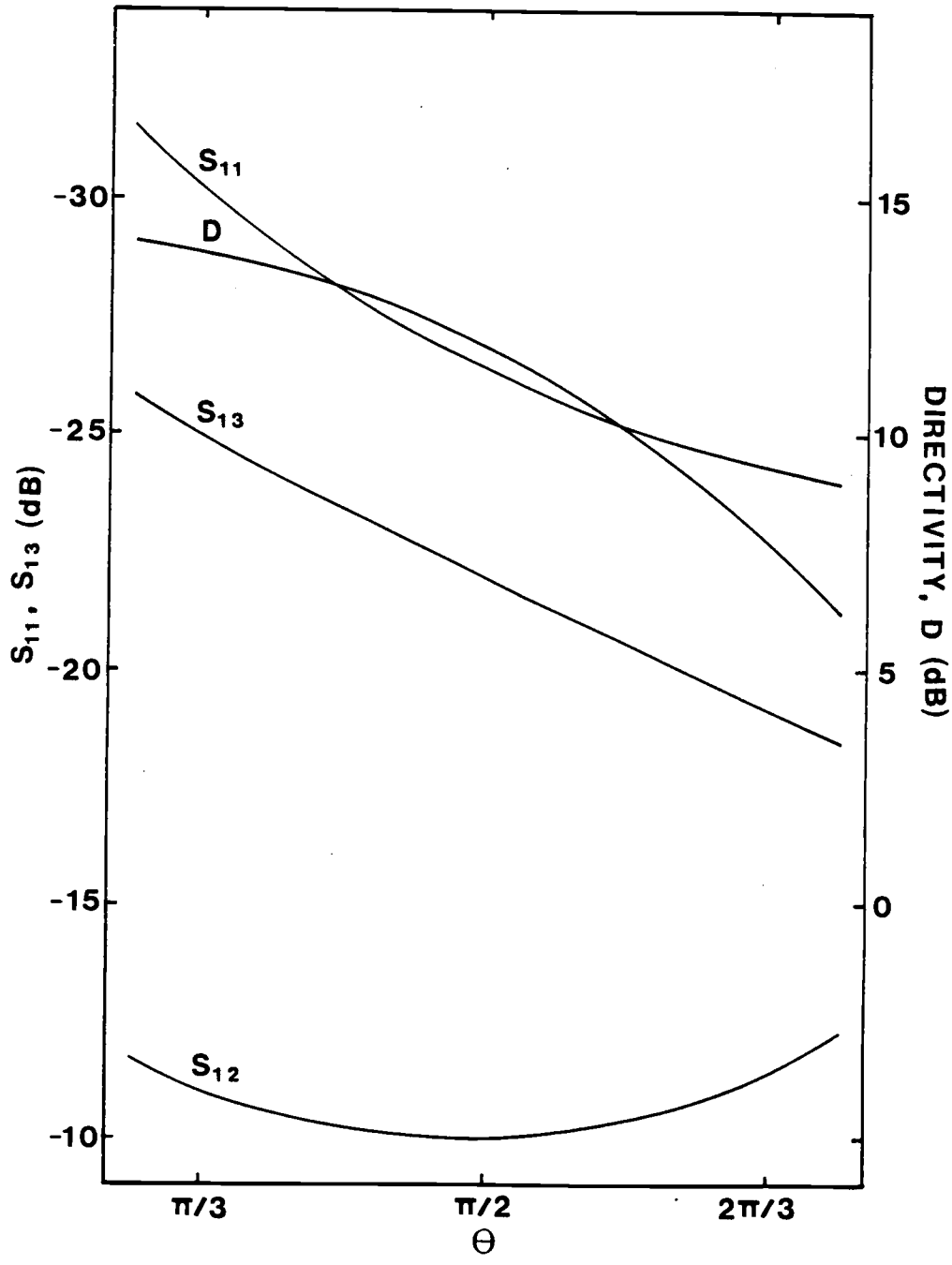

Figure 4-5. Coupling $|S_{12}|$, reflection coefficient $|S_{11}|$, isolation $|S_{13}|$ and directivity D vs normalized frequency Θ for nominal 10-dB coupling with ε_r=10 (where $w_1/h = w_2/2h = s/3h = 0.156$), when terminated in $Z_1 = Z_2 = 50$ ohms.

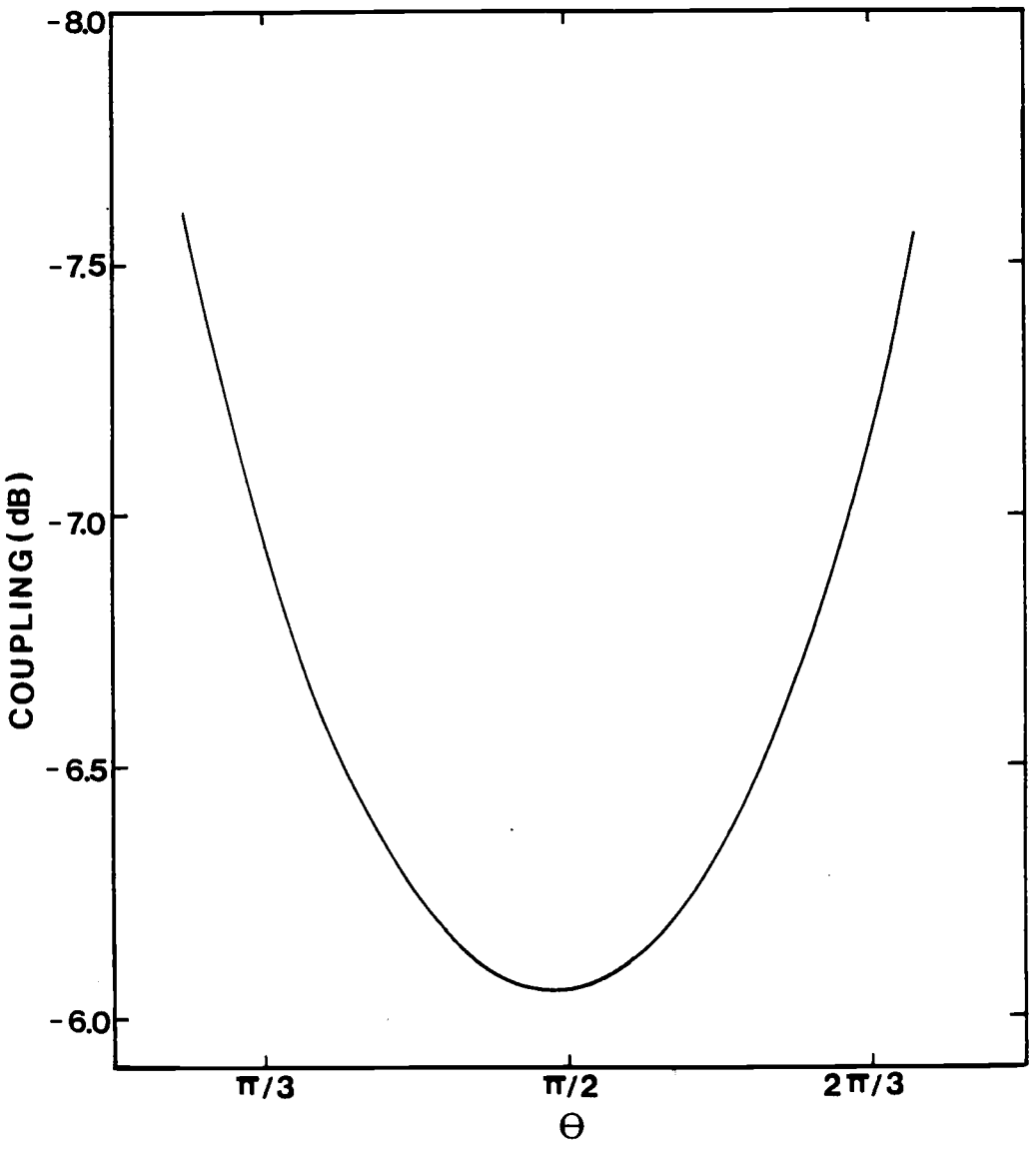

Figure 4-6(a). Coupling $|S_{12}|$ vs normalized frequency Θ for nominal 6-dB coupling with $\varepsilon_r = 2.55$ (where $w_1/h = 0.663$, $w_2/h = 1.755$, $s/h = 0.117$), when terminated in $Z_1 = Z_2 = 50$ ohms

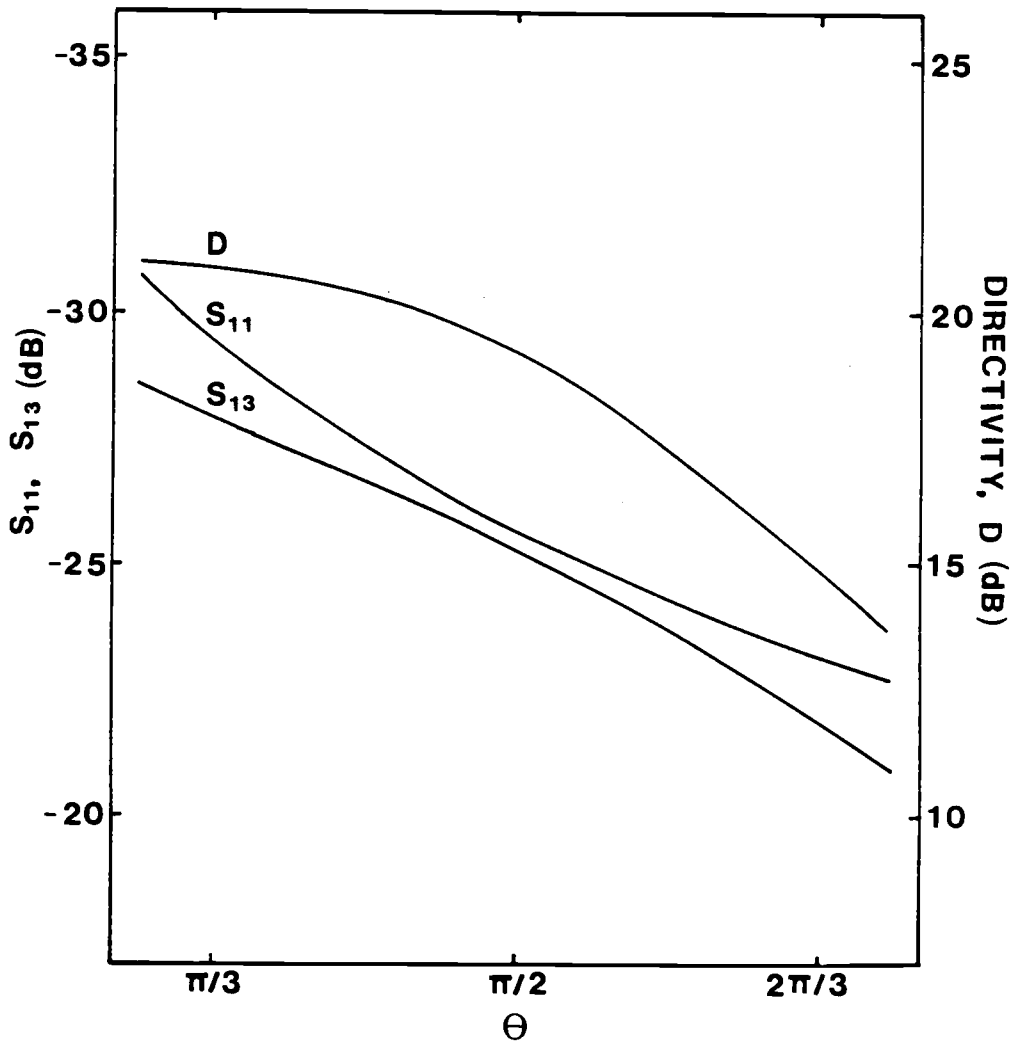

Figure 4-6(b). Reflection coefficient $|S_{11}|$, isolation $|S_{13}|$ and directivity D vs normalized frequency Θ for nominal 6-dB coupling with $\varepsilon_r = 2.55$ (where $w_1/h = 0.663$, $w_2/h = 1.755$, $s/h = 0.117$), when terminated in $Z_1 = Z_2 = 50$ ohms.

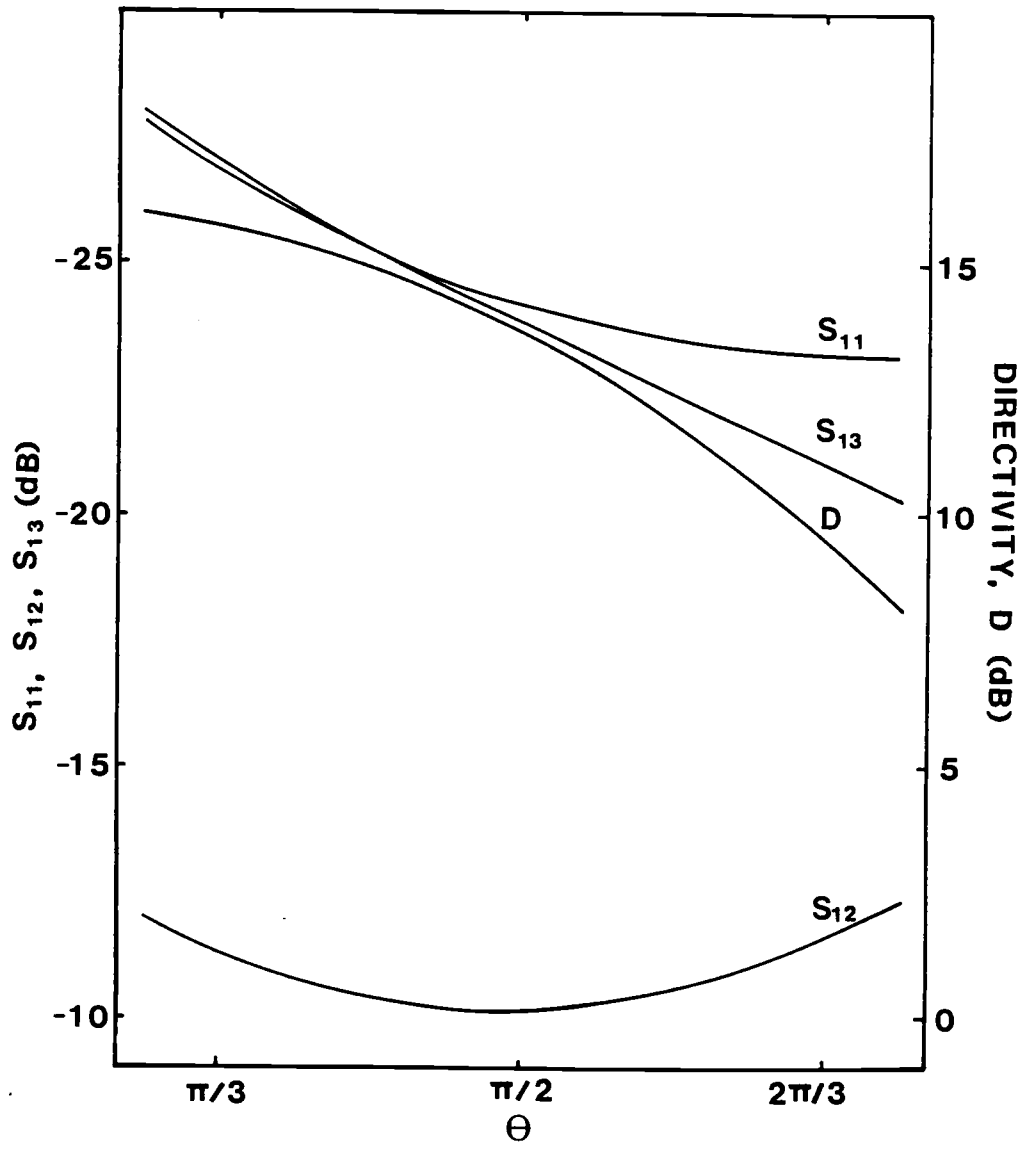

Figure 4-7. Coupling $|S_{12}|$, reflection coefficient $|S_{11}|$, isolation $|S_{13}|$ and directivity D vs normalized frequency Θ for nominal 10-dB coupling ε_r= 2.55 (where w_1/h = 0.858, w_2/h = 1.716, s/h = 0.429), when terminated in Z_1= Z_2= 50 ohms.

Table 4-1. Design Parameters of Symmetrical and Nonsymmetrical Interdigitated Couplers Consisting of Symmetrical Three Lines

(1) 3 dB Case with $\varepsilon_r = 10$.

Dimensions (where $w_1 = w_3$, h is thickness of subs.)			Effective Dielectric Constants			Effective Velocity ($\times 10^8$ m/sec)			Voltage Ratio (where $R_{va} = 0.$)		Mode-line Characteristic Impedance (Ohms) (where $Z_{a1} = Z_{a3}$, $Z_{a2} = 0.$, $Z_{b1} = Z_{b3}$, $Z_{c1} = Z_{c3}$)					Absolute Scattering Parameters at Center Frequency (dB) with $Z_1 = Z_2 = 50\,\Omega$			
w_1/h	s/h	w_2/h	ε_a	ε_b	ε_c	v_a	v_b	v_c	R_{vb}	R_{vc}	Z_{a1}	Z_{b1}	Z_{b2}	Z_{c1}	Z_{c2}	S_{11}	S_{12}	S_{13}	S_{14}
.078	.039	.078	5.5102	6.2999	5.5001	1.2771	1.1944	1.2783	1.0031	-2.1906	63.107	213.737	234.836	31.963	35.118	-31.47	-3.16	-2.96	-19.86
		.117	5.5114	6.3244	5.5002	1.2770	1.1921	1.2783	1.0037	-1.8523	63.778	219.387	203.936	33.711	31.337	-31.0	-3.03	-3.05	-21.72
		.156	5.5131	6.3595	5.5002	1.2768	1.1888	1.2783	1.0046	-1.5280	64.558	226.204	173.616	35.916	27.566	-30.63	-2.95	-3.11	-24.34
		.195	5.5143	6.3821	5.5003	1.2767	1.1867	1.2783	1.0052	-1.3769	64.965	230.025	159.187	37.179	25.730	-29.29	-3.09	-2.95	-28.34
		.234	5.5160	6.4150	5.5003	1.2765	1.1837	1.2783	1.0062	-1.2058	65.456	235.006	142.566	38.842	23.563	-30.17	-2.95	-3.1	-28.25
		.273	5.5171	6.4363	5.5004	1.2763	1.1817	1.2783	1.0069	-1.1165	65.722	237.944	133.753	39.827	22.388	-29.98	-2.97	-3.08	-29.32
		.312	5.5187	6.4675	5.5005	1.2762	1.1788	1.2783	1.0080	-1.0077	66.051	241.910	122.855	41.157	20.902	-29.82	-3.0	-3.03	-29.86
		.351	5.5198	6.4878	5.5006	1.2760	1.1770	1.2783	1.0087	-.9475	66.234	244.316	116.749	41.963	20.052	-29.55	-3.04	-3.0	-29.5
		.390	5.5214	6.5177	5.5007	1.2759	1.1743	1.2782	1.0098	-.8709	66.466	247.638	108.886	43.069	18.938	-29.29	-3.09	-2.95	-28.34
		.429	5.5224	6.5372	5.5008	1.2757	1.1725	1.2782	1.0105	-.8270	66.598	249.691	104.330	43.749	18.280	-29.14	-3.13	-2.92	-27.43
		.468	5.5239	6.5659	5.5010	1.2756	1.1700	1.2782	1.0117	-.7695	66.767	252.570	98.307	44.694	17.396	-28.9	-3.2	-2.86	-26.13
		.507	5.5249	6.5847	5.5012	1.2754	1.1683	1.2782	1.0125	-.7357	66.864	254.374	94.737	45.281	16.864	-28.75	-3.24	-2.83	-25.34
		.546	5.5264	6.6125	5.5014	1.2753	1.1658	1.2782	1.0136	-.6906	66.991	256.931	89.930	46.104	16.137	-28.54	-3.31	-2.77	-24.25

Table 4-1 (Cont.)

(2) 6 dB case with $\epsilon_r = 10$

w_1/h	s/h	w_2/h	ϵ_a	ϵ_b	ϵ_c	v_a	v_b	v_c	R_{vb}	R_{vc}	Z_{a1}	Z_{b1}	Z_{b2}	Z_{c1}	Z_{c2}	S_{11}	S_{12}	S_{13}	S_{14}
.125	.187	.125	5.5772	6.6487	5.5037	1.2695	1.1627	1.2779	1.0289	-1.5771	79.916	161.762	131.246	51.765	42.000	-28.75	-6.17	-1.25	-21.57
		.156	5.5793	6.6699	5.5042	1.2692	1.1608	1.2778	1.0305	-1.4470	80.003	164.130	122.362	52.523	39.157	-28.38	-6.04	-1.28	-22.35
		.187	5.5815	6.6899	5.5048	1.2690	1.1591	1.2778	1.0320	-1.3430	80.009	166.180	115.164	53.241	36.899	-28.13	-5.97	-1.3	-22.99
		.218	5.5836	6.7092	5.5053	1.2687	1.1574	1.2777	1.0335	-1.2570	80.196	167.996	109.125	53.924	35.028	-27.96	-5.92	-1.32	-23.49
		.250	5.5857	6.7279	5.5059	1.2685	1.1558	1.2776	1.0351	-1.1839	80.292	169.634	103.935	54.575	33.438	-27.81	-5.9	-1.33	-23.86
		.312	5.5897	6.7638	5.5072	1.2680	1.1527	1.2775	1.0382	-1.0650	80.471	172.510	95.363	55.789	30.840	-27.58	-5.89	-1.33	-24.19
		.374	5.5936	6.7983	5.5085	1.2676	1.1498	1.2773	1.0412	-.9712	80.629	174.994	88.478	56.901	28.769	-27.43	-5.92	-1.32	-24.12
		.406	5.5955	6.8150	5.5092	1.2674	1.1484	1.2773	1.0428	-.9310	80.701	176.125	85.496	57.423	27.875	-27.35	-5.94	-1.31	-23.97
		.437	5.5973	6.8315	5.5099	1.2672	1.1470	1.2772	1.0443	-.8945	80.767	177.195	82.759	57.925	27.054	-27.29	-5.97	-1.3	-23.78
		.468	5.5991	6.8477	5.5107	1.2670	1.1457	1.2771	1.0458	-.8610	80.829	178.211	80.235	58.408	26.297	-27.23	-6.00	-1.29	-23.56
		.546	5.6025	6.8794	5.5122	1.2666	1.1430	1.2769	1.0488	-.8017	80.941	180.107	75.718	59.320	24.939	-27.13	-6.07	-1.27	-23.04
		.624	5.6073	6.9254	5.5147	1.2660	1.1392	1.2766	1.0532	-.7275	81.080	182.677	69.988	60.571	23.206	-26.97	-6.2	-1.24	-22.23

(3) 10 dB case with $\epsilon_r = 10$

w_1/h	s/h	w_2/h	ϵ_a	ϵ_b	ϵ_c	v_a	v_b	v_c	R_{vb}	R_{vc}	Z_{a1}	Z_{b1}	Z_{b2}	Z_{c1}	Z_{c2}	S_{11}	S_{12}	S_{13}	S_{14}
.156	.468	.125	5.7318	6.8363	5.5339	1.2522	1.1466	1.2744	1.0888	-1.3159	87.704	129.052	92.448	67.815	48.580	-25.29	-10.43	-.46	-21.91
		.156	5.7305	6.8228	5.5333	1.2524	1.1477	1.2745	1.0888	-1.3290	88.694	129.675	93.816	68.732	49.726	-26.74	-10.57	-.44	-21.82
		.250	5.7342	6.9113	5.5423	1.2520	1.1404	1.2734	1.0982	-1.0393	88.540	134.913	76.993	70.205	40.065	-26.36	-10.12	-.49	-22.01
		.312	5.7364	6.9474	5.5464	1.2517	1.1374	1.2730	1.1025	-.9509	88.522	136.817	71.714	70.863	37.143	-26.30	-10.06	-.49	-21.91
		.374	5.7388	6.9806	5.5503	1.2515	1.1347	1.2725	1.1067	-.8802	88.520	138.457	67.436	71.478	34.814	-26.27	-10.04	-.5	-21.73
		.468	5.7411	7.0116	5.5542	1.2512	1.1322	1.2721	1.1107	-.8217	88.527	139.906	63.846	72.055	32.882	-26.25	-10.06	-.5	-21.52
		.624	5.7476	7.0962	5.5655	1.2505	1.1254	1.2708	1.1221	-.6913	88.572	143.481	55.649	73.591	28.542	-26.25	-10.22	-.48	-20.88
		.780	5.7516	7.1476	5.5726	1.2501	1.1214	1.2700	1.1294	-.6276	88.607	145.43	51.538	74.479	26.394	-26.27	-10.38	-.47	-20.48
		.936	5.7569	7.2192	5.5829	1.2495	1.1158	1.2688	1.1397	-.5529	88.659	147.931	46.608	75.647	23.834	-26.27	-10.65	-.45	-19.97
		1.092	5.7601	7.2641	5.5894	1.2491	1.1123	1.2681	1.1462	-.5128	88.690	149.391	43.903	76.333	22.433	-26.25	-10.85	-.44	-19.69

Table 4 (Cont.)

(4) 6 dB case with $\varepsilon_r = 2.55$

w_1/h	s/h	w_2/h	ε_a	ε_b	ε_c	v_a	v_b	v_c	R_{vb}	R_{vc}	Z_{a1}	Z_{b1}	Z_{b2}	Z_{c1}	Z_{c2}	S_{11}	S_{12}	S_{13}	S_{14}
.663	.117	.780	1.8276	2.1084	1.7822	2.2176	2.0646	2.2457	1.0581	-1.7476	80.148	165.022	152.568	46.770	43.240	-25.66	-5.59	-1.47	-21.00
		.975	1.8301	2.1173	1.7840	2.2161	2.0603	2.2445	1.0645	-1.5155	80.462	166.944	134.665	49.240	39.719	-25.63	-5.61	-1.45	-22.25
		1.170	1.8333	2.1299	1.7869	2.2142	2.0542	2.2427	1.0737	-1.2625	80.795	169.573	114.925	52.397	35.511	-25.63	-5.71	-1.40	-23.90
		1.365	1.8350	2.1379	1.7888	2.2131	2.0504	2.2415	1.0794	-1.1351	80.956	171.193	104.878	54.205	33.207	-25.65	-5.79	-1.36	-24.72
		1.560	1.8372	2.1492	1.7917	2.2118	2.0450	2.2397	1.0877	-.9847	81.140	173.465	92.894	56.561	30.290	-25.65	-5.94	-1.31	-25.3
		1.755	1.8385	2.1564	1.7936	2.2110	2.0416	2.2385	1.0928	-.9042	81.236	174.889	86.404	57.935	28.623	-25.65	-6.05	-1.27	-25.26
		1.950	1.8400	2.1666	1.7963	2.2101	2.0367	2.2369	1.1002	-.8046	81.353	176.906	78.299	59.754	26.447	-25.63	-6.23	-1.22	-24.72

(5) 10 dB case with $\varepsilon_r = 2.55$

w_1/h	s/h	w_2/h	ε_a	ε_b	ε_c	v_a	v_b	v_c	R_{vb}	R_{vc}	Z_{a1}	Z_{b1}	Z_{b2}	Z_{c1}	Z_{c2}	S_{11}	S_{12}	S_{13}	S_{14}
.858	.429	.429	1.8792	2.1260	1.7946	2.1870	2.0561	2.2379	1.0966	-2.2472	86.946	125.363	154.470	59.689	73.548	-24.90	-10.6	-.46	-20.34
		.858	1.8853	2.1527	1.8071	2.1834	2.0433	2.2302	1.1233	-1.4085	87.337	130.823	103.488	65.295	51.652	-24.24	-9.93	-.51	-22.63
		1.287	1.8883	2.1675	1.8144	2.1817	2.0363	2.2257	1.1390	-1.1431	87.546	133.196	86.708	68.001	44.267	-24.19	-9.95	-.50	-23.54
		1.716	1.8917	2.1873	1.8239	2.1797	2.0271	2.2199	1.1604	-.8930	87.777	135.996	70.458	71.100	36.836	-24.19	-10.20	-.47	-23.84
		2.145	1.8934	2.1991	1.8294	2.1787	2.0216	2.2165	1.1734	-.7788	87.892	137.563	62.855	72.717	33.226	-24.18	-10.44	-.45	-23.53
		2.574	1.8954	2.2154	1.8356	2.1776	2.0142	2.2122	1.1913	-.6524	88.024	139.623	54.257	74.674	29.018	-24.12	-10.85	-.42	-22.90
		3.003	1.8964	2.2253	1.8407	2.1770	2.0097	2.2097	1.2022	-.5881	88.094	140.851	49.789	75.742	26.774	-24.05	-11.14	-.39	-22.45
		3.432	1.8977	2.2391	1.8462	2.1762	2.0035	2.2064	1.2173	-.5115	88.177	142.524	44.374	77.082	23.899	-23.93	-11.60	-.36	-21.88

between strips (s/h) fixed in Fig. 4-8 and 9, since this non-mode converting set of terminations is a convenient and perhaps---starting point in the design of the coupler. This results in an ideal coupler if the normal mode phase velocities are equal [7,100].

From these design curves or Table 4-1, one can determine the physical dimensions, w_1/h, w_2/h and s/h of a symmetrical interdigitated four-port coupler such that $Z_1 = Z_2 = 50\ \Omega$ for a desired coupling, e.g., for $\varepsilon_r = 10$, $w_1/h = .078$, $w_2/h = .312$ and $s/h = .039$ for a 3 dB coupler. Similarly, the dimension of a non-symmetrical interdigitated four-port coupler can be determined for a given Z_1 and Z_2 such that $Z_1 = \sqrt{Z_{b1}\ Z_{c1}}/2$ and $Z_2 = \sqrt{Z_{b2}\ Z_{c2}}$ for a desired coupling. The scattering parameters of the non-symmetrical coupler can be found by utilizing equation(C-3). However, as stated in the analysis of this section, the examination of scattering parameters for the non-symmetrical case reveals that the isolation is maximum at the center frequency, but the coupler is not matched. Hence, the new terminations Z_1 and Z_2 required for the optimum performance are determined by using the impedance renormalization procedure as given by equation (2-19) and (2-20) in an interative manner as described in Section 3.3 The method to determine the optimum terminations is illustrated in the following example of a non-symmetrical three-line coupler.

Example: For the symmetrical three line coupled structure with the relative dielectric constant $\varepsilon_r = 10$ and the geometry given by

$w_1/h = w_3/h = .078$, $w_2/h = .117$ and $s/h = .039$, the quasi-TEM normal mode parameters are shown in Table 4-1.

These parameters are substituted into the explicit expressions for scattering parameters given by equation (C-3), in which Z_{1o}/Z_{2o} has been taken as $-2/R_{vb}R_{vc}$ where $R_c = R_{vb}$ and $R_\pi = R_{vc}$. The scattering parameters for a 3 dB non-symmetrical interdigitated three-line four-port coupler when terminated in $Z_1 = Z_{1o}/2 = \sqrt{Z_{b1}Z_{c1}}/2 = 43\ \Omega$ and $Z_2 = Z_{2o} = \sqrt{Z_{b2}Z_{c2}} = 79.94\ \Omega$ shown in Fig. 4-2(b), are found to be:

$\|S_{11}\|$	$\|S_{12}\|$	$\|S_{13}\|$	$\|S_{14}\|$	$\|S_{22}\|$	$\|S_{23}\|$
.2190	.6994	.0245	.6797	.1473	.6872

The same parameters when terminated in real impedances $Z_1 = 54\ \Omega$ and $Z_2 = 65.7\ \Omega$, found after three iterations by using the procedure described in Section 3.3, are:

$\|S_{11}\|$	$\|S_{12}\|$	$\|S_{13}\|$	$\|S_{14}\|$	$\|S_{22}\|$	$\|S_{23}\|$
.0272	.7165	.0277	.6965	.0324	.6963

It can be seen that the coupler matching is considerably improved with minimal change in the others.

The coupling, reflection coefficient and directivity are also plotted as a function of normalized frequency in Fig. 4-10 for both cases.

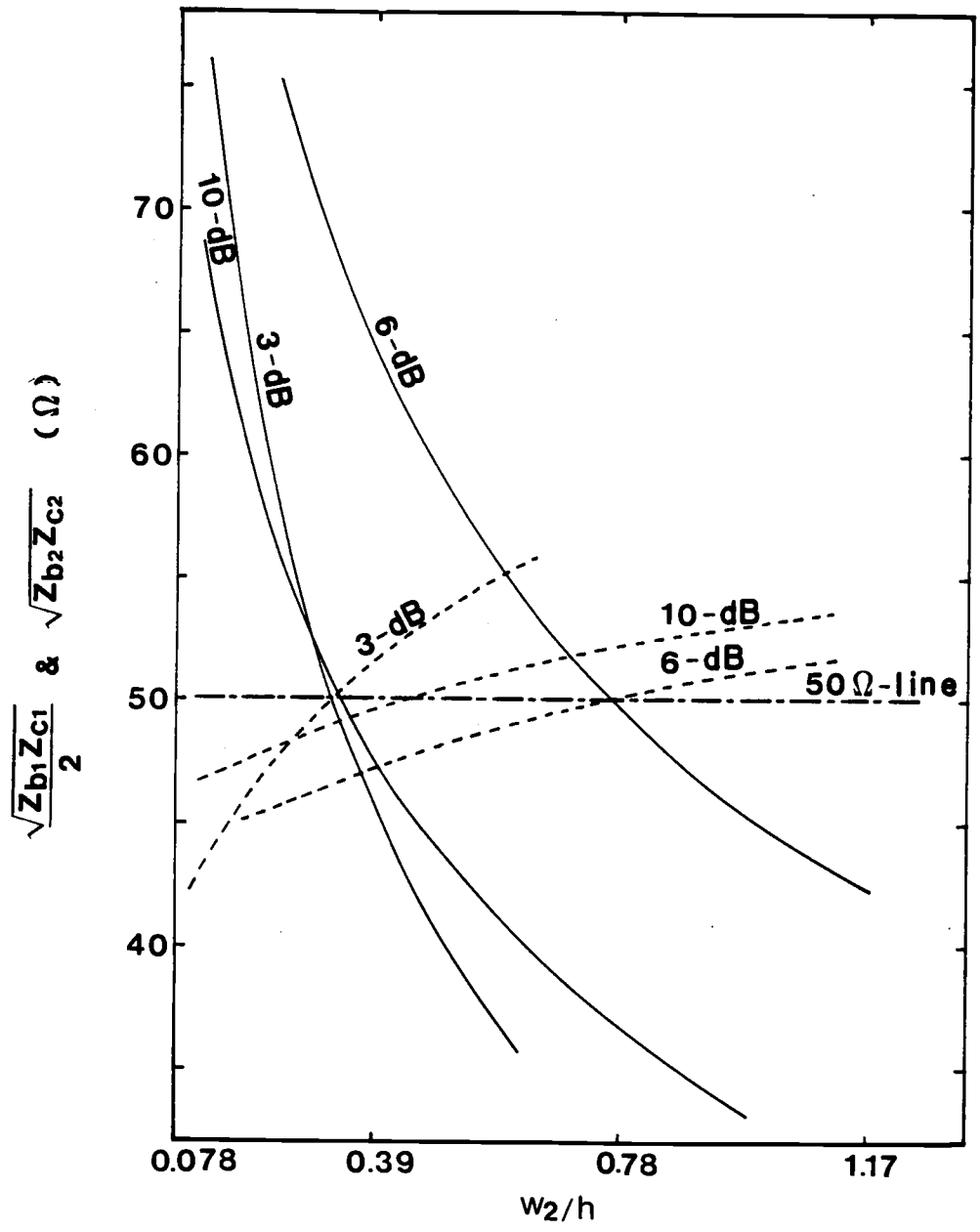

Figure 4-8. Design curves for alumina($\varepsilon_r = 10$) interdigitated three-line couplers(where, $w_1/h = 0.078$ and $s/h = 0.039$ for 3-dB, $w_1/h = 0.125$ and $s/h = 0.187$ for 6-dB, $w_1/h = 0.156$ and $s/h = 0.468$ for 10-dB).

-------- $Z_{10}=\sqrt{Z_{b1}Z_{c1}}\ /\ 2$

———— $Z_{20}=\sqrt{Z_{c2}Z_{c2}}$

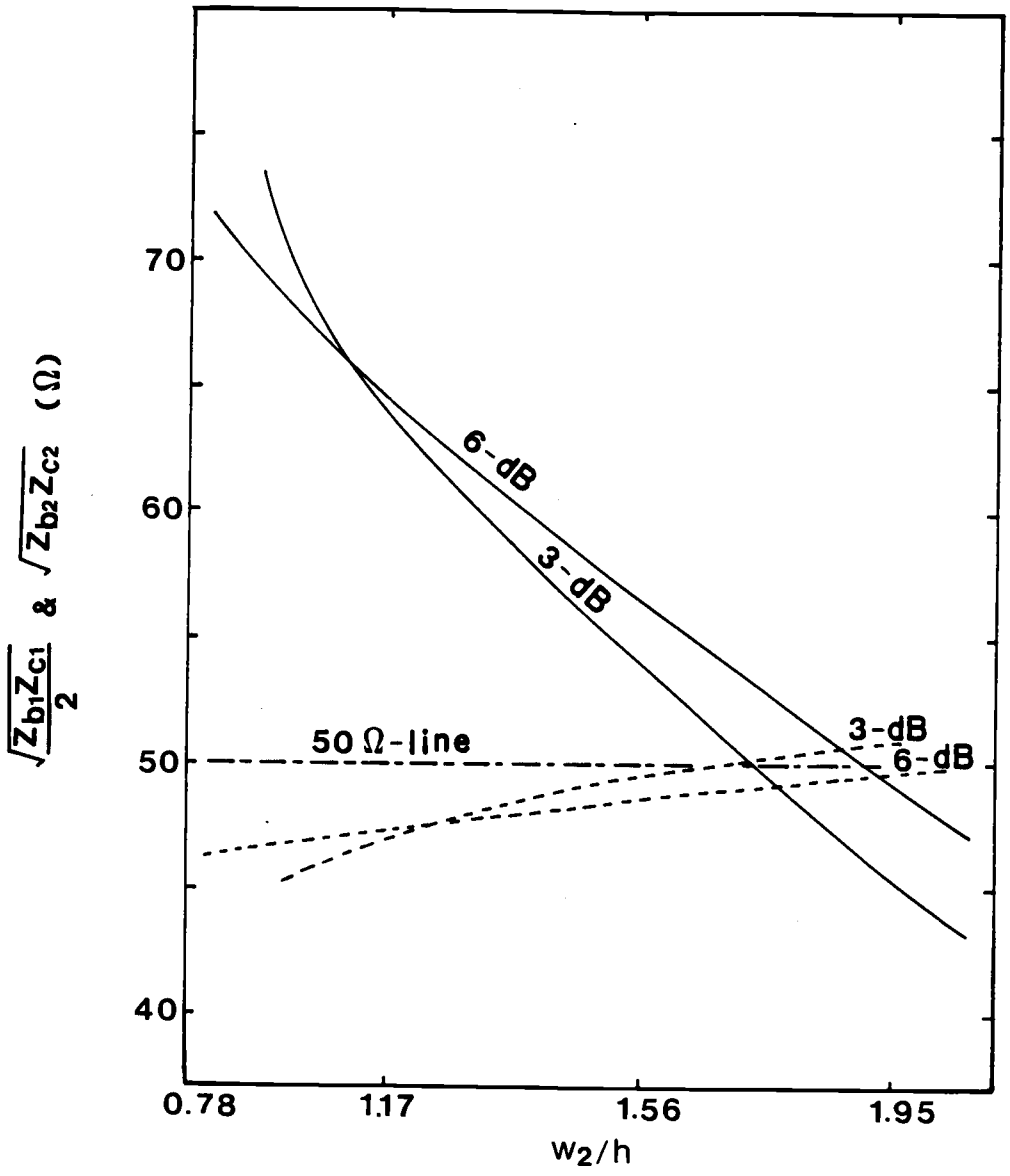

Figure 4-9. Design curves for polystyrene(ε_r = 2.55) interdigitated three-line couplers (where, w_1/h = 0.663 and s/h = 0.117 for 6-dB, w_2/h = 0.858 and s/h = 0.429 for 10-dB).

------ $Z_{10}=\sqrt{Z_{b1}Z_{c1}}\,/\,2$

——— $Z_{20}=\sqrt{Z_{b2}Z_{c2}}$

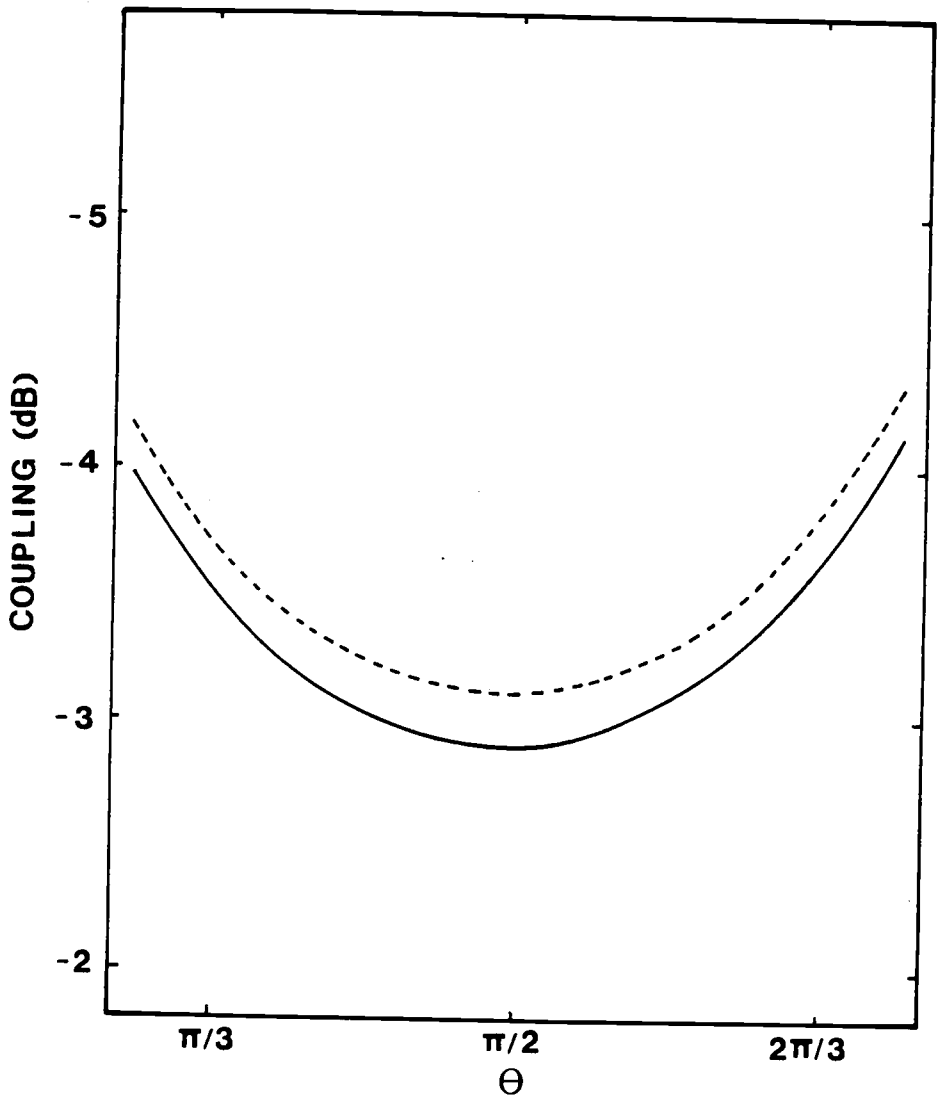

Figure 4-10(a). Coupling $|S_{12}|$ vs normalized frequency Θ for the non-symmetrical interdigitated three-line structure with $\varepsilon_r = 10$.

------- Characteristic terminations, $Z_{10} = 43$ ohms and $Z_{20} = 79.94$ ohms.

——— Optimized terminations, $Z_1 = 54$ ohms and $Z_2 = 65.7$ ohms.

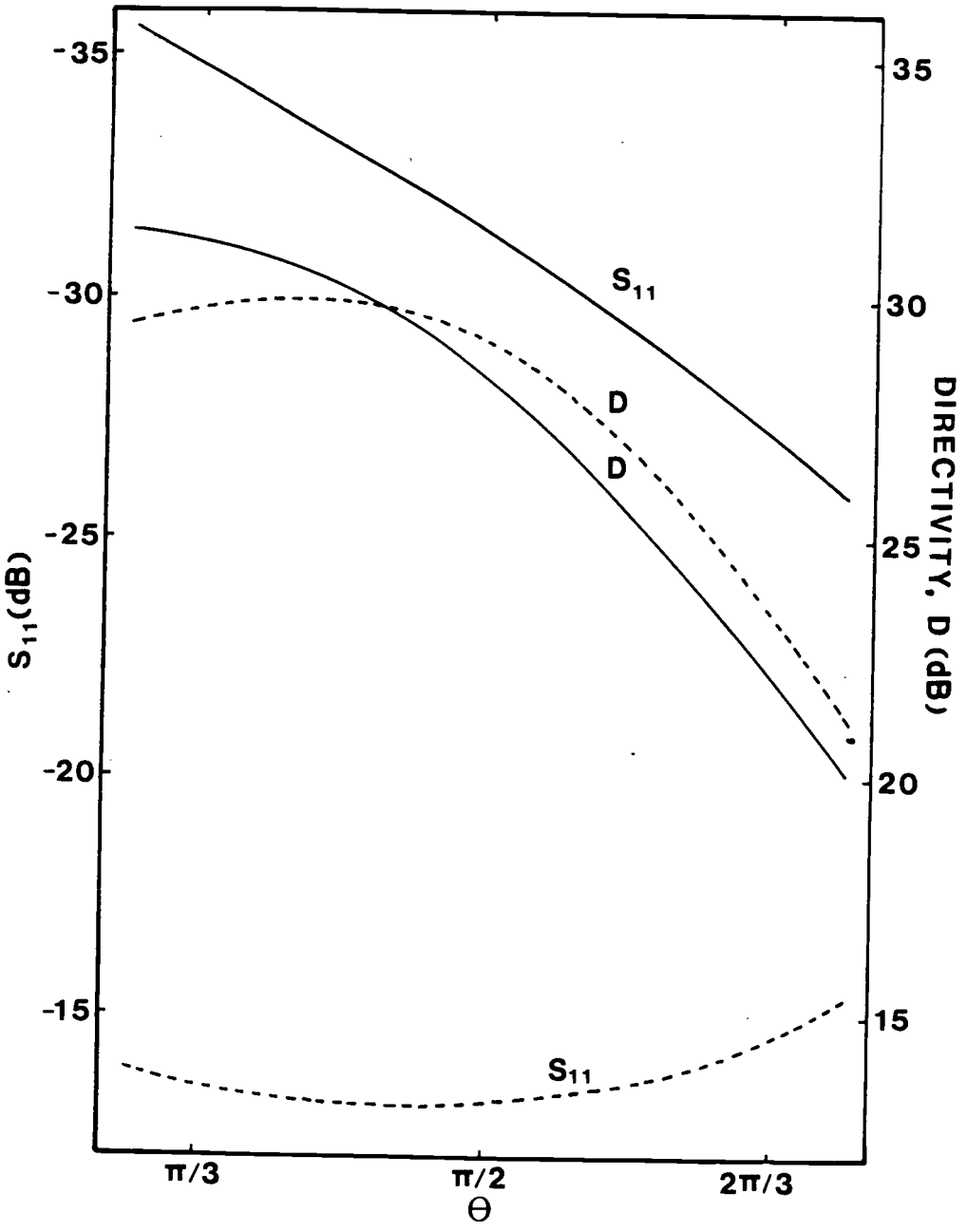

Figure 4-10(b). Reflection coefficient $|S_{11}|$ and directivity D vs normalized frequency Θ for the non-symmetrical interdigitated three-line structure with $\varepsilon_r = 10$.
------ Charateristic terminations, $Z_{10} = 43$ ohms and $Z_{20} = 79.94$ ohms.
——— Optimized terminations, $Z_1 = 54$ ohms and $Z_2 = 65.7$ ohms.

The curves for the center band fl product shown in Fig. 4-11 and Fig. 4-12 are useful and convenient to determine the length for the specific frequency, where f is frequency and l is the length of coupled lines. These curves are plotted as a function of the relative width of the middle strip for different values of coupling when terminated in 50 Ω. The design procedure is illustrated with an example.

Example: The dimension for the 3 dB symmetrical interdigitated three-line coupling structure with $\varepsilon_r = 10$ are taken from Tulaja's [94];

$h = .51$ mm, $w_1 = 40$ μm, $w_2 = 220$ μm, $s = 20$ μm, and

$l = 4.49$ mm

Normalizing w_1, w_2 and s with respect to h, $w_1/h = .078$, $w_2/h = .43$, and $s/h = .039$. The normal mode parameters for this geometry are found by using Table 4-1: for mode a;

$$\varepsilon_{eff} = 5.5224,\ R_{va} = 0,\ Z_{a1} = Z_{a3} = 66.598\ \Omega,\ Z_{a2} = 0$$

for mode b;

$$\varepsilon_{eff} = 6.5392,\ R_{vb} = 1.0098,\ Z_{b1} = Z_{b3} = 249.691\ \Omega,$$
$$Z_{b2} = 104.330\ \Omega$$

for mode c;

$$\varepsilon_{eff} = 5.5008,\ R_{vc} = -.8270,\ Z_{c1} = Z_{c3} = 43.749\ \Omega,$$
$$Z_{c2} = 18.28\ \Omega$$

Substituting the above characteristic mode impedances into

$Z_{1o} = \sqrt{Z_{b1}Z_{c1}}/2$ and $Z_{2o} = \sqrt{Z_{b2}Z_{c2}}$ gives:

$Z_{1o} = 52.26\ \Omega$ and $Z_{2o} = 43.67\ \Omega$

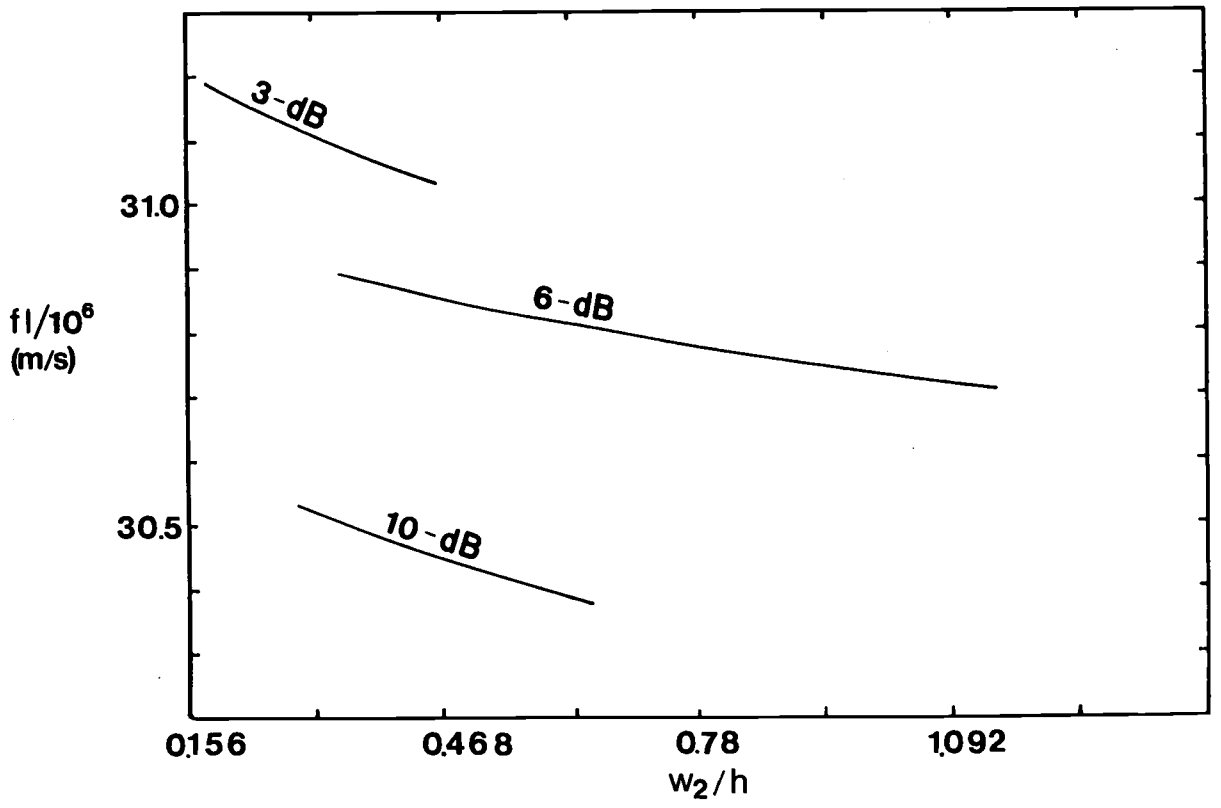

Figure 4-11. Center-band fl product for alumina (ε_r= 10) interdigitated three-line couplers(Dimensions; w_1/h = 0.078 and s/h = 0.039 for 3-dB, w_1/h = 0.125 and s/h = 0.187 for 6-dB, w_1/h = 0.156 and s/h = 0.468 for 10-dB)

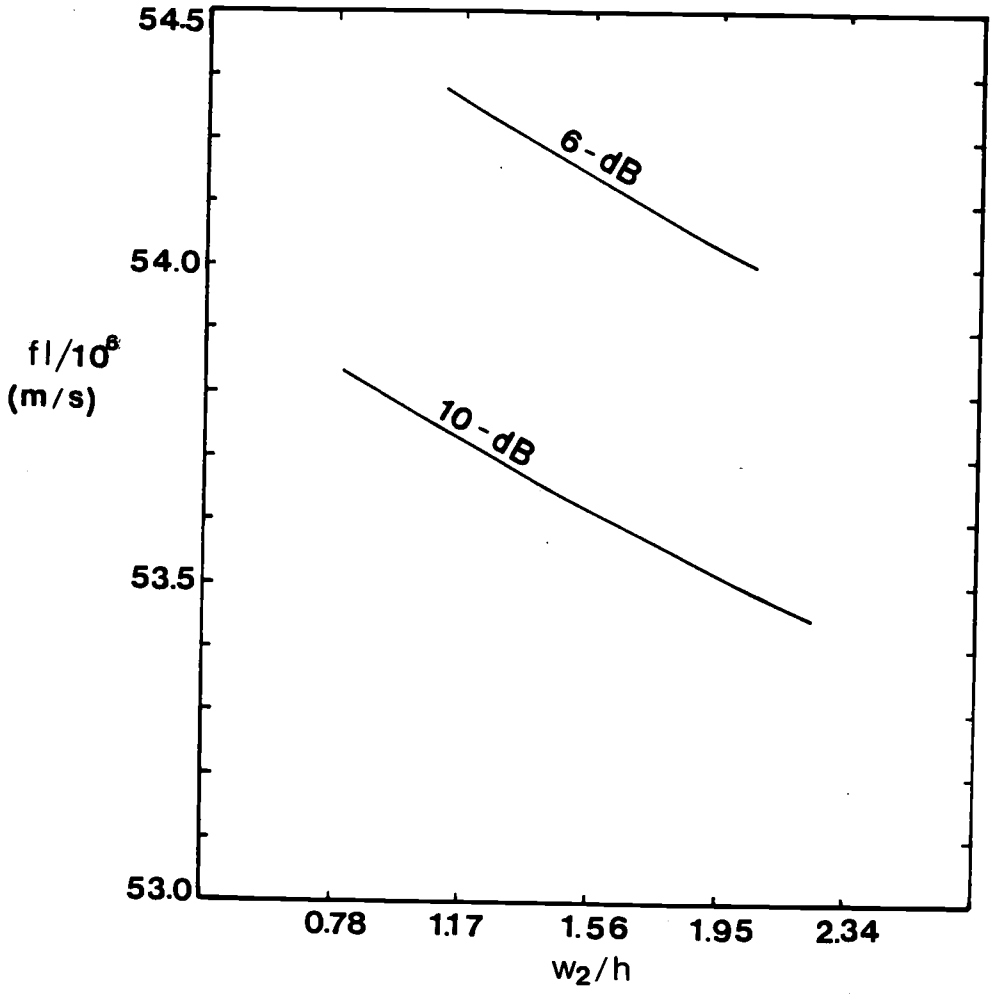

Figure 4-12. Center-band fl product for polystyrene (ε_r= 2.55) interdigitated three-line couplers(Dimension; w_1h = 0.663 and s/h = 0.117 for 6-dB, w_1/h = 0.858 and s/h = 0.429 for 10-dB).

From Fig. 4-11, fl for w_2/h = .43 and 3 dB is found to be:

$$fl = 31.05 \times 10^6 \text{ cm/sec}$$

Hence, for l = 4.49 mm, f = 6.915 GHz.

The scattering parameters, given by the explicit expressions, equation (C-3) at the center frequency, when terminated in Z_{1o} = 52.26 Ω and Z_{2o} = 43.67 Ω are found to be:

$\|S_{11}\|$	$\|S_{12}\|$	$\|S_{13}\|$	$\|S_{14}\|$	$\|S_{22}\|$	$\|S_{23}\|$
.0785	.6965	.0348	.7124	.0774	.7125

The same parameters when terminated in Z_1 = 47.5 Ω and Z_2 = 43.67 Ω found after two iterations by using the procedure described in the above example are:

$\|S_{11}\|$	$\|S_{12}\|$	$\|S_{13}\|$	$\|S_{14}\|$	$\|S_{22}\|$	$\|S_{23}\|$
.0338	.6973	.0415	.7148	.0574	.7133

When terminated in $Z_1 = Z_2$ = 50 Ω and using the general expressions given by equation (2-12), these parameters are:

$\|S_{11}\|$	$\|S_{12}\|$	$\|S_{13}\|$	$\|S_{14}\|$	$\|S_{22}\|$	$\|S_{23}\|$
.0349	.6973	.0425	.7146	.0555	.7133

According to the design procedure presented here, the geometry which was fabricated by Tulaja has the physical dimensions of a

non-symmetrical interdigitated four-port coupler such that $Z_{1o} = \sqrt{Z_{b1}Z_{c1}}/2 = 48.5\,\Omega$ and $Z_{2o} = \sqrt{Z_{b2}Z_{c2}} = 46.4\ \Omega$ for 3 dB coupling, and $l = 4.49$ mm is not the quarter wavelength at the frequency, $f = 6$ GHz, but $f = 6.915$ GHz. The terminations Z_1 and Z_2 required for optimum performance found by using the impedance renormalization procedure described above are found to be:

$$Z_1 = 47.5\ \Omega \quad \text{and} \quad Z_2 = 43.67\ \Omega$$

From the design curves shown in Fig. 4-8, the physical dimensions of a 3 dB symmetrical coupler satisfying $Z_1 = Z_2 = 50\ \Omega$ are found to be:

$$w_1/h = .078, \quad w_2/h = .312, \quad s/h = .039$$

4.3 CONCLUDING REMARKS

Analysis and design procedure for both the symmetrical and non-symmetrical interdigitated four-port directional couplers consisting of symmetrical three lines have been presented. Physical dimensions of 3, 6 and 10 dB couplers with substrates having typical dielectric constant values of 2.55 and 10 can be found by using the tables and charts given in Section 4.2. The symmetrical coupler was analyzed by using the explicit expressions for scattering parameters of four-port with characteristic non-mode converting terminations. It was shown that non-symmetrical couplers with non-mode converting terminations were not the optimum ones because of the difference in phase velocities of the normal modes of the system. A procedure to optimize the four-port for maximum isolation and matching in terms of the terminating impedances was presented.

CHAPTER V. Broadband Filters/DC Blocks

5.1 INTRODUCTION

The work to date in the area of DC blocks has been confined only to the coupled two-line microstrip structures.

Symmetrical and non-symmetrical two-port coupled microstrip line structures consisting of a pair of lines in an inhomogeneous medium [21] have various applications as filters and impedance matching network. One of the two-port prototypes [83], the open circuited interdigital filters, shown in Fig. 5-1(a) and (b), is a wideband filter with DC isolated input and output ports. This filter has been used for application as DC blocks [84-86] because of its improved performance at higher frequency as compared to a lumped capacitor. These DC blocks were introduced by La Combe and Cohen [84], who, for their analysis, used an approximate equivalent circuit, based on the even- and odd-mode propagation in coupled microstrip. A more general approach was presented by Rizzoli [85], who derived the conditions for both flat and first order Chebyshev frequency response and obtained design formulas for DC blocks with a pair of lines. The circuit is physically realizable in microstrip form and can be incorporated in microwave integrated circuits. The bandwidth of DC blocks depends on the coupling between the two lines and the structure becomes either impractical or unrealizable by conventional MIC technology for larger bandwidths.

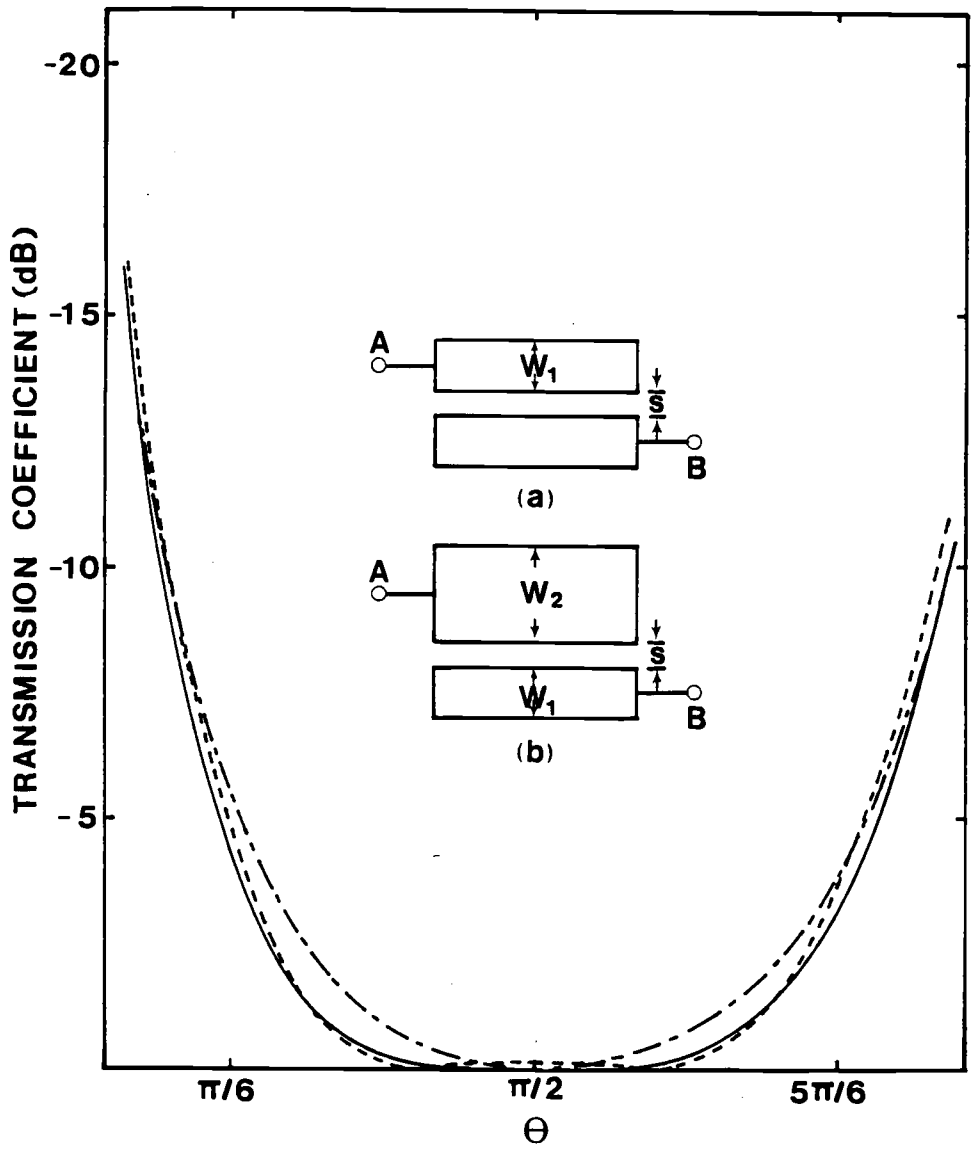

Figure 5-1. Transmission coefficient $|S_{12}|$ vs normalized frequency Θ for two-line (a) symmetrical(where $w_1/h = w_2/h = 0.078$) and (b) non-symmetrical(where $w_1/h = w_2/4h = 2s/h = 0.078$) DC blocks with $\varepsilon_r = 10$.

———— Flat response for (a) with terminations R = 69.1 ohms.

- — - — Flat response for (b) with terminations R_1= 40.76 ohms and R_2=71.48 ohms.

--------- Ripple response for (a) with terminations R = 58.3 ohms given by $|S_{11}|_{\theta = \pi/2} = 1/6$.

Since, for a larger bandwidth, the lines have to be very tightly coupled, it is more convenient to use more than two lines. The bandwidth for a given coupling, and hence the line widths and spacing can be increased significantly by utilizing more than two lines.

In this chapter the analysis and design procedures for open-circuited interdigital multiple coupled microstrip-line structures for applications as wideband DC blocks and filters are presented. These are derived by utilizing the expressions for scattering parameters of two-port network.

5.2 GENERAL ANALYSIS AND DESIGN PROCEDURE

The scattering parameters of a non-symmetrical two-port terminated in R_1 on line 1 and R_2 on line 2 are given by:

$$S_{11} = \frac{(Z_{11} - R_1)(Z_{22} + R_2) - Z_{12}^2}{(Z_{11} + R_1)(Z_{22} + R_2) - Z_{12}^2} \tag{5-1}$$

$$S_{12} = S_{21} = \frac{2 Z_{12}\sqrt{R_1 R_2}}{(Z_{11} + R_1)(Z_{22} + R_2) - Z_{12}^2} \tag{5-2}$$

$$S_{22} = \frac{(Z_{11} + R_1)(Z_{22} - R_2) - Z_{12}^2}{(Z_{11} + R_1)(Z_{22} + R_2) - Z_{12}^2} \tag{5-3}$$

where Z_{11}, Z_{22}, and Z_{12} are the elements of the two-port impedance matrix.

For a symmetrical case terminated in $R_1 = R_2 = R$ the above equations are simplified as:

$$S_{11} = S_{22} = \frac{Z_{11}^2 - Z_{12}^2 - R^2}{(Z_{11} + R)^2 - Z_{12}^2} \tag{5-4}$$

$$S_{12} = S_{21} = \frac{2 R Z_{12}}{(Z_{11} + R)^2 - Z_{12}^2} \tag{5-5}$$

where Z_{11}, Z_{12} and Z_{22} are the elements of the two-port impedance matrix.

S_{11} and S_{22} are simply the reflection coefficients Γ_1 and Γ_2 at points 1 and 2, respectively, as defined in the following:

$$\Gamma_1 = \frac{R_1 - Z_{o1}}{R_1 + Z_{o1}} \tag{5-6a}$$

$$\Gamma_2 = \frac{R_2 - Z_{o2}}{R_2 + Z_{o2}} \tag{5-6b}$$

where Z_{o1} and Z_{o2} are the characteristic impedance of the coupled lines at ports 1 and 2, respectively.

The matching conditions for the non-symmetrical case can be obtained by setting $S_{11} = S_{22} = 0$. These are given by:

$$R_1 = \sqrt{Z_{11} / Z_{22} \, (Z_{11} Z_{22} - Z_{12}^2)} \tag{5-7a}$$

$$R_2 = Z_{22}/Z_{11} \cdot R_1 \tag{5-7b}$$

In the symmetrical case the above equations reduce to:

$$R = R_1 = R_2 = \sqrt{Z_{11}^2 - Z_{12}^2} \tag{5-8}$$

The equations (5-6) results in a flat frequency response at the center frequency given by $\Theta = \frac{\pi}{2}$ for $R_1 = Z_{o1}$ and $R_2 = Z_{o2}$ and the first order Chebyshev (single ripple) frequency response for $R_i < Z_{oi}$ $(i = 1,2)$ is characterized by:

$$S_{ii}|_{\text{at } \Theta = \frac{\pi}{2}} = \frac{Z_{oi}^2 - R_i^2}{Z_{oi}^2 + R_i^2}\Bigg|_{\Theta = \frac{\pi}{2}} > 0 \qquad (5\text{-}9)$$

The above equation has been derived by letting $Z_{o1}^2 = Z_{11}^2 - Z_{12}^2$ and $Z_{o2} = Z_{o1}$, and substituting into expressions for S_{11} and S_{12} given by equations (5-1) and (5-3) respectively.

The closed-form design equations for both flat frequency response and single ripple response with the specified maximum ripple can be derived by utilizing the above equations with the assumption of TEM mode propagation (i.e., all normal mode velocities are equal as follows:

For the case of the homogeneous medium [6,7], the eigenvalues are degenerated and $\beta_c = \beta_\pi = j\omega\sqrt{\mu_0\varepsilon_0}$ and the voltage ratios can be chosen as $R_c = -R_\pi = 1$. In terms of the even- and odd-mode impedances of the n-line structure Z_{11}, Z_{12} and Z_{22} for the non-symmetrical two-port coupled lines are given by:

$$Z_{11} = -j \frac{1}{2} (Z_e{}^a + Z_o{}^a) \cot \theta$$

$$Z_{12} = -j \frac{1}{2} (Z_e{}^a - Z_o{}^a) \csc \theta$$

$$Z_{22} = -j \frac{1}{2} (Z_e{}^b + Z_o{}^b) \cot \theta$$

where, $\theta = \beta \ell$, is the normalized frequency and $Z_e{}^a$, $Z_o{}^a$, $Z_e{}^b$, $Z_o{}^b$ are the even- and odd-mode inpedances of line 1 and lines 2, respectively.

Substituting these impedance parameters into S_{11} given by equation (5-1),

$$S_{11} = \frac{k - j \frac{1}{2} (A-B) \cot \theta}{k + j\, 2\, R_1 R_2 - j \frac{1}{2} (A+B) \cot \theta} \qquad (5\text{-}10)$$

where, $Z_e{}^a - Z_o{}^a = Z_e{}^b - Z_o{}^b$

$$k = \frac{1}{4} (Z_e{}^a - Z_o{}^a) (Z_e{}^b - Z_o{}^b) - \frac{1}{2} (Z_o{}^a Z_e{}^b + Z_e{}^a Z_o{}^b) \cdot \cot^2 \theta - R_1 R_2$$

$$= \frac{1}{4} (Z_e{}^a - Z_o{}^a)^2 - \frac{1}{2} (Z_o{}^a Z_e{}^b + Z_e{}^a Z_o{}^b) \cot^2 \theta - R_1 R_2$$

$$A = R_1 (Z_e{}^a + Z_o{}^a)$$

$$B = R_1 (Z_e{}^b + Z_o{}^b)$$

For the symmetrical case the above equation leads to:

$$S_{11} = \frac{- Z_e Z_o \cot^2 \theta + \frac{(Z_e - Z_o)^2}{4} - R^2}{[-Z_e Z_o \cot^2 \theta + \frac{(Z_e - Z_o)^2}{4} + R^2] - j R (Z_e + Z_o) \cot \theta}$$

(5-11)

where, $Z_e = Z_e{}^a = Z_e{}^b$, $Z_o = Z_o{}^a = Z_o{}^b$ and $R_1 = R_2$.

The equation (5-10) results in a flat frequency response at the center frequency given by $\theta = \frac{\pi}{2}$ for

$$R_1 = \frac{1}{2}\left(Z_e{}^a - Z_o{}^a\right)\sqrt{\frac{Z_e{}^a + Z_o{}^a}{Z_e{}^b + Z_o{}^b}} \qquad (5\text{-}12a)$$

and

$$R_2 = \frac{1}{2}\left(Z_e{}^a - Z_o{}^a\right)\sqrt{\frac{Z_e{}^b + Z_o{}^b}{Z_e{}^a + Z_o{}^a}} \qquad (5\text{-}12b)$$

The equation (5-10) also results in a simple ripple response for $R_1R_2 < \frac{1}{4}\left(Z_e{}^a - Z_o{}^a\right)\left(Z_e{}^b - Z_o{}^b\right) = \frac{1}{4}\left(Z_e{}^a - Z_o{}^a\right)^2$ with the maximum ripple given by:

$$\left|S_{11}\right|_{\text{at } \theta = \frac{\pi}{2}} = \frac{\left(Z_e{}^a - Z_o{}^a\right)^2\left(Z_e{}^b - Z_o{}^b\right) - 4R_1R_2}{\left(Z_e{}^a - Z_o{}^a\right)^2\left(Z_e{}^b - Z_o{}^b\right) - 4R_1R_2}$$

$$= \frac{\left(Z_e{}^a - Z_o{}^a\right)^2 - 4R_1R_2}{\left(Z_e{}^a - Z_o{}^a\right)^2 + 4R_1R_2} \qquad (5\text{-}13)$$

For the symmetrical case equations (5-12) and (5-13) lead to

$$R = \frac{\left(Z_e - Z_o\right)}{2} \qquad (5\text{-}14)$$

$$\left|S_{11}\right|_{\text{at } \theta = \frac{\pi}{2}} = \frac{\left(Z_e - Z_o\right)^2 - 4R^2}{\left(Z_e - Z_o\right)^2 + 4R^2} \qquad (5\text{-}15)$$

where $R = R_1 = R_2$ and $R < \frac{\left(Z_e - Z_o\right)}{2}$

For specified R_1, R_2 and bandwidth, Z_e^i and Z_o^i (i = a,b) can be determined from equation (5-10) for flat frequency response and from equations (5-10) and (5-13) for a single ripple response with the specified maximum ripple. Consider the DC block with flat frequency response. For this case, the normalized cut off frequency θ_c, where $S_{11} = \Gamma_c$ (for instance, typical value of $\Gamma_c = \frac{1}{6}$ for maximum SWR = 1.4) is found from equation (5-10) to be:

$$\theta_c = \tan^{-1} \left\{ \left[\frac{-1 + \sqrt{1 + \chi^2 \left(\frac{1}{\Gamma_c^2} - 1\right)}}{2} \right]^{\frac{1}{2}} \right\}$$

or

$$\theta_c = \tan^{-1} \left\{ \chi \left[\frac{(1/\Gamma_c^2) - 1}{2 \left(1 + \sqrt{1 + \chi^2 \left(\frac{1}{\Gamma_c^2} - 1\right)}\right)} \right]^{\frac{1}{2}} \right\} \qquad (5\text{-}16)$$

where a characteristic parameter χ,

$$\chi = \frac{2 \left(Z_e^a Z_o^b + Z_o^a Z_e^b\right)}{\left(Z_e^a - Z_o^a\right)\left(Z_e^b - Z_o^b\right)} = \frac{2 \left(Y_e^a Y_o^b + Y_o^a Y_e^b\right)}{\left(Y_o^a - Y_e^a\right)\left(Y_o^b - Y_e^b\right)}$$

$$= \frac{2 \left(Z_e^a Z_o^b + Z_o^a Z_o^b\right)}{\left(Z_e^a - Z_o^a\right)^2} \qquad (5\text{-}17)$$

For the symmetrical case

$$\chi = \frac{4 Z_e Z_o}{\left(Z_e - Z_o\right)^2} \qquad (5\text{-}18)$$

The closed-form design equations for a symmetrical coupled line two-port structure can be derived as follows by letting $|S_{11}|$ at $\theta = \frac{\pi}{2} = \Gamma_t$ given by equation (5-15) and substituting into equation (5-11).

$$\theta_c = \tan^{-1} \left\{ \left[\frac{-(2 + q\chi) + 2\sqrt{1 + q\chi + \frac{qs}{s-1}\chi^2}}{4 - (1 - \frac{1}{s})\, q} \right]^{\frac{1}{2}} \right\} \qquad (5\text{-}19)$$

where

$$s = \frac{1 + \Gamma_t}{1 - \Gamma_t}, \quad \text{is the maximum SWR.}$$

$$q = s\,(1 - \frac{1}{s})\,(\frac{1}{\Gamma_c 2} - 1)$$

For $\Gamma_t = 0$, the above equation (5-19) leads to equation (5-16) for the flat frequency response. The smaller the χ is, the larger is the fractional bandwidth $[= 2\,(1 - \frac{2\,\theta_c}{\pi})]$.

The design equation for non-symmetrical DC blocks with a Chebyshev frequency response can be formulated in a manner similar to the one presented above for the symmetrical case.

The design procedure for DC blocks, as in the case of other coupled inhomogeneous line structures, can be formulated by assuming TEM mode of propagation (all normal mode velocities are equal) in terms of the equivalent even- and odd-mode immittance of the n-line structure.

The design procedure for DC blocks is illustrated with an example of both symmetrical and non-symmetrical two-line open circuited interdigital two-port structures shown in Fig. 5-1(a) and 5-1(b).

Example: For a specified R = 70 Ω and a predicted fractional bandwidth of 80 % taking $|S_{11}| = \Gamma_c \cong .33$, one can determine Z_e , Z_o and χ for a symmetrical coupled line two-port structure with a flat frequency response from equations (5-14) and (5-16), so that $Z_e = 184 \quad \Omega$, $Z_o = 44 \quad \Omega$ and $\chi = 1.65$.

The values of Z_e and Z_o can be translated into a physical configuration by using published results on a pair of coupled lines [59]. These physical dimensions and effective dielectric constants are:

$$\frac{w_1}{h} = \frac{2s}{h} = .078, \; \varepsilon_{re} = 6.1420 \quad \text{and} \quad \varepsilon_{ro} = 5.5023.$$

In order to verify the above bandwidth, the transmission coefficient for the same structure is derived in terms of the equivalent impedance parameters, as follows. By the use of the boundary condition given by

$$I_2 = I_3 = 0$$

the remaining two-ports are described by the following impedance matrix:

$$[Z] = \begin{bmatrix} Z_{11} & Z_{14} \\ Z_{14} & Z_{22} \end{bmatrix}$$

where the elements of [Z] are expressed by Tripathi [21].

For the symmetrical case, Z_{11} must be chosen such that it is equal to Z_{22}. Substituting the above parameters into expressions for S_{12} given by equation (5-2) gives the exact frequency response shown in Fig. 5-1(c). From this curve, the exact fractional bandwidth taking 0.5 dB ($\Gamma_c \simeq .33$) is found to be 78.9%, while the predicted one is 80 %. The predicted bandwidth is within 1.4 % of the exact one.

For the same symmetrical structure with a single ripple response having the maximum ripple given by $S_{11}|_{\text{at } \theta = \frac{\pi}{2}} = \Gamma_t = \frac{1}{6}$ (SWR = 1.4), the required termination, R, is found by equation (5-15) to be R = 58.3 Ω. The predicted fractional bandwidth taking $\Gamma_c \simeq .33$ is the symmetrical case above with a single ripple response is found by equation (5-19) to be 85.42%. In a manner similar to the case of a flat frequency response, the exact fractional bandwidth taking $\Gamma_c \simeq .33$ is found to be 83.33%. The predicted bandwidth is within 2.5% of the exact value.

Examination of the results reveals that the bandwidth of the ripple response is slightly improved, e.g., by about 5.3% from that of the flat response.

Consider a non-symmetrical two-line structure with the relative dielectric constant $\varepsilon_r = 10$ and the geometry given by $\frac{w_1}{h} = \frac{w_2}{h} = \frac{2s}{h} = 0.78$.

The normal mode parameters found by using the technique [67] are found to be:

Mode c; $\varepsilon_{eff} = 6.3395$, $Z_{c1} = 226.60\ \Omega$, $Z_{c2} = 101.55\ \Omega$,

$R_{vc} = 1.0033$

Mode π; $\varepsilon_{eff} = 5.5069$, $Z_{\pi 1} = 52.02\ \Omega$, $Z_{\pi 2} = 23.31\ \Omega$,

$R_{v\pi} = -.4466$

Since $(Z_{c1} - Z_{\pi 1})$ is greater enough not to compare with $(Z_{c2} - Z_{\pi 2})$, the design equation for the non-symmetrical two-line DC blocks given by equation (5-10) can not be applied, where $Z_e^a - Z_o^a = Z_e^b - Z_o^b = Z_c - Z_\pi$ for TEM mode is given by Tripathi [21].

However, the terminations, R_1, R_2, and a fractional bandwidth in a non-symmetrical two-line DC block with a flat frequency response can be found as follows by using equations (5-2) and (5-7) derived in terms of the equivalent impedance described above. The exact flat frequency response obtained is shown in Fig. 5-1(c). In the non-symmetrical case with the flat response, the fractional bandwidth taking $\Gamma_c = .33$ is 53.3%. The fractional bandwidth in the symmetrical case with the flat frequency response is about 32% wider than the one in the non-symmetrical case.

5.3 ANALYSIS AND DESIGN FOR THREE-LINE STRUCTURES

Both symmetrical and non-symmetrical two-port DC blocks and filters shown in Fig. 5-2(a) and (b) can be realized with a symmetrical three-line structure. In this case, ports 2, 4 and 6 are open circuited and ports 1 and 3 are interconnected. The design procedure for both cases is the same as the one presented in the previous section for two-line DC blocks.

As stated in the previous section, for the case of the symmetrical three-line two-port DC block shown in Fig. 5-2(a) with specified termination R and bandwidth, one can determine Z_e and Z_o from equations (5-14) and (5-16) for a flat frequency response and from equations (5-15) and (5-16) for a single ripple response having a specified maximum ripple.

In the case of the non-symmetrical three-line two-port DC block shown in Fig. 5-2(b), with specified terminations, R_1, R_2 and bandwidth, one can determine Z_e^a , Z_o^b and Z_o^a , Z_o^b (where, i = a, b, and Z_e^a , Z_e^b and Z_o^a , Z_o^b are the even- and odd-mode impedances of line 1 and 2, respectively) from equations (5-12) and (5-16) for a flat frequency response and from equations (5-12), (5-13) and (5-16) for a single ripple frequency response having a specified maximum ripple. However, since, in the interdigital three-line structure, mode a is not excited (as described in the design of Section 4.2) in the symmetrical three-line interdigital two-port structure, Z_e and Z_o must be replaced by Z_{b2} and Z_{c2}, respectively, and in the non-symmetrical case, Z_e^a , Z_e^b and Z_o^a , Z_o^b must be replaced by Z_{b1}, Z_{b2} and Z_{c1}, Z_{c2}, respectively.

Once the characteristic impedances of lines are determined as described above, these values must be translated into the physical dimensions to design the specified DC blocks and filters. The physical dimensions for design and normal mode parameters for the exact analysis can be found by trial and error method in a manner

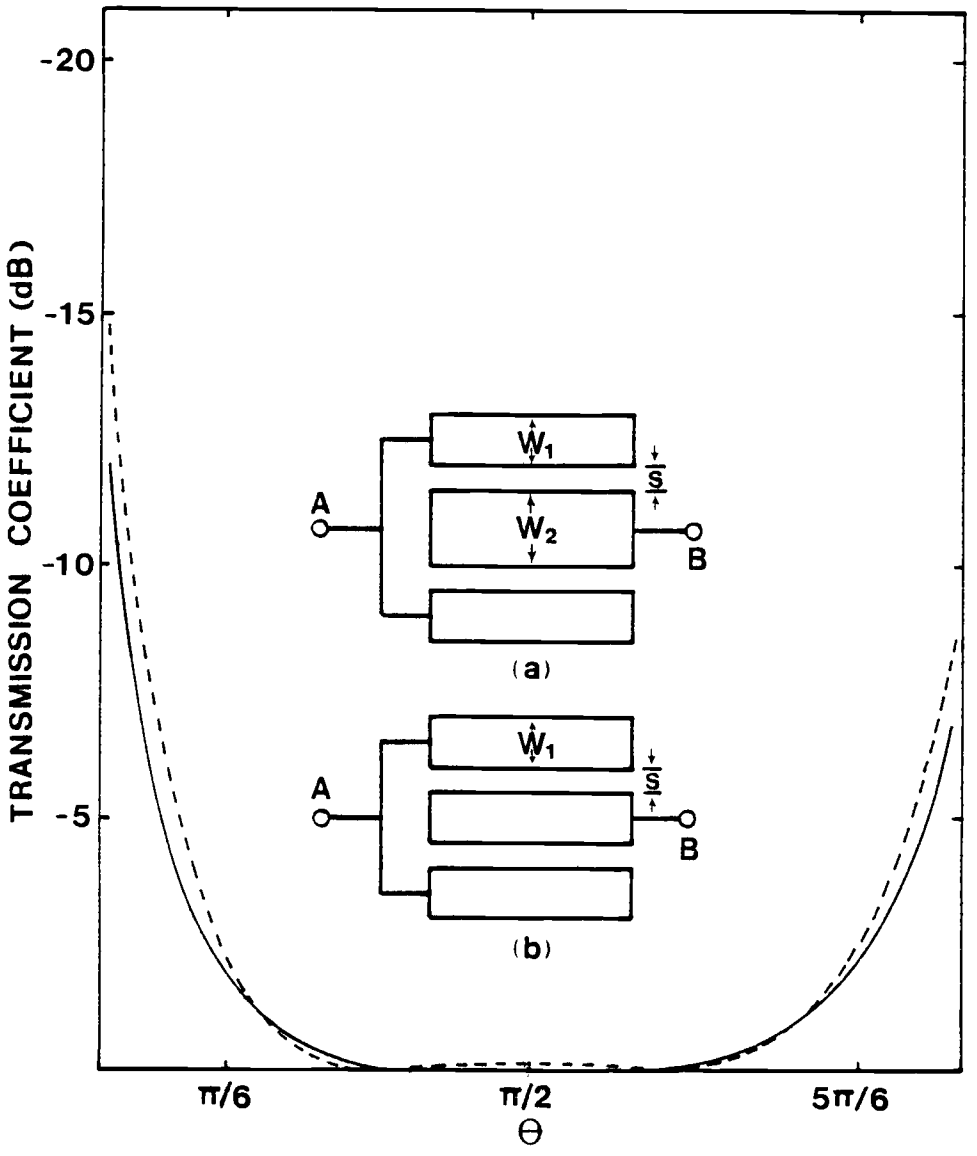

Figure 5-2. Transmission coefficient $|S_{12}|$ vs normalized frequency for open-circuited interdigital three-line coupled (a) symmetrical(where $w_1/h = w_2/4h = 2s/h = 0.078$) and (b) non-symmetrical(where $w/h = 2s/h = 0.078$) DC blocks with $\varepsilon_r = 10$.

———— Flat response for (a) with terminations R = 50 ohms, and for (b) with terminations R_1= 58.61 ohms and R_2= 66.73 ohms.

--------- Ripple response for (a) with terminations R = 42.39 ohms given by $|S_{11}|_{\theta = \pi/2} = 1/6$.

similar to the approach described in section 4.2. Since the immittance parameters can be derived in terms of the normal mode parameters one can design the specified circuit by analyzing the circuit exactly, as follows.

Using the boundary conditions given by $I_2 = I_4 = I_6 = 0$ and $V_1 = V_3$ with $I_a = I_1 + I_3 = 2I_1$, the two-port circuit is described by the following impedance matrix:

$$[Z] = \begin{bmatrix} Z_{22} & Z_{15} \\ Z_{15} & \frac{Z_{11} + Z_{13}}{2} \end{bmatrix}$$

where the elements of [Z] are expressed by Tripathi [95] and for the symmetrical case Z_{22} must be chosen such that it is equal to $(Z_{11} + Z_{13})/2$.

These parameters are substituted into expressions for a flat response or for a single ripple response to determine the terminations. For example, for a flat frequency response, terminations can be found from the matching conditions given by equations (5-7). These parameters and the terminations are also substituted into expressions for the transmission coefficient given by equation (5-2) to find the flat frequency response or the single ripple response. Through this response, the predicted bandwidth can be checked exactly.

A procedure to analyze and design three-line DC blocks is illustrated with an example.

Example: Consider the symmetrical case with a flat frequency response. $Z_{b2} = 122.86\ \Omega$ and $Z_{c2} = 20.9\ \Omega$ can be found by the procedure described above, such that Z_{b2} and Z_{c2} satisfy a specified termination of 50 Ω and a predicted fractional bandwidth of 100.02%.

The physical dimensions and normal mode parameters for Z_{b2} and Z_{c2} obtained above can be determined as follows by the trial and error method presented in Section 4.2: $w_1/h = 2s/h = w_2/4h = .078$ and the normal mode parameters are given in Table 4-1.

Since it is very difficult to find the exact symmetrical structure for $Z_{22} = (Z_{11} + Z_{13})/2$, the matching terminations for the symmetrical two-port case above are calculated by equation (5-7) as $R_1 = 50.97\ \Omega$ and $R_2 = 50.17\ \Omega$. The exact flat frequency response is shown in Fig. 5-2(c). Then, the exact fractional bandwidth obtained is 100%.

The same symmetrical structure, having a single ripple response and terminating in $R_1 = 43.1\ \Omega$ and $R_2 = 42.4\ \Omega$ found by equation (5-9) for the maximum ripple given by $\Gamma_c = \frac{1}{6}$, has a predicted fractional bandwidth of 105%. The exact bandwidth found through equation (5-2) is 105.56%. The exact ripple frequency responce is shown in Fig. 5-2(c).

A comparison between the two cases shows the bandwidth for the single ripple response is improved by 5% more than that bandwidth for the flat response.

In the non-symmetrical case with a flat frequency response, the physical dimensions and normal mode parameters for $Z_{b1} = 213.7\ \Omega$,

Z_{c1} = 32 Ω, Z_{b2} = 203.9 Ω and Z_{c2} = 35.1 Ω satisfying specified terminations, R_1 = 58.6 Ω, R_2 = 66.7 Ω and the predicted fractional bandwidth of 103.34%, are: $w_1/h = w_2/h = 2s/h = .078$ and the normal mode parameters are given in Table 4-1. The exact flat frequency response obtained as decribed above is shown in Fig. 5-2. The exact fractional bandwidth is 100%. A comparison of two cases reveals that the predicted one is 3% more than the exact one.

The design procedure for Chebyshev frequency response in the non-symmetrical case can be formulated in a manner similar to the one presented above in the symmetrical case with Chebyshev frequency response.

5.4 ANALYSIS AND DESIGN OF INTERDIGITATED MULTIPLE COUPLED TWO-PORT WITH FOUR OR MORE LINES

For an n-line open circuited interdigital structure as shown in Fig. 5-3, the scattering parameters can be found from the 2n-port impedance matrix with (2 n-2) boundary conditions. For example, for n even, these conditions are $I_A = I_1 + I_3 + \ldots + I_{n-1}$; $I_B = I_{n+1} + I_{n+3} + \ldots + I_{2\,n-1}$; $I_2 = I_4 = \ldots = I_n = I_{n+2} = \ldots = I_{2n} = 0$; $V_A = V_1 = V_3 = \ldots = V_{n-1}$ and $V_B = V_{n+1} = V_{n+3} = \ldots = V_{2n-1}$. The expressions for the elements of the impedance matrix for a 2n-port are known in a closed form for the symmetrical four-line case given in Appendix A. For a larger number of lines it is more convenient to compute the frequency response of the DC block on a digital computer by utilizing the boundary conditions and the general expressions for the immittance matrix of this n-line system.

As is the case of other coupled inhomogeneous line structures, the design procedure for DC blocks can be formulated by assuming the TEM mode of propagation in terms of the equivalent even- and odd-mode immittances of the n-line structure. For the n-line interdigital structure, these are found in the same manner as for the case of interdigitated couplers and are given below for even and odd number of lines.

n-even

$$\frac{1}{Z_{en}} = Y_{en} \simeq v_p[C_{11} - C_{12} + (\frac{n}{2} - 1)\ (C_{22} - 2\ C_{12})] \qquad (5\text{-}20a)$$

$$\frac{1}{Z_{on}} = Y_{on} \simeq v_p[C_{11} + C_{12} + (\frac{n}{2} - 1)\ (C_{22} + 2\ C_{12})] \qquad (5\text{-}20b)$$

n-odd

$$\frac{1}{Z_{en}^{(A)}} = Y_{en}^{(A)} \simeq v_p\ [2\ (C_{11} - C_{12}) + (\frac{n-3}{2})(C_{22} - C_{12})] \qquad (5\text{-}21a)$$

$$\frac{1}{Z_{on}^{(A)}} = Y_{on}^{(A)} \simeq v_p\ [2\ (C_{11} + C_{12}) + (\frac{n-3}{2})(C_{22} + 2\ C_{12})] \qquad (5\text{-}21b)$$

$$\frac{1}{Z_{en}^{(B)}} = Y_{en}^{(B)} \simeq v_p\ [(\frac{n-1}{2})\ (C_{22} - 2\ C_{12})] \qquad (5\text{-}21c)$$

$$\frac{1}{Z_{on}^{(B)}} = Y_{on}^{(B)} \simeq v_p\ [(\frac{n-1}{2})\ (C_{22} + 2\ C_{12})] \qquad (5\text{-}21d)$$

In the above equations, v_p is the phase velocity, C_{11} is the self capacitance of lines 1 and n, C_{22} is the self capacitance of lines 2 through n-1, and C_{12} is the mutual capacitance between adjacent lines. In addition, all the lines are assumed to have equal widths and the

coupling between nonadjacent lines is neglected. A structure with an odd number of lines is inherently nonsymmetrical and in order to design a symmetrical two-port, the widths of lines 2, 4, ..., n-1 must be chosen differently from the width of lines 1, 3, ..., n [with C_{22} in equations (5-21 c) and (5-21 d) changed accordingly] such that $Y_{on}^{(A)} = Y_{on}^{(B)}$ and $Y_{en}^{(A)} = Y_{en}^{(B)}$ as described in the previous section for three-line structure.

For a given n-line structure, χ can be estimated by the following equation derived in terms of even- and odd-mode impedances of a pair of lines [59] by using equation (5-20) and the relationship between C_{11} and C_{22} given by Ou [87].

$$\chi = \frac{\frac{n}{2}(Z_e + Z_o) + (\frac{n}{2} - 1)\frac{(Z_e - Z_o)^2}{(Z_e + Z_o)} - (n-1)^2 (Z_e - Z_o)^2}{(n-1)^2 (Z_e - Z_o)^2} \qquad (5-22)$$

As an example, consider the two-line structure of La Combe and Cohen [84] with $Z_e = 130\ \Omega$, $Z_o = 24\ \Omega$ and a fractional bandwidth of 68.35% for $\Gamma_c = \frac{1}{6}$. The fractional bandwidth is increased to 104.4% for the four-line and 118% for the six-line structures. Examination of typical cases indicates that increasing the number of lines beyond four may not be very advantageous. Consider the symmetrical four-line structure as an example.

In a symmetrical four-line DC blocks with ports, 2, 4, 5 and 7 open-circuited as shown in Fig. 5-4 and having a flat frequency response, for a specified termination of $R = 67.6\ \Omega$ and a predicted fraction bandwidth of 117.47%, one can determine $Z_e = 181.61\ \Omega$,

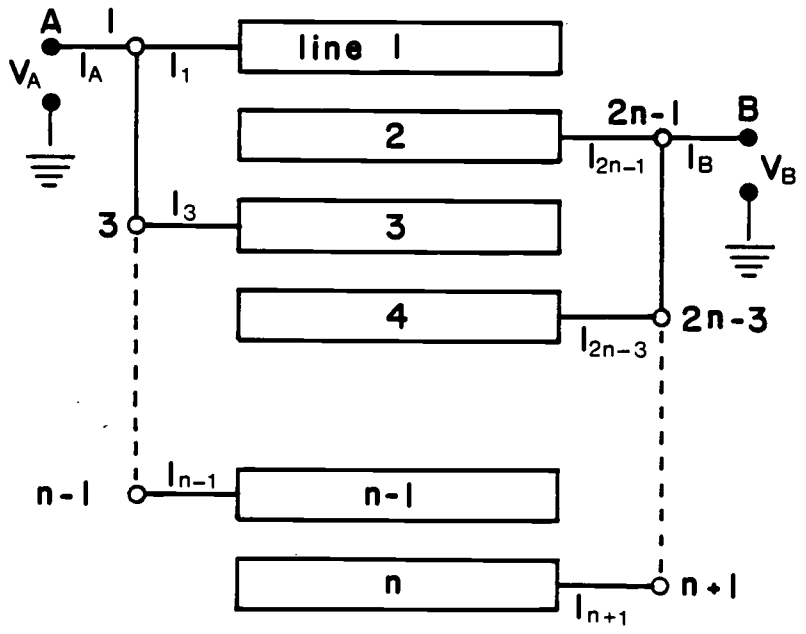

Figure 5-3. Schematic of an open-circuited interdigital multiple coupled line two-port.

Z_o = 43.44 and χ = .6644 by using equation (5-14), (5-16) and (5-22). Then the physical dimensions and normal mode parameters can be found as follows in a manner similar to the three-line case described in the previous section.

The results obtained are: w/h = 2s/h = .078 and

Mode a; ε_{eff} = 6.3354, Z_{a1} = 224.67 Ω, Z_{a2} = 377.76 Ω, R_{va} = 1.00393

Mode b; ε_{eff} = 5.5142, Z_{b1} = 73.56 Ω, Z_{b2} = 127.99 Ω, R_{vb} = 3.4045

Mode c; ε_{eff} = 5.5001, Z_{c1} = 34.61 Ω , Z_{c2} = 58.19 Ω , R_{vc} = -1.67482

Mode d; ε_{eff} = 5.5000, Z_{d1} = 21.52 Ω , Z_{d2} = 37.44 Ω , R_{vd} = -5.11101

In order to find the exact flat frequency response, one must first derive the equivalent impedance matrix from the boundary conditions given by $I_2 = I_4 = I_5 = I_7 = 0$.

The impedance matrix obtained is:

$$\begin{bmatrix} V_1 \\ V_3 \\ V_6 \\ V_8 \end{bmatrix} = \begin{bmatrix} Z_{11} & Z_{13} & Z_{16} & Z_{18} \\ Z_{13} & Z_{22} & Z_{17} & Z_{16} \\ Z_{16} & Z_{27} & Z_{22} & Z_{13} \\ Z_{18} & Z_{16} & Z_{13} & Z_{11} \end{bmatrix} \begin{bmatrix} I_1 \\ I_3 \\ I_6 \\ I_8 \end{bmatrix}$$

where the elements of the impedance matrix are given in Appendix A.

Then, taking the inverse of the above matrix and using the boundary conditions given by $I_a = I_1 + I_3$, $I_b = I_6 + I_8$, $V_a = V_1 = V_3$ and $V_b = V_6 = V_8$, the final equivalent admittance matrix of the two-port circuit is found to be:

$$[Y] = \begin{bmatrix} Y_{11} & Y_{12} \\ Y_{12} & Y_{11} \end{bmatrix}$$

where

$$\begin{bmatrix} y_{11} & y_{12} & y_{13} & y_{14} \\ y_{21} & y_{22} & y_{23} & y_{24} \\ y_{31} & y_{32} & y_{33} & y_{34} \\ y_{41} & y_{42} & y_{43} & y_{44} \end{bmatrix} = \begin{bmatrix} z_{11} & z_{13} & z_{16} & z_{18} \\ z_{13} & z_{22} & z_{17} & z_{16} \\ z_{16} & z_{27} & z_{22} & z_{13} \\ z_{18} & z_{16} & z_{13} & z_{11} \end{bmatrix}^{-1}$$

$$Y_{11} = y_{11} + 2\,Y_{12} + y_{22}$$

$$Y_{12} = y_{13} + y_{14} + y_{24}$$

Using the matching condition for an admittance expression given by

$$R = \frac{1}{G} = \frac{1}{\sqrt{y_{11}^2 - y_{12}^2}},$$

the termination is found to be R = 67.6 Ω.

The exact flat frequency response terminated in R = 67.6 Ω and the simple ripple response terminated in R = 57.1 Ω (found by using equation (5-15) for a specified maximum ripple given by $S_{11} \mid_{\text{at } \theta = \frac{\pi}{2}} = \frac{1}{6}$) are shown in Fig. 5-4.

The exact fractional bandwidth of the flat case is 111.11%. The exact fractional bandwidth of the simple ripple case is 117.78%, while the predicted one is 121.02%. The exact flat frequency response for transmission coefficients of two, three and four-line cases is shown in Fig. 5-5 for their comparison.

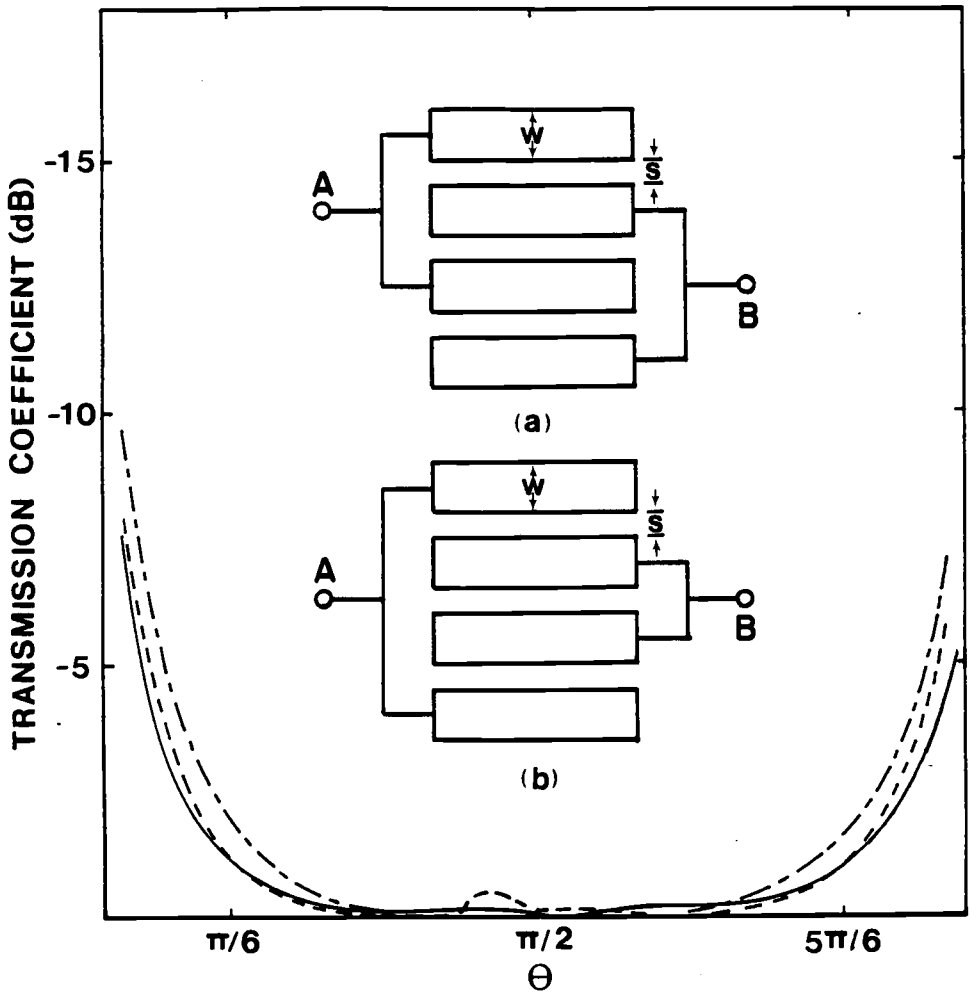

Figure 5-4. Transmission coefficient $|S_{12}|$ vs normalized frequency Θ for open-circuited interdigital four-line coupled for (a) symmetrical and (b) non-symmetrical DC blocks(where w/h = 2s/h = 0.078) with ε_r= 10.

——— Flat response for (a) with terminations R = 67.62 ohms.

- — - — Flat response for (b) with terminations R_1= 61.07 ohms and R_2= 58.23 ohms.

--------- Ripple response for (a) wth terminations R = 57.14 ohms given by $|S_{11}|_{\theta = \pi/2}$= 1/6.

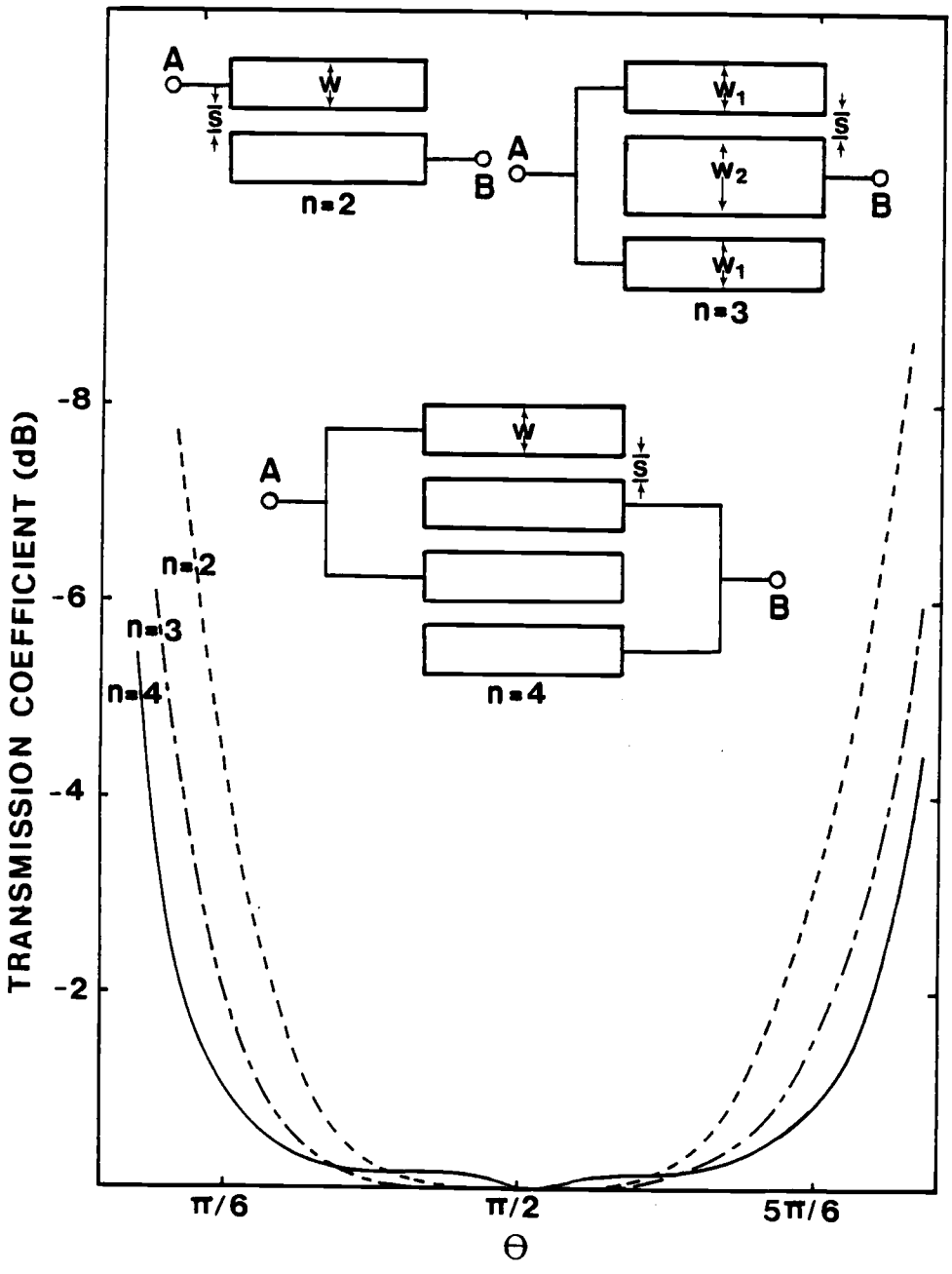

Figure 5-5. Transmission coefficient $|S_{12}|$ vs normalized frequency Θ for multiple coupled microstrip line DC block with ε_r=10 (where w/h = 2s/h = 0.078 and R = 69.1 ohms for n = 2 ; w_1/h= 2s/h = w_2/4h = 0.078 and R = 50.6 ohms for n = 3; w/h = 2s/h = 0.078 and R = 67.6 ohms for n = 4).

5.5 EXPERIMENTAL RESULTS

A three-line DC block was fabricated at Chalmers University of Technology in Gothenburg, Sweden on R T Duroid substrate(ε_r= 10.5) with its thickness h = 1.25 mm[115]. The original design geometry for a symmetrical block with 50 Ω terminations was computed to be w_1= w_3= .0875 mm , w_2= .37 mm and s = .0488 mm . However, because of the overetching of the thin lines the final geometry measured was w_1= w_3= .0375 mm , w_2= .375 mm and s = .0875 mm shown in Fig.5-6(a), which results in a non-symmetrical block with input and output matching impedances of 50 Ω and 44 Ω respectively. The computed and measured results for the transmission and reflection coefficients are shown in Fig.5-6(b) and(c), and as seen the experimental results are in good agreement with the theoretically predicted ones. The minor discrepancy is primarily due to the junction discontinuities, conductor and radiation losses.

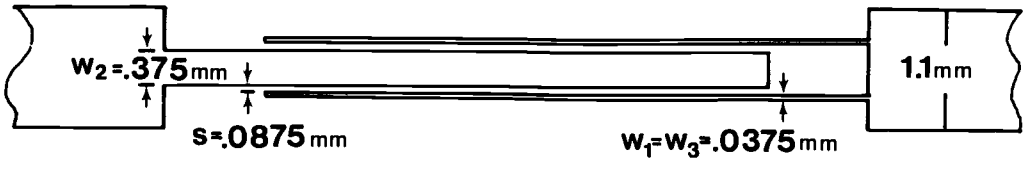

Figure 5-6(a) Measured geometrical layout of an interdigitated three-line DC block with ε_r= 10.5 (where, the substrate thickness h = 1.25 mm).

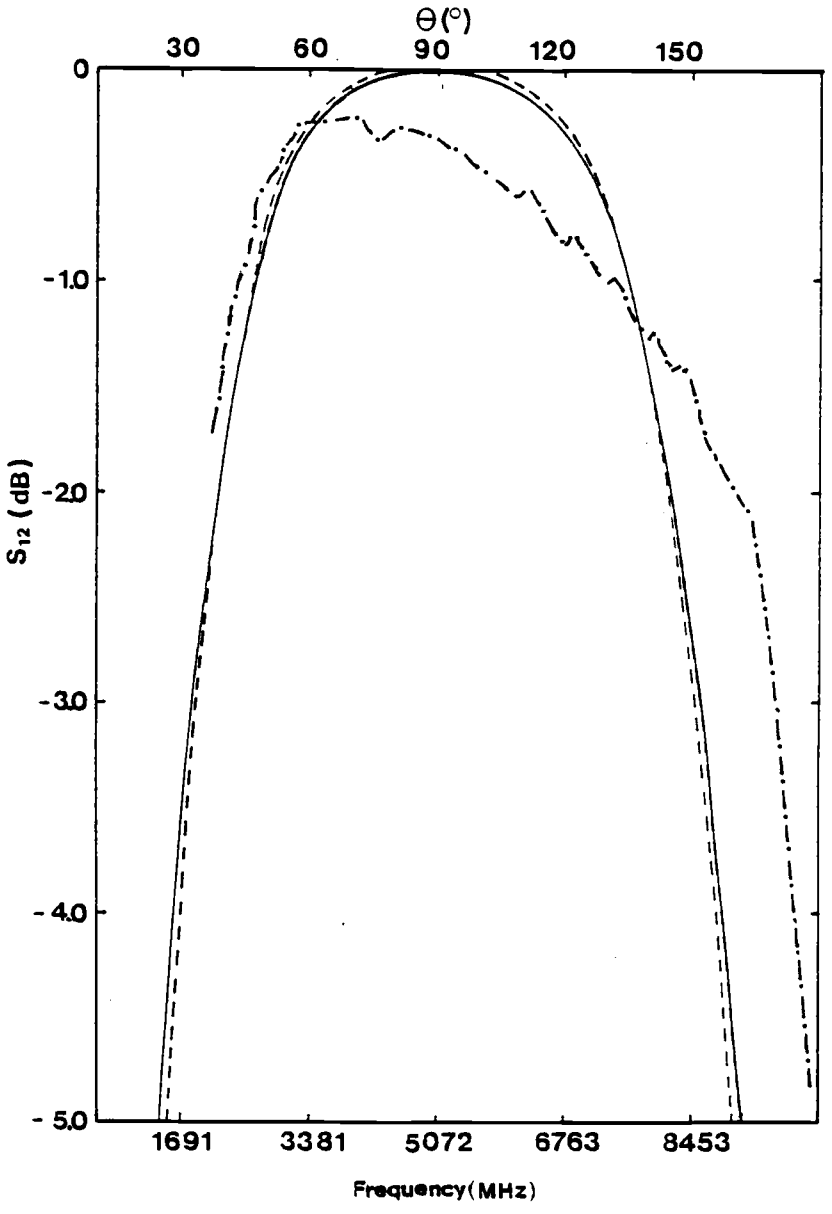

Figure 5-6 (b). Transmission coefficients $|S_{12}|$ vs frequency for an open-circuited interdigital three-line coupled non-symmetrical DC block as that in Figure 5-6(a).

— - — - — Measured response with terminations $R_1 = R_2 = 50\,\Omega$.

——————— Theoretical response with terminations $R_1 = R_2 = 50\,\Omega$.

---------- Theoretical response with perfect matching terminations $R_1 = 50.16\,\Omega$ and $R_2 = 43.83\,\Omega$.

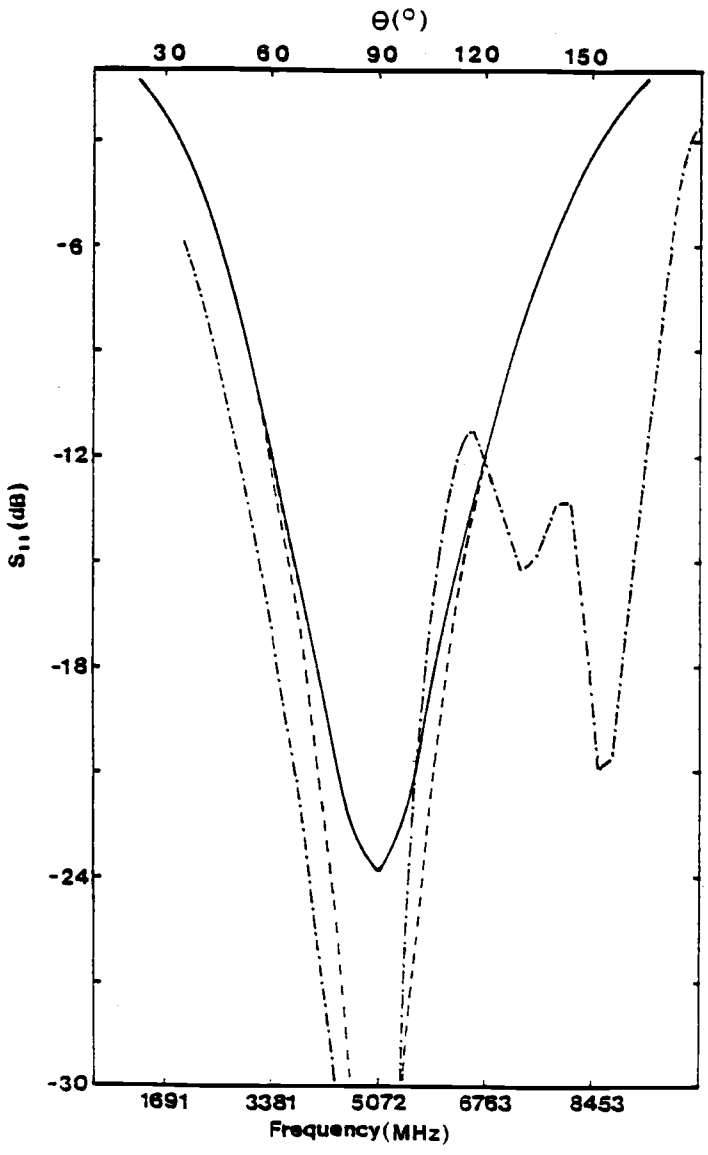

Figure 5-6(c). Reflection coefficients $|S_{11}|$ vs frequency for the same open-circuited interdigital three-line coupled non-symmetrical DC block as that in Figure 5-6 (a).

5.6 CONCLUDING REMARKS

Analysis and design procedures for both symmetrical and non-symmetrical open-circuited interdigital multiple coupled microstrip line structures for applications as wideband DC blocks and filters have been presented. The design equations, as is the case of other microstrip structures, are based on a simplified TEM model.

The structures can be designed for a specified bandwidth for the flat frequency or Butterworth response and for a specified bandwidth and maximum ripple for a single rippled response characteristics. The exact frequency responses for the transmission coefficient computed by utilizing the quasi-TEM parameters of coupled microstrip lines for the two, three and four-line cases have been presented in terms of their respective equivalent immittance parameters. These results are fairly close to the ones obtained by the approximate TEM model.

Examination of typical cases indicates that increasing the number of lines beyond four may not be remunerative.

CHAPTER VI. Conclusions

The procedure for finding the immittance of a general n-line coupled structure in an inhomogeneous medium has been presented in terms of the normal mode parameters of the n-line coupled system. The expressions are in a convenient form for both computational purposes and deriving the explicit closed form expressions for the elements of the 2n-port immittance matrix. As an example, the closed form expressions for the elements of the admittance matrix of a symmetrical eight-port structure are given in Appendix A.

The scattering parameters of a general coupled line four-port with arbitrary terminations are derived directly from the normal mode parameters of the system by using the definition of the scattering parameters. It is shown that these can also be derived in terms of the scattering parameters of the four-port with non-mode terminations and the new arbitrary terminations. This formulation is quite general and can be applied to various coupled guided wave systems including coupled microstrip lines, slot lines, comb lines, dielectric waveguides and various other uniformly coupled transmission systems. The results obtained have been used to present the procedure to determine the optimum terminations for directional couplers and derive the expressions for the sensitivity of four-port couplers to changes in terminations.

Analysis and design procedures for both the symmetrical and non-symmetrical interdigitated four-port directional couplers of

symmetrical three lines have been presented. Physical dimensions of 3, 6 and 10 dB couplers with substrates having typical dielectric constant values of 2.55 and 10 can be found by using the tables and charts given in Chapter IV. Analysis and design procedures for both symmetrical and non-symmetrical open-circuited interdigital multiple coupled microstrip line structures for applications as wide-band DC blocks and filters have been presented. The design equations, as is the case of other microstrip structures, are based on a simplified TEM model. The structures can be designed for a specified bandwidth for the flat frequency response and for a specialized bandwidth and maximum ripple for a single rippled response characteristics.

Examination of typical cases indicates that increasing the number of lines beyond four may not be renumerative.

Some suggestions for further work are included in the following paragraphs. There is a need for obtaining the analytical solutions leading to the conditions for infinite directivity and impedance matching in a general non-symmetrical directional couplers in an inhomogeneous medium, though the same has been presented by Cristal [7] in a homogeneous medium. Since the general expressions for finding the network functions, e.g., the immittance and scattering parameters of a general, uniformly coupled n-line structure in an inhomogeneous medium are in a convenient form and have wider applications than those presented in this thesis.

The technique for analysis and design of multiple coupled interdigital two-port with three and four lines offers satisfactory results

which are close to the exact results. Further investigation is needed for improving the bandwidth and for additioned applications of such structures as power dividers/combiners, comb-line band-pass filters and other multiple coupled two-port filters. These can be carried out by similar techniques to the ones presented in this thesis.

It would be very useful from a practical standpoint to know how well and over what frequency range, these models work, where the assumption of a TEM mode of propagation is not strictly valid. In particular dispersion effects are not known and could have a significant effects on bandwidth and directivity of the couplers.

BIBLIOGRAPHY

1. Carson, J.R. and Hoyt, R.S. "Propagation of Periodic Waves Over a System of Parallel Wires," Bell System Tech. Jour., Vol. 6, pp. 495-545; 1927.

2. Pipes, L.A., "Matrix Theory of Multiconductor Transmission Lines," Phi. Mag., Vol. 24, pp. 97-113; July 1937.

3. Rice, S.Q., "Steady State Solution of Transmission Line Equations," Bell System Tech. Jour., Vol. 20, pp. 131-178; 1941.

4. Oliver, B.M., "Directional Electromagnetic Couplers," Proc. IRE, Vol. 42, No. 11, pp. 1686-1692; November 1954.

5. Jones, E.M.T., and Bolljahn, J.T., "Coupled-Strip-Transmission Line Filters and Directional Couplers," IRE Trans. Microwave Theory and Techniques, Vol. MIT-4, pp. 75-81; April 1956.

6. Ozaki, H. and Ishii, J., "Synthesis of a Class of Strip Line Filters," IRE Trans. Circuit Theory, Vol. CT-5, pp. 104-109; June 1958.

7. Cristal, E.G., "Coupled-Transmission-Line Directional Couplers With Coupled Lines of Unequal Characteristic Impedance," IEEE Trans. Microwave Theory and Techniques, Vol. MIT-14, pp. 337-346; July 1966.

8. Vlostovskiy, E.G., "Theory of Coupled Transmission Lines," Telecommun. and Radio Engg., Vol. 21, pp. 87-93; April 1967.

9. Amemiya, H., "Time Domain Analysis of Multiple Parallel Transmission Lines," RCA Review, Vol. 28, pp. 241-276; June 1967.

10. Sharpe, C.B., "An Equivalence Principle for Non-Uniform Transmission Line Directional Couplers; IEEE Trans. Microwave Theory and Techniques, Vol. MIT-15, pp. 398-405; July, 1967.

11. Zysman, G.I. and Johnson, A.D., "Coupled Transmission Line Networks in an Inhomogeneous Dielectric Medium," IEEE Trans. Microwave Theory and Techniques, Vol. MIT-17, pp. 753-759; October 1969.

12. Krage, M.K., and Haddad, G.I., "Characteristics of Coupled Microstrip Transmission Lines - I: Coupled Mode Formulation of Inhomogeneous Lines," IEEE Trans. Microwave Theory and Techniques, Vol. MIT-18, pp. 217-222; April 1970.

13. Chang, F.Y., "Transient Analysis of Lossless Coupled Transmission Lines in a Nonhomogeneous Dielectric Medium," IEEE Trans. Microwave Theory and Techniques, MTT-18, pp. 616-626; September 1970.

14. Guckel, H. and Sun, Y.Y., "Uniform Multimode Transmission Lines," IEEE Trans. Microwave Theory and Techniques, Vol. 6, pp. 412-413, June 1972.

15. Marx, D.K., "Propagation Modes, Equivalent Circuits, and Characteristics Terminations for Multiconductor Transmission Lines with Inhomogeneous Dielectrics," IEEE Trans. Microwave Theory and Techniques, Vol. MTT-21, pp. 450-457; July 1973.

16. Noble, D.F. and Carlin, H.J., "Circuit Properties of Coupled Dispersive Transmission Lines," IEEE Trans. Circuit Theory, Vol. CT-20, No. 1, pp. 56-54; January 1973.

17. Ekinge, R.B., "A New Method of Synthesizing Matched Broad-Band TEM-mode Three-ports," IEEE Trans. Microwave Theory and Techniques, Vol. MTT-19, pp. 81-88; January 1971.

18. Speciale, R.A., "Fundamental Even- and Odd-Mode Waves for Non-Symmetrical Coupled Lines in Non-Homogeneous Media," 1974 IEEE S-MIT International Microwave Symp. Digest Tech. Papers, pp. 156-158; June 1974.

19. Allen, J.L., "Non-Symmetrical Coupled Lines in an Inhomogeneous Dielectric Medium," International Jour. Electronics, Vol. 38, pp. 337-347; March 1975.

20. Speciale, R.A., "Even- and Odd-Mode Waves for Non-symmetrical Coupled Lines in a Nonhomogeneous Media," to appear in IEEE Trans. Microwave Theory and Techniques, Vol. 23, No. 11; November 1975.

21. Tripathi, V.K., "Asymmetric Coupled Transmission Lines in an Inhomogeneous Medium," IEEE Trans. Microwave Theory and Techniques, Vol. 23, No. 9, pp. 734-739; September 1975.

22. Tripathi, V.K., "Properties and Applications of Asymmetric Coupled Line Structures in an Inhomogeneous Medium," Proc. 5th European Microwave Conference; pp. 278-282, Hamburg; September 1975.

23. Kaupp, H.R., "Pulse Crosstalk Between Microstrip Transmission Lines," 7th Intl. Electronic Circuit Packaging Symp. Record (WESCON 66) 2/4; August 1966.

24. Arvanitakis, N.C., et al., "Coupled Noise Prediction in Printed Circuit Boards for High-Speed Computer System," 7th Intl. Electronic Circuit Packaging Symp. Record (WESCON 66), 2/6; August, 1966.

25. Catt, I., "Crosstalk (Noise) in Digital Systems," IEEE Trans. Electronic Computers, Vol. EC-16, pp. 743-763; December 1967.

26. Okugawa, S. and Hagiwara, H., "Analysis and Computation of Crosstalk Noise Between Microstrip Transmission Lines," Electronics and Communication (Japan), Vol. 53-C, No. 7, pp. 128-135; 1970.

27. Young, Leo, Ed., Artech House, A comprehensive set of publications on the theory and design of coupled lines in a homogeneous medium is compiled in: "Parallel Coupled Lines and Directional Couplers" and "Microwave Filters Using Parallel Coupled Lines," 1972.

28. Matthaei, G.L., et al., "Microwave Filters, Impedance Matching Networks, and Coupling Structures," McGraw-Hill Book Co., Inc., New York; 1964.

29. Matsumato, A., Ed., "Microwave Filters and Circuits," Advances in Microwavew Supplement I, Academic Press; 1970.

30. Cohn, S.B., "Slot Line on a Dielectric Substrate," IEEE Trans. Microwave Theory and Techniques, Vol. MTT-17, No. 10, pp. 768-778; October 1969.

31. Knorr, J.B. and Kuchler, K.D., "Analysis of Coupled Slots and Coplanar Strips on Dielectric Substrates," IEEE Trans. Microwave Theory and Techniques, Vol. MTT-23, No. 7, pp. 541-548; July 1975.

32. Itoh, T. and Mittra, R., "Dispersion Characteristics of Slot Lines," Electronics Letters, Vol. 7, pp. 364-365; July 1971.

33. Mariani, E.A., Heinzman, C.P., Agrios, J.P. and Cohn, S.B., "Slot Line Characteristics," IEEE Trans. Microwave Theory and Techniques, Vol. MTT-17, pp. 1091-1096; December 1969.

34. Kitazawa, T., Fujiki, Y., Hayashi, Y. and Suzuki, M., "Slot Line with Thick Metal Coating," IEEE Trans. Microwave Theory and Techniques, Vol. MTT-21, pp. 580-582; September 1973.

35. Wen, C.P., "Coplanar Waveguide: A surface Strip Transmission Line Suitable for Nonreciprocal Gyromagnetic Device Applications," IEEE Trans. Microwave Theory and Techniques, Vol. MTT-17, pp. 1087-1090; December 1969.

36. Knorr, J.B. and Kuchler, K.D., "Analysis of Coupled Slots and Coplanar Strips on Dielectric Substrate," IEEE Trans. Microwave Theory and Techniques, Vol. MTT-23, pp. 541-548; July 1975.

37. Pregla, R. and Pintzos, S.G., "Determination of the Propagation Constants in Coupled Microslots by a Variational Method," Proc. 5th Colloquium on Microwave Comm., Vol. IV, pp. MT-491-500; Budapest, Hungary; June 24-30, 1974.

38. Kitzzawa, T., Hayashi, Y. and Suzuki, M., "A Coplanar Waveguide with Thick Metal Coating," IEEE Trans. Microwave Theory and Techniques, Vol. MTT-24, pp. 604-608; September 1976.

39. Wen, C.P., "Coplanar-Waveguide Directional Couplers," IEEE Trans. Microwave Theory and Techniques, Vol. MTT-18, pp. 318-322; June 1970.

40. Allen, J.L., "Inhomogeneous Coupled Line Filters with Large Mode Velocity Ratios," IEEE Trans. Microwave Theory and Techniques, Vol. MTT-22, pp. 1182-1186; December 1974.

41. Schneider, M.V., "Microstrip Lines for Microwave Integrated Circuits," Bell System Tech. Jour., Vol. 48, pp. 1421-1444; May-June 1969.

42. Wheeler, H. A.,"Transmission Line Properties of Parallel Wide Strips by Conformal Mapping Approximation," IEEE Trans. Microwave Theory and Techniques, Vol. MTT-12, pp. 280-289; 1964.

43. Wheeler, H. A., "Transmission Line Properties of Parallel Strips Separated by a Dielectric Sheet," IEEE Trans. Microwave Theory and Techniques, Vol. MTT-13, pp. 172-185; March 1965.

44. Smith, J.I., "The Even- And Odd-Mode Capacitance Parameters for Coupled Lines in Suspended Substrate," IEEE Trans. Microwave Theory and Techniques, Vol. MTT-19, pp. 424-431; May 1971.

45. Pregla, R., "Calculation of the Distributed Capacitances and Phase Velocities in Coupled Microstrip Lines by Conformal Mapping Techniques," Arch. Elek. Ubertragung, Vol. 26, pp. 470-474; November 1972.

46. Liebmann, G., "Solution of Partial Differential Equations with a Resistive Network Analogue," British J. Appl. Phys., Vol. 1, pp. 92-103; April 1952.

47. Green, H.E., "The Numerical Solution of Some Important Transmission-Line Problems," IEEE Trans. Microwave Theory and Techniques, Vol. MTT-13, pp. 676-692; September 1965.

48. Green H.E., "The Numerical Solution of Transmission Line Problems," Advances in Microwaves, Vol. 2, Ed. Leo Young, pp. 327-393, Academic Press; 1967.

49. Hill, Y.M. et al., "A General Method for Obtaining Impedance and Coupling Characteristics of Parallel Microstrip and Triplate Transmission Line Configuration," IBM J. Res. Develop., Vol. 13, pp. 314-322; May 1969.

50. Farrar, A. and Adams, A.T., "Matrix Methods for Microstrip Three-Dimensional Problem," IEEE Trans. Microwave Theory and Techniques, Vol. MTT-20, pp. 497-504; August 1972.

51. Lennartsson, B.I., "A Network Analogue Method for Computing the TEM Characteristics of Planar Transmission Lines," IEEE Trans. Microwave Theory and Techniques, Vol. MTT-20, pp. 586-591; September 1972.

52. Stinehelfer, H.E., "An Accurate Calculation of Uniform Microstrip Transmission Lines," IEEE Trans. Microwave Theory and Techniques, Vol. MTT-16; pp. 439-444; July 1968.

53. Silvester, P., "TEM Wave Properties of Microstrip Transmission Lines," Proc. IEEE Vol. 115, pp. 43-48; January 1968.

54. Krammler, D.W., "Caclculation of Characteristic Admittances and Coupling Coefficients on Strip Transmission Lines," IEEE Trans. Microwave Theory and Techniques, Vol. MTT-16, pp. 925-937; November 1968.

55. Bryant, T.G., and Weiss, J.A., "Parameters of Microstrip Transmission Lines and of Coupled Paws of Microstrip Lines," IEEE Trans. Microwave Theory and Techniques, Vol. MTT-16, pp. 1021-1027; December 1968.

56. Maesel, M., "A Numerical Solution of the Characteristics of Coupled Microstrips," 1969 European Microwave Conf. (London), pp. 118-121, IEE Conf. Publication No. 58; September 1969.

57. Chen, W.H., "Even and Odd Mode Impedance of Coupled Pairs of Microstrip Lines," IEEE Trans. Microwave Theory and Techniques, Vol. MTT-18, pp. 55-57; January 1970.

58. Weeks, W.T., "Calculation of Coefficients of Capacitance of Multiconductor Transmission Lines in the Presence of a Dielectric Surface," IEEE Trans. Microwave Theory and Techniques, Vol. MTT-18, pp. 35-43; January 1970.

59. Bryant, T.G., and Weiss, J.A., "MSTRIP (Parameters of Microstrip)", IEEE Trans. Microwave Theory and Techniques, Vol. MTT-19, pp. 418-419; April 1971.

60. Patel, P.D., "Calculation of Capacitance Coefficients for a System of Irregular Finite Conductors on a Dielectric Sheet," IEEE Trans. Microwave Theory and Techniques, Vol. MTT-19, pp. 862-869; November 1971.

61. Benedek, P. and Silvester, P., "Capacitance of Parallel Rectangular Plates Separated by a Dielectric Sheet," IEEE Trans. Microwave Theory and Techniques, Vol. MTT-20, pp. 504-510; August 1972.

62. Allen, J.L., and Estes, M.F., "Broadside-Coupled Strips in a Layered Dielectric Medium," IEEE Trans. Microwave Theory and Techniques, Vol. MTT-20, pp. 662-669; October 1972.

63. Chao, C.L., "Characteristics of Unsymmetrical Broadside-Coupled Strips in an Inhomogeneous Dielectric Medium," IEEE-MIT-S Intl. Microwave Symp. Digest, pp. 113-121; May 1975.

64. Yamashita, E. and Mittra, R. "Variational Method for the Analysis of Microstrip Lines," IEEE Trans. Microwave Theory and Techniques, Vol. MTT-13, pp. 251-256; April 1968.

65. Yamashita, E., "Variational Method for the Analysis of Microstrip-like Transmission Lines," IEEE Trans. Microwave Theory and Techniques, Vol. MTT-16, pp. 529-535; August 1968.

66. Yamashita, E. and Yamasaki S., "Parallel Strip Line Embedded in or Printed on a Dielectric Sheet," IEEE Trans. Microwave Theory and Techniques, Vol. MTT-16, pp. 972-973; November 1968.

67. Lee, H.J., Ph.D. Thesis to be published, Electrical & Computer Eng. Dept., O.S.U.

68. Hornsby, J.S. and Gopinath, A., "Numerical Analysis of a Dielectric Loaded Wave Guide with a Microstrip Line - Finite Difference Methods," IEEE Trans. Microwave Theory and Techniques, Vol. MTT-17, pp. 684-690; September 1969.

69. Gelder, D., "Numerical Determination of Microstrip Properties Using the Transverse Field Components," Proc. IEE, Vol. 117, pp. 699-705; April 1970.

70. Denlinger, E.J., "Frequency Dependence of a Coupled Pair of Microstrip Lines," IEEE Trans. Microwave Theory and Techniques, Vol. MTT-18, pp. 731-733; October 1970.

71. Denlinger, E.J., "A Frequency Dependent Solution for Microstrip Transmission Lines," IEEE Trans. Microwave Theory and Techniques, Vol. MTT-19; pp. 30-39; January 1971.

72. Daly, P., "Hybrid-Mode Analysis of Microstrip by Finite-Element Methods," IEEE Trans. Microwave Theory and Techniques, Vol. MTT-19, pp. 19-25; January 1971.

73. Pregla, R. and Schlosser, W., "Waveguide Modes in Dielectric Supported Strip Lines," Ark. Elek. Ubertragung, Vol. 22, pp. 379-386; August 1968.

74. Mittra, R. and Itoh, T., "A New Technique for the Analysis of the Dispersion Characteristics of Microstrip Lines," IEEE Trans. Microwave Theory and Techniques, Vol. MTT-19, pp. 47-56; January 1971.

75. Gauld, J.W. and Talboys, E.C., "Even- And Odd-Mode Guide Wavelengths of Coupled Lines in Microstrips," Electronics Letters, Vol. 8, pp. 121-122; March 1972.

76. Krage, M.K., and Haddad, G.I., "Frequency Dependent Characteristics of Microstrip Transmission Lines," IEEE Trans. Microwave Theory and Techniques, Vol. MTT-20, pp. 678-688; October 1972.

77. Getsinger, W.J., "Microstrip Dispersion Model," IEEE Trans. Microwave Theory and Techniques, Vol. MTT-20, pp. 34-39; January 1973.

78. Getsinger, W.J., "Dispersion of Parallel Coupled Microstrip," IEEE Trans. Microwave Theory and Techniques, Vol. MTT-21, pp. 144-145; March 1973.

79. Allen, J.L. and Barnes, W.J., "Unequal Coupled Mode Velocity C Section Filters," Electronics Letters, Vol. 10, pp. 128-129; April 1974.

80. Allen, J.L., "Multi-Section Inhomogeneous Coupled-Line Filters with Large Mode-Velocity Ratios," IEEE-MTT-S International Microwave Symp. Digest, pp. 113-115, May 1975, IEEE Cat. No. CH0955-5.

81. Gysel, U., "Microwave Band-Pass Filter Design in an Inhomogeneous Transmission Media," IEEE International Symposium on Circuits and Systems, Boston, Mass; April 1975.

82. Briechle, R., "Microstrip Comb Line Filters," Proc. 5th European Microwave Conf., pp. 436-440, Hamburg; Spetember 1975.

83. Tripathi, V.K., "Equivalent Circuits and Characteristics of Inhomogeneous Nonsymmetrical Coupled-Line Two-Port Circuits," IEEE Trans. Microwave Theory and Techniques, Vol. MTT-25, pp. 140-142; February 1977.

84. LaCombe, D. and Cohen, J., "Octove-band Microstrip DC Blocks," IEEE Trans. Microwave Theory and Techniques, Vol. MTT-20, pp. 555-55 ; August 1972.

85. Rizzoli, V., "Analysis and Design of Microstrip DC Blocks," Microwave Jour., Vol. 20, pp. 109-110; June 1977.

86. Kajfez, et al., "Asymmetric Microstrip DC Block with Rippled Response," IEEE, MTT-S Intl. Microwave Symp. Digest, pp. 301-303; 1981.

87. Ou, W.P., "Design Equations for an Interdigitated Directional Coupler," IEEE Trans. Microwave Theory and Techniques, Vol. MTT-23, pp. 253-255; February 1975.

88. Rizzoli, V., "Stripline Interdigitated Couplers; Analysis and Design Considerations," Electronics Letters, Vol. 11, pp. 392-393; August 1975.

89. Malherbe, J.A.G., "Interdigital Directional Couplers with an Odd- or Even-Number of Lines and Unequal Characteristic Impedances," Electronics Letters, Vol. 12, pp. 464-465; September 1976.

90. Hewitt, S.J. and Pengelly, R.S., "Design Data for Interdigital Directional Couplers," Electronics Letters, Vol. 12, pp. 86-87; February 1976.

91. Paolino, D.D., "Design More Accurate Interdigitated Couplers," Microwaves, pp. 34-38; May 1976.

92. Lange, J., "Interdigitated Stripline Quadrature Hybrid," IEEE Trans. Microwave Theory and Techniques, Vol. MTT-17, pp. 1150-1151; December 1969.

93. Waugh, R. and LaCombe, D., "Unfolding the Lange Coupler," IEEE Trans. Microwave Theory and Techniques, Vol. MTT-20, pp. 777-779; November 1972.

94. Tulaja, V., Schiek, B. and Kohler, J., "An Interdigitated 3-dB Coupler with Three Strips," IEEE Trans. Microwave Theory and Techniques, Vol. MTT-26, pp. 643-645; September 1978.

95. Tripathi, V.K., "On the Analysis of Symmetrical Three-Line Microstrip Circuits," IEEE Trans. Microwave Theory and Techniques, Vol. MTT-25, pp. 726-729; September 1977.

96. Tripathi, V.K., "The Scattering Parameters and Directional Coupler Analysis of Characteristically Terminated Three-Line Structures in an Inhomogeneous Medium," IEEE Trans. Microwave Theory and Techniques, Vol. MTT-29, pp. 22-26; January 1981.

97. Paul, C.R., "On Uniform Multimode Transmission Lines," IEEE Trans. Microwave Theory and Techniques, Vol. MTT-21, pp. 556-558; August 1973.

98. Paul, C.R., "Useful Matrix Chain Parameter Identities for the Analysis of Multiconductor Transmission Lines, IEEE Trans. Microwave Theory and Techniques, Vol. MTT-23, pp. 756-760; September 1975.

99. Carlin, H.J. and Giordano, A.B., "Network Theory; An Introduction to Reciprocal and Nonreciprocal Circuits," Englewood Cliffs, N.J.; Prentice-Hall, Inc.; Chapter 4; 1964.

100. Gunton, D.J. and Paige, E.G.S., "An Analysis of the General Asymmetric Directional Coupler with Non-mode-Converting Terminations," Microwaves, Optics and Acoustics, Vol. 2, pp. 31-36; January 1978.

101. Garg, R., "The Effect of Tolerances on Microstrip Line and Slot Line Performance," IEEE Trans. Microwave Theory and Techniques, Vol. MTT-26, pp. 16-19; January 1978.

102. Shamasundara, S.D. and Gupta, K.C., "Sensitivity Analysis of Coupled Microstrip Directional Coupler," IEEE Trans. Microwave Theory and Techniques, Vol. MTT-26, pp. 788-794; October 1978.

103. Brenner, H.E., "Perturbations of the Critical Parameters of Quarter Wave Directional Couplers," IEEE Trans. Microwave Theory and Techniques, Vol. MTT-15, pp. 384-385; June 1967.

104. Sun, Y.Y., "Analyasis of Generalized Coupled-Transmission Line Directional Coupler," Int. J. Electronics, Vol. 41, pp. 125-136; 1976.

105. Tripathi, V.K. and Chang, C.L., "Quasi-TEM Parameters of Nonsymmetrical Coupled Microstrip Lines," Int. J. Electronics, Vol. 45, No. 21, pp. 215-223; August 1978.

106. Shibata, K., Hatori, K., Tokumitsu, Y. and Komizo, H., "Microstrip Spiral Directional Coupler," IEEE Trans. Microwave Theory and Techniques, Vol. MTT-29, pp. 680-689, July 1981.

107. Presser, A., "Interdigitated Microstrip Coupler Design," IEEE Trans. Microwave Theory and Techniques, Vol. MTT-26, No. 10, pp. 801-805; October 1978.

108. Rizzoli, V. and Lipparini, A., "The Design of Interdigitated Couplers for MIC Applications," IEEE Trans. Microwave Theory and Techniques, Vol. MTT-26, pp. 7-15; January 1978.

109. Tajima, Y. and Kamihashi, S., "Multiconductor Couplers," IEEE Trans. Microwave Theory and Techniques, Vol. MTT-26, pp. 795-801; October 1978.

110. Collier, R. J. and El-Deeb, N. A., "On the Use of a Microstrip Three-Line System as a Six-Port Reflectometer," IEEE Trans. Microwave Theory and Techniques, Vol. MTT-27, pp. 847-853; October 1979.

111. Tajima, Y. and Kamihashi, S., "Multiconductor Couplers," IEEE Trans. Microwave Theory and Techniques, Vol. MTT-26, pp. 795-801; October 1978.

112. Kajfez, D., Paunovic, Z. and Pavlin, S., "Simplified Design of Lange Coupler," IEEE Trans. Microwave Theory and Techniques, Vol. MTT-26, No. 10, pp. 806-808; October 1978.

113. Yamamoto, S., Azakami, T., and Itakura, K., "Coupled Strip Transmission Line with Three Center Conductors," IEEE Trans. Microwave Theory and Techniques, Vol. MTT-14, pp. 446-461; October 1966.

114. Pavlidis, D. and Hartnagel, H.L., "The Design and Performance of Three-Line Microstrip Couplers," IEEE Trans. Microwave Theory and Techniques, Vol. MTT-24, pp. 631-640; October 1976.

115. Tripathi, V. K., Chin, Y. K., and Lee, H.," Interdigital Multiple Coupled Microstrip DC blocks", to be published, 12th European Microwave Conference, September 1982, in Helsinki, Finland.

116. Levy, R., "Transmission-Line Directional Couplers for Very Broad Band Operation," Proc. Inst. Elec. Eng., Vol. 112, pp. 469-476; March 1965.

APPENDICES

APPENDIX A

The Symmetrical Four-Line Eight-Port Structure

Let the voltage and current eigenvector matrices for the symmetrical four-line structure be presented by

$$[M_V] = \begin{bmatrix} 1 & 1 & 1 & 1 \\ R_a & R_b & R_c & R_d \\ R_a & -R_b & R_c & -R_d \\ 1 & -1 & 1 & -1 \end{bmatrix} \qquad \text{(A-1)}$$

$$[M_I] = \begin{bmatrix} Y_{a1} & Y_{ba} & Y_{c1} & Y_{d1} \\ R_a Y_{a2} & R_b Y_{b2} & R_c Y_{c2} & R_d Y_{d2} \\ R_a Y_{a2} & -R_b Y_{b2} & R_c Y_{c2} & -R_d Y_{d2} \\ Y_{a1} & -Y_{b1} & Y_{c1} & -Y_{d1} \end{bmatrix} \qquad \text{(A-2)}$$

where $Y_{\chi i}$ represents the mode admittance of line i (1,2,3,4) for mode χ (a,b,c,d).

The inverse matrix of (A-1) is then given by:

$$[M_V]^{-1} = \begin{bmatrix} -R_c/R_1 & 1/R_1 & 1/R_1 & -R_c/R_1 \\ -R_d/R_2 & 1/R_2 & -1/R_2 & R_d/R_2 \\ R_a/R_1 & -1/R_1 & -1/R_1 & R_a/R_1 \\ R_b/R_2 & -1/R_2 & 1/R_2 & -R_b/R_2 \end{bmatrix} \qquad \text{(A-3)}$$

where

$$R_1 = 2\ (R_a - R_c)$$

$$R_2 = 2\ (R_b - R_d)$$

The orthogonal condition $[M_I]^T\ [M_V] = [U]$ leads to the following relations;

$$\frac{Y_{a1}}{Y_{a2}} = \frac{Y_{c1}}{Y_{c2}} = \frac{Z_{a2}}{Z_{a1}} = \frac{Z_{c2}}{Z_{c1}} = -\ R_a\ R_c \qquad \text{(A-4a)}$$

$$\frac{Y_{b1}}{Y_{b2}} = \frac{Y_{d1}}{Y_{d2}} = \frac{Z_{b2}}{Z_{b1}} = \frac{Z_{d2}}{Z_{d1}} = -R_b\ R_d \qquad \text{(A-4b)}$$

According to equation (2-8), the admittance matrix for the symmetrical eight-port structures are given by

$$[Y] = \begin{bmatrix} [Y]_{11} & [Y]_{12} \\ [Y]_{12} & [Y]_{11} \end{bmatrix} \qquad \text{(A-5)}$$

where

$$[Y]_{11} = \begin{bmatrix} Y_{11} & Y_{12} & Y_{13} & Y_{14} \\ Y_{12} & Y_{22} & Y_{23} & Y_{24} \\ Y_{13} & Y_{32} & Y_{33} & Y_{34} \\ Y_{14} & Y_{42} & Y_{43} & Y_{44} \end{bmatrix}$$

$$= \begin{bmatrix} Y_{a1} & Y_{b1} & Y_{c1} & Y_{d1} \\ R_a Y_{a2} & R_b Y_{b2} & R_c Y_{c2} & R_d Y_{d2} \\ R_a Y_{a2} & -R_b Y_{b2} & R_c Y_{c2} & -R_d Y_{d2} \\ Y_{a1} & -Y_{b1} & Y_{c1} & -Y_{d1} \end{bmatrix} \begin{bmatrix} \coth \gamma_a \ell & 0 & 0 & 0 \\ 0 & \operatorname{Coth} \gamma_b \ell & 0 & 0 \\ 0 & 0 & \operatorname{Coth} \gamma_c \ell & 0 \\ 0 & 0 & 0 & \operatorname{Coth} \gamma_d \ell \end{bmatrix}$$

$$\cdot \begin{bmatrix} -R_c/R_1 & 1/R_1 & 1/R_1 & -R_c/R_1 \\ -R_d/R_2 & 1/R_2 & -1/R_2 & R_d/R_2 \\ R_a/R_1 & -1/R_1 & -1/R_1 & R_a/R_1 \\ R_b/R_2 & -1/R_2 & 1/R_2 & -R_b/R_2 \end{bmatrix}$$

$$[Y_{12}] = \begin{bmatrix} Y_{15} & Y_{16} & Y_{17} & Y_{18} \\ Y_{25} & Y_{26} & Y_{27} & Y_{28} \\ Y_{35} & Y_{36} & Y_{37} & Y_{38} \\ Y_{45} & Y_{46} & Y_{47} & Y_{48} \end{bmatrix}$$

$$= -\begin{bmatrix} Y_{a1} & Y_{b1} & Y_{c1} & Y_{d1} \\ R_a Y_{a2} & R_b Y_{b2} & R_c Y_{c2} & R_d Y_{ds} \\ R_a Y_{a2} & -R_b Y_{b2} & R_c Y_{c2} & -R_d Y_{d2} \\ Y_{a1} & -Y_{b1} & Y_{c1} & -Y_{d1} \end{bmatrix} \begin{bmatrix} \operatorname{csch} \gamma_a \ell & 0 & 0 & 0 \\ 0 & \operatorname{csch} \gamma_b \ell & 0 & 0 \\ 0 & 0 & \operatorname{csch} \gamma_c \ell & 0 \\ 0 & 0 & 0 & \operatorname{csch} \gamma_d \ell \end{bmatrix}$$

$$\begin{bmatrix} -R_c/R_a & 1/R_1 & 1/R_1 & -R_c/R_1 \\ -R_d/R_2 & 1/R_2 & -1/R_2 & R_d/R_2 \\ R_a/R_1 & -1/R_1 & -1/R_2 & R_d/R_2 \\ R_b/R_2 & -1/R_2 & 1/R_2 & -R_b/R_2 \end{bmatrix}$$

The expressions for the admittance parameters are obtained as follows by manipulating the partitioned matrix above.

$$Y_{11} = Y_{44} = Y_{55} = Y_{88} = -(A + B) \qquad \text{(A-6a)}$$

$$Y_{14} = Y_{41} = Y_{58} = Y_{85} = -(A - B) \qquad \text{(A-6b)}$$

$$Y_{12} = Y_{21} = Y_{34} = Y_{43} = Y_{56} = Y_{65} = Y_{78} = Y_{89} = C + D \qquad \text{(A-6c)}$$

$$Y_{13} = Y_{31} = Y_{24} = Y_{42} = Y_{57} = Y_{75} = Y_{68} = Y_{86} = C - D \qquad \text{(A-6d)}$$

$$Y_{15} = Y_{51} = Y_{48} = Y_{84} = E + F$$

$$Y_{18} = Y_{81} = Y_{45} = Y_{54} = E - F$$

$$Y_{16} = Y_{61} = Y_{25} = Y_{52} = Y_{38} = Y_{83} = Y_{47} = Y_{74} = -(G + H) \qquad \text{(A-6e)}$$

$$Y_{17} = Y_{71} = Y_{28} = Y_{82} = Y_{35} = Y_{53} = Y_{46} = Y_{64} = -(G - H) \qquad \text{(A-6f)}$$

$$Y_{22} = Y_{33} = Y_{66} = Y_{77} = I + J \qquad \text{(A-6g)}$$

$$Y_{23} = Y_{32} = Y_{67} = Y_{76} = I - J \qquad \text{(A-6h)}$$

$$Y_{26} = Y_{62} = Y_{37} = Y_{73} = -(K + L) \qquad \text{(A-6i)}$$

$$Y_{27} = Y_{72} = Y_{36} = Y_{63} = -(K - L) \qquad \text{(A-6j)}$$

where

$$A = \frac{1}{R_1}\left(R_c Y_{a1} \coth \gamma_a \ell - R_a Y_{c1} \coth \gamma_c \ell\right)$$

$$B = \frac{1}{R_2}\left(R_d Y_{b1} \coth \gamma_b \ell - R_b Y_{d1} \coth \gamma_d \ell\right)$$

$$C = \frac{1}{R_1}\left(Y_{a1} \coth \gamma_a \ell - Y_{c1} \coth \gamma_c \ell\right)$$

$$D = \frac{1}{R_2}\left(Y_{b1} \coth \gamma_b \ell - Y_{d1} \coth \gamma_d \ell\right)$$

$$E = \frac{1}{R_1}\left(R_c Y_{a1} \operatorname{csch} \gamma_a \ell - R_a Y_{c1} \operatorname{csch} \gamma_c \ell\right)$$

$$F = \frac{1}{R_2}\left(R_d Y_{b1} \operatorname{csch} \gamma_b \ell - R_b Y_{d1} \operatorname{csch} \gamma_d \ell\right)$$

$$G = \frac{1}{R_1}\left(Y_{a1} \operatorname{csch} \gamma_a \ell - Y_{c1} \operatorname{csch} \gamma_c \ell\right)$$

$$H = \frac{1}{R_2}\left(Y_{b1} \operatorname{csch} \gamma_b \ell - Y_{d1} \operatorname{csch} \gamma_d \ell\right)$$

$$I = \frac{1}{R_1}\left(R_a Y_{a2} \coth \gamma_a \ell - R_c Y_{c2} \coth \gamma_c \ell\right)$$

$$J = \frac{1}{R_2}\left(R_b Y_{b2} \coth \gamma_b \ell - R_d Y_{d2} \coth \gamma_d \ell\right)$$

$$K = \frac{1}{R_1}\left(R_a Y_{a2} \operatorname{csc} \gamma_a \ell - R_c Y_{c2} \operatorname{csc} \gamma_c \ell\right)$$

$$L = \frac{1}{R_2}\left(R_b Y_{b2} \operatorname{csch} \gamma_b \ell - R_d Y_{d2} \operatorname{csch} \gamma_d \ell\right)$$

The validity and correctness of the above expressions has been tested by evaluating these parameters for the example given in section 2.3 and comparing the results with the values computed from the general matrix expressions given in section 2.2.

APPENDIX B

Analysis of Symmetrical Three-Line Microstrip Circuits [95]

The voltages and currents for the case of uniformly coupled lines are found by equations (2-3) and (2-4);

$$\frac{d^2[V]}{dx^2} + [Z]\,[Y]\,[V] = 0 \tag{2-3}$$

$$\frac{d^2[I]}{dx^2} + [Y]\,[Z]\,[I] = 0 \tag{2-4}$$

where

$$[Z] = \begin{bmatrix} z_{11} & z_{12} & z_{13} \\ z_{12} & z_{22} & z_{12} \\ z_{13} & z_{12} & z_{11} \end{bmatrix}$$

$$[Y] = \begin{bmatrix} y_{11} & y_{12} & y_{13} \\ y_{12} & y_{22} & y_{12} \\ y_{13} & y_{12} & y_{11} \end{bmatrix}$$

The characteristic product matrices [Z] [Y] and [Y] [Z] are of the form

$$[Z]\,[Y] = \begin{bmatrix} A & B & C \\ D & E & D \\ C & B & A \end{bmatrix} \tag{B-1a}$$

and

$$[Y]\,[Z] = \{[Z]\,[Y]\}^{T} \tag{B-1b}$$

where

$$A = z_{11}\,y_{11} + z_{12}\,y_{12} + z_{13}\,y_{13}$$

$$B = z_{11}\,y_{12} + z_{12}\,y_{22} + z_{13}\,y_{12}$$

$$C = z_{11}\,y_{13} + z_{12}\,y_{12} + z_{13}\,y_{11}$$

$$D = z_{12}\,y_{11} + z_{22}\,y_{12} + z_{12}\,y_{13}$$

$$E = z_{22}\,y_{22} + 2\,z_{12}\,y_{12}$$

Assuming the solutions of equation (2-3) the form $e^{\gamma x}$, the eigen values of [Z] [Y] are determined from

$$\det\ \{[Z]\,[Y] - \gamma^{2}\,[U]\} = 0 \tag{B-2}$$

where [U] is the 3 x 3 identity matrix.

These eigenvalues lead to the propagation constants for the normal modes of the system and are given by

$$\gamma_{c}^{2} = A - C \tag{B-3a}$$

$$\gamma_{b}^{2} = \frac{A + C + E}{2} + 1/2\sqrt{(A + C - E)^{2} + 8DB} \tag{B-3b}$$

$$\gamma_{c}^{2} = \frac{A + C + E}{2} - 1/2\sqrt{(A + C - E)^{2} + 8DB} \tag{B-3c}$$

The eigenvector matrices corresponding to the eigenvalues can be calculated by substituting the eigenvalues above into equations (2-3) and (2-4) and are given by

$$[M_V] = \begin{bmatrix} 1 & 1 & 1 \\ 0 & R_{vb} & R_{vc} \\ -1 & 1 & 1 \end{bmatrix} \tag{B-4a}$$

and

$$[M_I] = \begin{bmatrix} 1 & 1 & 1 \\ 0 & R_{Ib} & R_{Ic} \\ -1 & 1 & 1 \end{bmatrix} \tag{B-4b}$$

where $[M_V]$ is voltage eigenvector matrix and $[M_I]$ is current eigenvector matrix, which gives the ratio of voltages and currents, respectively, on the three lines for the three normal modes of propagation.

$$R_{vb,c} = -\frac{A + C - E}{2B} \pm \sqrt{\left(\frac{A + C - E}{2B}\right)^2 + 2\frac{D}{B}} \tag{B-5}$$

and

$$R_{vb,c} = -\frac{2}{R_{vc,b}} \tag{B-6}$$

From (B-5) and (B-6) it is seen that

$$R_{vb}R_{vc} = -2\frac{D}{B} \tag{B-7a}$$

$$R_{Ib}R_{Ic} = -2\frac{D}{B} \tag{B-7b}$$

Therefore, $R_{vb,c} \neq R_{Ib,c}$ unless $D = B$.

The voltage and current eigenvectors may be used to find the characteristic impedances and admittances of the three lines for the

three normal modes. From (2-1) and (2-2), these are found to be

$$Z_{a1} = Z_{a3} = \frac{Z_{11} - Z_{13}}{\gamma_a} = \frac{\gamma_a}{y_{11} - y_{13}} = \frac{1}{Y_{a1}} = \frac{1}{Y_{a3}} \tag{B-8a}$$

$$Z_{b1} = Z_{b3} = \frac{z_{11} + z_{13} + R_{Ib} Z_{12}}{\gamma_b} = \frac{\gamma_b}{y_{11} + y_{13} + R_{vb} y_{12}} = \frac{1}{Y_{b1}}$$

$$= \frac{1}{Y_{b3}} \tag{B-8b}$$

$$Z_{b2} = \frac{R_{Ib} Z_{22} + 2 Z_{12}}{R_{Ib} \gamma_b} = \frac{R_{vb} \gamma_b}{R_{Vb} Y_{22} + 2 Y_{12}} = \frac{1}{Y_{b2}} \tag{B-8c}$$

$$Z_{c1} = Z_{c3} = \frac{z_{11} + z_{13} + R_{Ic} z_{12}}{\gamma_c}$$

$$= \frac{\gamma_c}{y_{11} + y_{13} + R_{vc} Y_{12}} = \frac{1}{Y_{c1}} = \frac{1}{Y_{c3}} \tag{B-8d}$$

$$Z_{c2} = \frac{R_{Ic} z_{22} + 2 z_{12}}{R_{Ic} \gamma_c} = \frac{R_{v2} \gamma_c}{R_{v2} y_{22} + 2 y_{12}} = \frac{1}{Y_{c2}} \tag{B-8e}$$

where Z_{jk} and Y_{jk} (j = a,b,c and k = 1,2,3) are the characteristic impedance and admittance, respectively, of line k for mode j. From (B-5) to (B-7), it is seen that the characteristic immittances of the lines for the three normal modes are related through

$$\frac{Y_{b1}}{Y_{b2}} = \frac{Y_{c1}}{Y_{c2}} = \frac{Z_{b2}}{Z_{b1}} = \frac{Z_{c2}}{Z_{c1}} = -\frac{R_{vb} R_{vc}}{2} \tag{B-9}$$

The immittance matrix parameters of the coupled line six-port shown in Fig. 4-1 are found in terms of these normal mode characteristic immittances of the three lines [95]. This can be done in a straight forward manner by using the approach described in Chaper II.

APPENDIX C

Scattering Parameters of a General Uniformly Coupled Line Four-Port With Characteristic Terminations [96]

The scattering parameters for the general two-line case and the symmetrical three-line four-port case are derived in terms of the reflection and transmission coefficients by using a system of voltage sources and terminating impedances (non-mode-converting terminations) which allow for the excitation of the individual modes of propagation. The reflection and transmission coefficients of each line for individual modes are given by Levy [116].

$$\Gamma_{\chi j} = \frac{j\,(Z_{\chi j}/Z_j - Z_j/Z_{\chi j})\,\sin\theta_\chi}{\phi_\chi} \qquad \text{(C-1a)}$$

$$T_\chi = \frac{2}{\phi_\chi}$$

where

$$\phi_\chi = 2\cos\theta_\chi + j\left(\frac{Z_{\chi j}}{Z_j} + \frac{Z_j}{Z_{\chi j}}\right)\sin\theta_\chi$$

In the above equations, $\chi = c,\pi$ represents the two normal modes of the system and $j = 1,2$ represents the lines. Thus, $Z_{\chi j}$ is the characteristic impedance of line j (1,2) for mode $\chi(c,\pi)$, Z_j is the terminating impedance for line j and θ_χ is the electric length of the line for a given mode. For the general two-line structure [21], the ratio of the line impedance for the two normal modes is equal and is given by

$$\frac{Z_{c2}}{Z_{c1}} = \frac{Z_{\pi 2}}{Z_{\pi 1}} = - R_c R_\pi \qquad \text{(C-2)}$$

where R_c and R_π represent the ratio of voltage on line 2 to that on line 1 for the two normal modes C and π respectively, and the elements of the voltage eigenvector matrix are given by

$$[M_v] = \begin{bmatrix} A & B \\ AR_c & BR_\pi \end{bmatrix}$$

Terminating of line 2 in Z_2 and line 1 in Z_1 with $Z_2/Z_1 = -R_c R_\pi$ then, enables us to excite the individual modes, since the ratio of the mode impedances of two lines is the same for all modes as given by equation (C-2). This results in

$$\Gamma_{\chi 1} = \Gamma_{\chi 2} \text{ and } T_{\chi 1} = T_{\chi 2} \text{ for } \chi = c \text{ and } \pi.$$

The scattering parameters are then found by utilizing the source configurations and terminations as shown in Figure C-1.

For $V_1 = 1$ and V_j $(j = 2,3,4) = 0$

letting $A + B = 1$ and $AR_c + BR_\pi = 0$, then

$$A \triangleq - \frac{R_\pi}{R_c - R_\pi} \quad , \quad B \triangleq \frac{R_c}{R_c - R_\pi}$$

Therefore, the scattering parameters are given by

$$S_{11} = S_{44} = A\Gamma_c + B\,\Gamma_\pi$$

$$= \frac{1}{R_c - R_\pi} (R_c\,\Gamma_\pi - R_\pi\,\Gamma_c) \qquad \text{(C-3a)}$$

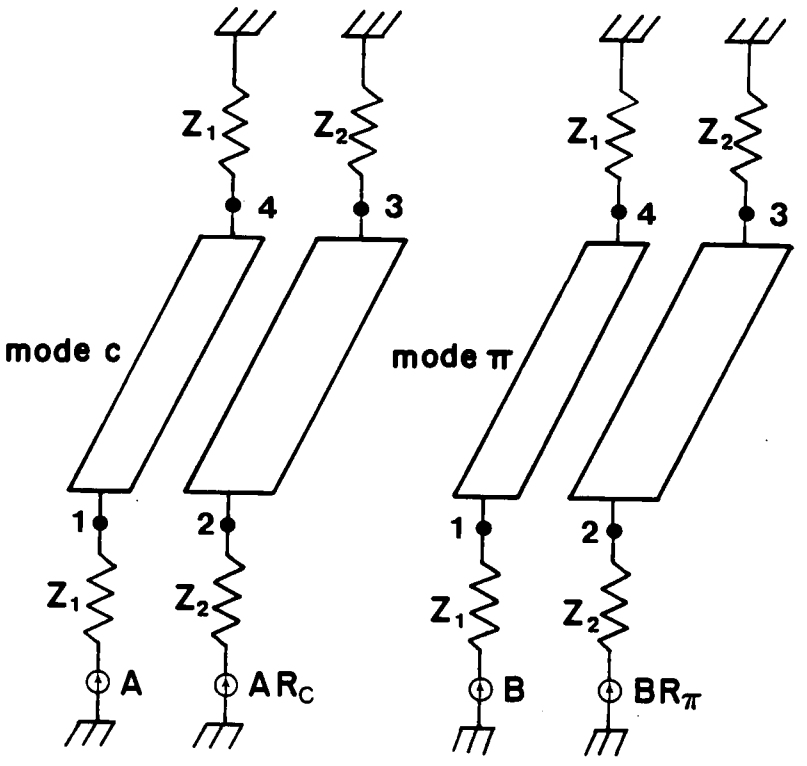

Figure c-1. Sources and terminations used to derive the scattering parameters: (a) Total signal input 1 V at port 1, zero at all the other ports. (b) Total signal input 1 V at port 2, zero at all the other ports.

$$S_{12} = S_{21} = S_{34} = S_{43} = (A\, R_c\, \Gamma_c + B\, R_\pi\, \Gamma_\pi)\sqrt{\frac{Z_{1o}}{Z_{2o}}}$$

$$= \sqrt{-R_c\, R_\pi}\ \frac{\Gamma_c - \Gamma_\pi}{R_c - R_\pi} \qquad \text{(C-3b)}$$

$$S_{14} = S_{41} = AT_c + B\, T_\pi$$

$$= \frac{R_c\, T_\pi - R_\pi\, T_c}{R_c - R_\pi} \qquad \text{(C-3c)}$$

$$S_{13} = S_{31} = S_{24} = S_{42} = (AR_c\, T_c + B\, R_\pi\, T_\pi)\sqrt{\frac{Z_{1o}}{Z_{2o}}}$$

$$= \sqrt{-\,R_c\, R_\pi}\quad \frac{T_c - T_\pi}{R_c - R_\pi} \qquad \text{(C-3d)}$$

Similarly, for $V_2 = 1$ and V_j $(j = 1,3,4) = 0$

$$A \triangleq \frac{1}{R_c - R_\pi}\ ,\quad B \triangleq \frac{-1}{R_c - R_\pi}$$

The scattering parameters are given by

$$S_{22} = S_{33} = AR_c\Gamma_c + B\, R_\pi\, \Gamma_\pi \qquad \text{(C-3e)}$$

$$= \frac{R_c\, \Gamma_c - R_\pi\, \Gamma_\pi}{R_c - R_\pi}$$

$$S_{23} = S_{32} = AR_cT_c + B\, R_\pi\, T_\pi \qquad \text{(C-3f)}$$

$$= \frac{R_c\, T_c - R_\pi\, T_\pi}{R_c - R_\pi}$$

The above expressions for $Z_{2o}/Z_{1o} = - R_{vb}R_{vc}/2$ with $R_c = R_{vb}$ and $R_\pi = R_{vc}$ lead to those obtained in Tripathi [95] for both the symmetrical and the non-symmetrical interdigitated four-port structures consisting of symmetrical three-line.